# Improved Resiliency of Transportation Networks through Connected Mobility

**Final Report**

by

Paul Ziehl
Email: ziehl@cec.sc.edu
University of South Carolina

Weichiang Pang
Robert Mullen
Rafal Anay
Nixon Wonoto

University of South Carolina

**January 31, 2019**

## Center for Connected Multimodal Mobility ($C^2M^2$)

*200 Lowry Hall, Clemson University*
*Clemson, SC 29634*

# DISCLAIMER

*The contents of this report reflect the views of the authors, who are responsible for the facts and the accuracy of the information presented herein. This document is disseminated in the interest of information exchange. The report is funded, partially or entirely, by the Center for Connected Multimodal Mobility ($C^2M^2$) (Tier 1 University Transportation Center) Grant, which is headquartered at Clemson University, Clemson, South Carolina, USA from the U.S. Department of Transportation's University Transportation Centers Program. However, the U.S. Government assumes no liability for the contents or use thereof. Non-exclusive rights are retained by the U.S. DOT.*

# Technical Report Documentation Page

| 1. Report No. | 2. Government Accession No. | 3. Recipient's Catalog No. |
|---|---|---|
| | | |

| 4. Title and Subtitle | 5. Report Date |
|---|---|
| Improved Resiliency of Transportation Networks through Connected Mobility | January 31, 2019 |
| | **6. Performing Organization Code** |

| 7. Author(s) | 8. Performing Organization Report No. |
|---|---|
| Paul Ziehl, Ph.D. https://orcid.org/0000-0002-4783-9255, Weichiang Pang, Ph.D. https://orcid.org/0000-0003-3050-5491, Robert Mullen, Ph.D. https://orcid.org/0000-0002-4321-5939/print, Rafal Anay, https://orcid.org/0000-0003-0425-9178, and Nixon Wonoto, Ph.D. https://orcid.org/0000-0002-2007-6614 | |

| 9. Performing Organization Name and Address | 10. Work Unit No. |
|---|---|
| University of South Carolina<br>300 Main St<br>Columbia, SC 29208 | **11. Contract or Grant No.**<br>69A3551747117 |

| 12. Sponsoring Agency Name and Address | 13. Type of Report and Period Covered |
|---|---|
| Center for Connected Multimodal Mobility (C2M2)<br>Clemson University<br>200 Lowry Hall<br>Clemson, SC 29634 | Final Report (August 2017 – Dec. 2018) |
| | **14. Sponsoring Agency Code** |

**15. Supplementary Notes**

Conducted in cooperation with the U.S. Department of Transportation, Federal Highway Administration

16. Abstract

A significant number of bridges (older bridges in particular) in the Southeastern and Central region of United States have been designed and constructed according to older seismic provisions. Based on an article by Wong et al. (2005), the economic loss from the Charleston region could reach over $14 billion if the 1886 Charleston earthquake were to happen again. Due to outdated seismic design strategies used for older bridges, recent research has investigated potential damage in Charleston. However, most of these investigations do not account for the simultaneous aspects of bridge importance (such as centrality, historical significance, and traffic capacity).

Furthermore, these prior investigations do not consider the actual detailing of critical structural connections, such as the critical pile to bent cap connection. This connection region is depended upon for energy dissipation while simultaneously providing structural integrity during an event. Full-scale experimental studies performed at the University of South Carolina were used to assess projected performance of these connections in a seismic event. This project develops a new tool that is informed with actual structural behavior gained through full-scale experimental investigations and combines centrality, historical significance, and traffic capacity to assess expected damage. The results are useful for informing placement of monitoring systems, identification of potential retrofit strategies, and optimizing network performance.

One goal of the work is technological transfer. The research findings can be used to assist the Department of Transportation in identification of the most critical bridges in the network for purposes of instrumentation, meaning which bridges should be monitored and, for those bridges, which specific regions should be monitored to rapidly assess damage after a seismic event. This information can then be utilized for routing of traffic and for the assessment of potential retrofitting strategies, thereby improving reliability of the transportation system. The tool runs on Matlab and includes transportation network and seismic demand visualization. Results are presented in sets of graphics and tables through a multi-window graphical user interface.

| 17. Keywords | 18. Distribution Statement |
|---|---|
| Bridge, retrofit, online monitoring, earthquake, fragility, optimization, tool development | **No restrictions.** |

| 19. Security Classif. (of this report) | 20. Security Classif. (of this page) | 21. No. of Pages | 22. Price |
|---|---|---|---|
| Unclassified | Unclassified | **103** | **$0.00** |

# ACKNOWLEDGMENT

*This research, titled "Improved Resiliency of Transportation Networks through Connected Mobility," was funded by the United States Department of Transportation (USDOT) Center for Connected Multimodal Mobility ($C^2M^2$). Parts of the research are used in the $C^2M^2$ collaborative work between Clemson University and University of South Carolina. Special thanks to Dr. Yohanna Mejia, Vafa Soltangharaei and Li Ai from USC who helped with the experimental part.*

# Table of Contents

## List of Tables

## List of Figures

# EXECUTIVE SUMMARY

***Overview:*** A significant number of bridges (older bridges in particular) in the Southeastern and Central region of United States have been designed and constructed according to older seismic provisions. Based on an article by Wong et al. (2005), the economic loss from the Charleston region could reach over $14 billion if the 1886 Charleston earthquake were to happen again. Due to outdated seismic design strategies used for older bridges, recent research has investigated potential damage in Charleston. However, most of these investigations do not account for the simultaneous aspects of bridge importance (such as centrality, historical significance, and traffic capacity).

Furthermore, these prior investigations do not consider the actual detailing of critical structural connections, such as the critical pile to bent cap connection. This connection region is depended upon for energy dissipation while simultaneously providing structural integrity during an event. Full-scale experimental studies conducted at the University of South Carolina were employed to assess projected performance of these connections in a seismic event. This project develops a new tool that is informed with actual structural behavior gained through full-scale experimental investigations and combines centrality, historical significance, and traffic capacity to assess expected damage. The results are useful for informing placement of monitoring systems, identification of potential retrofit strategies, and optimizing network performance.

***Findings:*** One goal of the work is technological transfer. The research findings can be used to assist the Department of Transportation in identification of the most critical bridges in the network for purposes of instrumentation, meaning which bridges should be monitored and, for those bridges, which specific regions should be monitored to rapidly assess damage after a seismic event. This information can then be utilized for routing of traffic and for the assessment of potential retrofitting strategies, thereby improving reliability of the transportation system. The tool runs on Matlab and includes transportation network and seismic demand visualization. Results are presented in sets of graphics and tables through a multi-window graphical user interface.

# CHAPTER 1

## Introduction

The ASCE infrastructure report card shows that the U.S. has almost four in every 10 bridges that are 50 years or older and deficient. Across a structurally deficient bridge, there are 188 million trips per day on average (Ironistic, 2018). After 1983's Loma Prieta earthquake, the American Association of State Highway and Transportation Officials (AASHTO), implemented "Guide Specifications for Seismic Design of Highway Bridges" as a mandatory requirement for states that are prone to seismic hazards (Roberts, 1996). However, many bridges in the Southeastern and Central region of United States (CSUS) are known to have designs that are in question for seismic consideration. Although the west coast is more prone to earthquakes phenomena compared to the east coast, some regions in the east coast are also susceptible to earthquakes, which mostly occur in the coastal plain from the break-up of Pangaea (when Africa and North America were one continent). One example of such a region is Charleston, SC.

Charleston is served by two interstates: I-26 and I-526. The length spans 50 km in Tennessee, 86 km in North Carolina, 356 km in South Carolina, which sums to 492 km span length. I-26 is predominantly a four-lane rural interstate with 100km/h speed limits but widens to six-lanes with lower speeds in the Charleston area. Another interstate passing through Charleston is the four-lane I-526 (span of 31 km). The three other major routes in Charleston are US 17, US 52, and US 78. A parameter called "ADT target" in the developed tool controls the study domain which includes most bridges that have high average daily traffic and fall under these major routes.

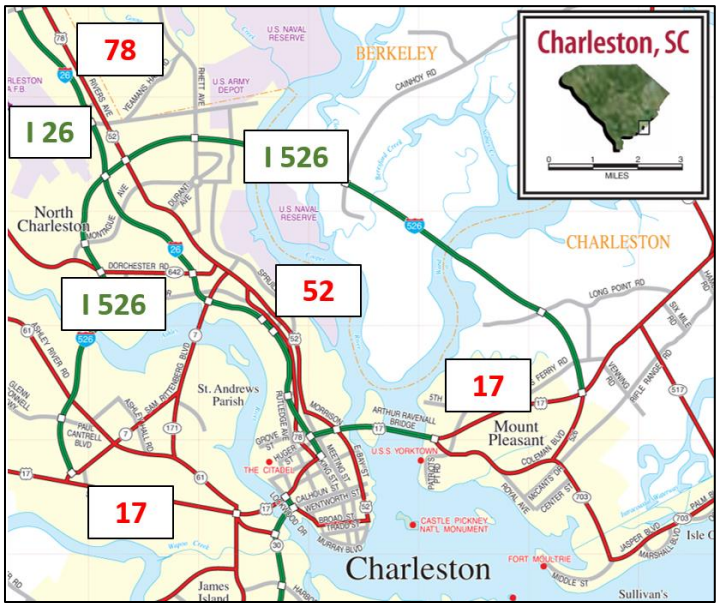


Figure 1.1: Charleston major transportation routes
(Adapted from TRIPmedia, 2018)

Charleston experienced on August 31, 1886 an earthquake of magnitude $M_w$ 6.9-7.3 with the geographical epicenter at 32.900° N 80.000° W and felt over 2.5 million square miles (Nuttli et al., 1986). The total damage was estimated to be around US $5 to $6 million with 60 casualties and an economic loss of $23 million (1978 dollars). It was also detected in several locations throughout the eastern part of the United States including Milwaukee; Cuba; Bermuda; Boston; Chicago; Massachusetts; Illinois and Wisconsin (Dutton, 1889; Bollinger, 1977; Stover and Coffman, 1993).

Extensive studies and research have been conducted on the 1886 earthquake since its occurrence. Until now, it is unclear what the cause of the event was. Some believe that the phenomenon was an instance of an intraplate earthquake, occurring on faults formed during the break-up of Pangaea. It was assumed by Johnston (1996) that the cause of the 1886 earthquake is a rupture along a fault with length and width varied from 20 to 160 km and between 16 and 25 km respectively.

After the 1886 earthquake, 300 aftershocks were noted in that area for a two- and half-year period. The results of a scientific study by the South Carolina Emergency Management Division (EMD) (for details, see EMD, 2012) showed that today an earthquake with similar magnitude and location to the one in 1886 could result a) an estimated of 45,000 victims; b) economic losses would exceed $20 billion and c) about 800 bridges would be damaged.

Moreover, some communities in the Charleston area are reachable by bridge routes only, which may be closed.

This research investigates two study cases for implementing the developed network optimization tool: (1) M7.1 (32.936° N 80.015° W), and (2) M7.3 (32.900° N 80.000° W). The second case simulates the 1886 scenario using the estimated earthquake magnitude and epicenter. The scenario data (earthquake locations and loads) from the Global Legacy Catalog (GLLEGACY) was extracted from the database: United States Geological Survey (USGS) (USGS, 2018). A series of scripts map the USGS data to the developed program for the usability of the tool.

In this project, one goal is to develop a versatile tool that can be used to generate optimized retrofit or monitoring programs. A script was developed to link the tool with the USGS database and SCDOT database (SCDOT, 2018) to model the network and seismic demand. The tool primarily focuses on, but is not limited to, an integer programming problem with two objective functions and the number of variables equivalent to the number of bridges in the transportation network under the study domain, or alternatively those that intersect with the traveling path. The developed tool generates fragility curves for every node of roads and bridges, performs Monte Carlo simulation, and uses Genetic Algorithms (GA) to optimize the network performance based on failure probability, traffic capacity, historical significance, centrality, retrofit cost, and traveling scenario. A Pareto frontier consisting of varying optima was then generated for the decision-making process. The tool can be used by the Department of Transportation for general case optimization

of the transportation network. The Charleston, SC, transportation network was used to demonstrate functionality and versatility of the developed tool.

# CHAPTER 2

## Literature Review

### 2.1 Retrofitting Strategies

This research addresses the need for structurally deficient U.S. bridges, primarily in CSUS, to be monitored or retrofit to anticipate future seismic demands. The first efforts to retrofit bridges affected by seismic events conducted after the 1971 San Fernando earthquake in southern California (FHWA, 2006). Expansion joint restrainers were fixed to limit relative longitudinal movements at expansion joints. This retrofitting method helps to avoid catastrophic failure of the bridge due to loss of support or unseating.

This retrofit strategy, however, was found to cause bridges to experience severe column damage (Wipf et al. 1997), which then increases interest in column retrofitting to increase column stability. Column jacketing helps to alleviate excessive plastic rotation demands in columns.

Another instance of a bridge retrofitting strategy is seismic isolation bearings for reducing the response during an earthquake by increasing the fundamental period of vibration. Seismic isolation bearings are a feasible alternative to rise the resiliency of weak bridges.

The other option for retrofitting is seat extenders, which are attached to the existing face of abutments or capped beams to reduce the likelihood of girder unseating during earthquake events (Wilson and Ryan, 2009). It is one of the retrofitting strategies combined into the optimization variables in this investigation.

Because retrofitting cost can be very expensive, priorities are given to bridges with certain criteria. FHWA uses the severity of the expected damage to assign the rank of retrofit priority (0 to 10) for bridges. However, this method does not address the issue of traffic flow, bridge centrality, and historical significance. In the tool developed, these various retrofitting strategies are the variables to maximize the network performance that includes historical significance, traffic flow, nodal centrality, and expected damage given the seismic load. However, to avoid excessive expenditures in retrofitting cost, priorities need to be assigned according to importance, and cost minimization becomes one of the goals of the optimization process. The same is true for making decisions related to monitoring of bridges.

### 2.2 Damage States

Bridge fragility curves are a means to represent the likelihood of bridges to experience various levels of damage in a probabilistic fashion. Based on FEMA (2005), for bridges, the various levels of damage can be described including: slight, moderate, extensive and complete damages.

## 2.3 Fragility Curves of Bridge Retrofitting Strategies

Prior research has addressed bridge retrofitting methods and related effects on structural capacity, usually represented as fragility CDF curves, showing the probability of damage exceedance as a function of intensity measures. For example, (1) nonlinear dynamic time history analysis was performed by Shinozuka and Kim (2000) to assess the effect of column retrofit on the responses of bridges under sixty ground acceleration time histories, (2) Billah et al. (2013) developed a two-dimensional finite element model subjected to forty earthquake excitations to attain the probability of exceedance, and (3) three-dimensional nonlinear analytical models were developed by Padgett and DesRoches (2009) using an open system for earthquake engineering simulation called the OpenSEES platform, (see Jeremic (2004) for details). The work reported here employs the measures of modification factors in Padgett and DesRoches (2009) for constructing fragility curves due to its rich variation of structural types and retrofitting strategies.

For this investigation retrofitting strategies can be classified into three categories including: (1) do nothing, (2) superstructure retrofit, and (3) superstructure and substructure retrofit. The strategy “do-nothing” involves the damage acceptance during a future earthquake and is related to options for structural monitoring, where information on damage can be rapidly gained but increase in capacity is not addressed. For the superstructure and substructure retrofits, the retrofit strategy from Padgett and DesRoches (2009) was employed.

The superstructure only option includes:

1. Restrainer cables to avoid collapsing of bridge spans.
2. Seat extenders to avoid unseating of bridge spans.

The combined superstructure and substructure option includes:

1. Column steel jacketing to improve shear of flexural strength.
2. Elastomeric isolation bearings to limit the loads transferred to the substructure.
3. Concrete shear keys to limit excessive lateral motion.
4. Restrainers and shear keys.
5. Seat extenders and shear keys.

As described previously, the purpose of seismic retrofitting is to minimize and avoid catastrophic bridge failures by strengthening bridges to resist future earthquakes. The purpose of structural monitoring is to provide information on damage that has occurred, potentially in near real-time, due to a seismic event. This information can be useful for re-routing of traffic and for prioritizing repairs and future retrofits.

For each retrofit strategy described above, the modification factor for the median shift for the fragility curves of the retrofitted bridges is provided in Padgett and DesRoches (2009).

## 2.4 Retrofitting Cost

Prior research has been performed to estimate retrofit costs. Parmelee (2013) relates the replacement cost to the traffic capacity. Chen (2013) estimated replacement cost based on the structural type and material. The retrofit cost for each bridge was estimated using data from the bridge replacement cost model by Chen (2013) and factored by the percent replacement cost based on California Department of Transportation data compiled by the FHWA (see FHWA, 2006). An example of retrofitting cost estimation can also be seen in Parmelee (2013). In general, new construction is less expensive than engineering costs of retrofit design (FHWA 2006). The reason is that special retrofit strategies are required due to uniqueness of many bridges. Moreover, it is difficult to achieve standardization of design and retrofit details.

## 2.5 Non-destructive Evaluation Techniques

Choosing the most appropriate evaluation methodology is based on several factors including type of structure, information about its existing condition, cost, availability, ease of installation, accuracy, and capability for data interpretation. In the United States, visual inspection is primarily used by bridge owners to evaluate the condition of bridges, however this method is inadequate for the identification of hidden defects and damage or in areas that are not easily accessible (Hadzor 2011). Instead, nondestructive evaluation (NDE) techniques have been performed in many industries to assess the condition of a structural component without impairing its future usefulness or causing damage (Cartz 1995).

A promising technology for assessing damage to pile to bent cap connections in the field is remote monitoring with acoustic emission. Acoustic emission is defined ASTM E1316 (ASTM 2014) as “the release of transient stress waves due to a localized release of energy within a structural system”. In the case of bridge members such as piles and bent caps, acoustic emission data is generated by slippage of strands, breaking of wires, corrosion of steel reinforcement, and cracking of concrete. One often cited complication with acoustic emission monitoring is that relatively common environmental factors such as wind-borne debris, rain, hail, and ambient traffic loading may also case acoustic emission data. However, because the signatures of these acoustic emission events are different, pattern recognition can be utilized to minimize data that is not related to structural damage and degradation (Anay et al. 2018, Soltangharaei et al. 2018).

## 2.6 Bridge Monitoring Using Acoustic Emission

On-site load tests of reinforced and prestressed concrete bridges have been performed and documented under regular traffic and overloading while monitoring with AE. Golaski et al. (2002) conducted load tests on five bridges having different types of structures including reinforced and prestressed concrete. They found that AE is the most suitable method for inspection of older bridges. On site AE monitoring was performed for evaluation of a prestressed concrete double-tee beam bridge without plans (Anay et al.

2015). In this case, the AE data showed that damage was more prevalent near the supports than in the midspan. Recently, Takamine et al. (2018) proposed a new method to inspect the condition of bridge decks using AE waves generated by heavy rain. Cracks deep inside reinforced concrete bridge decks were successfully detected by analyzing rain-induced data. Świt (2018) presented the results of AE application for categorizing active destructive processes during the active operation of different types of structures including steel bridges, steel columns supporting a structure for a cable car, gas pipelines and the My Thuan cable-stayed bridge. The recorded AE signals from each field test were divided into classes to which different damage mechanisms based on the structure type were assigned. Based on these and other studies, AE can be employed as a monitoring method for selected bridges from the network to provide useful information of bridge condition before and after an extreme event.

## 2.7 Full Scale Pile-to-Bent Cap Connections

Full scale pile-to-bent cap connections were tested under lateral loading at USC including; a) testing of full-scale interior and exterior bent cap connections (Figure 2.1a), and b) testing of three piles connected to a single bent cap (Figure 2.1b) (Larosche et al., 2014a and 2014b).

(a) interior and exterior bent cap connections (b) three piles connected to a single bent cap

Figure 2.1: Pile cap connection tests
(Larosche et al., 2014a and 2014b)

Through the experimental and numerical investigations, the structural capacity of the pile to bent cap connections for typical South Carolina connection details was addressed (Larosche et al., 2014a and 2014b, Larosche et al. 2015). One finding of the project was that the exterior bent details had limited structural capacity prior to the redesign of this connection, leading to a redesigned connection subsequently tested at full-scale (Figure 2.1). The results of this experiment were combined into the analyses explained in this report to enhance the resolution of the network models, both with the initial and re-designed conditions.

# CHAPTER 3

## Modeling of the Network and Seismic Demand

### 3.1 Modeling the Network

To make the tool adaptive to cases other than the one used in this research , i.e., the Charleston network, the modeling is very important. Essentially, the network and seismic load modeling portion was conducted by creating an algorithm that can read and filter information from databases that have varying syntax and be able to extract the information needed for the analysis and optimization. For the network modeling, geospatial vector data from SCDOT was translated into graphical representations of the networks under both the geographic coordinate system and the Universal Transverse Mercator system (UTM). Figure 3.1 shows the geographical coordinate of the bridges and roads based on the SCDOT database and NBI. To select the bridges that fell under major highways, the developed program incorporated an adjustable parameter for ADT target. In this study case, the ADT target was set to be 5,000 vehicles/day, which means that bridges with ADT lower than that were not included in the study domain. The program automatically increases the number of bridges to be under the study domain if the ADT target parameter is adjusted by the potential users. In this case, 44 bridges fell under the study domain.

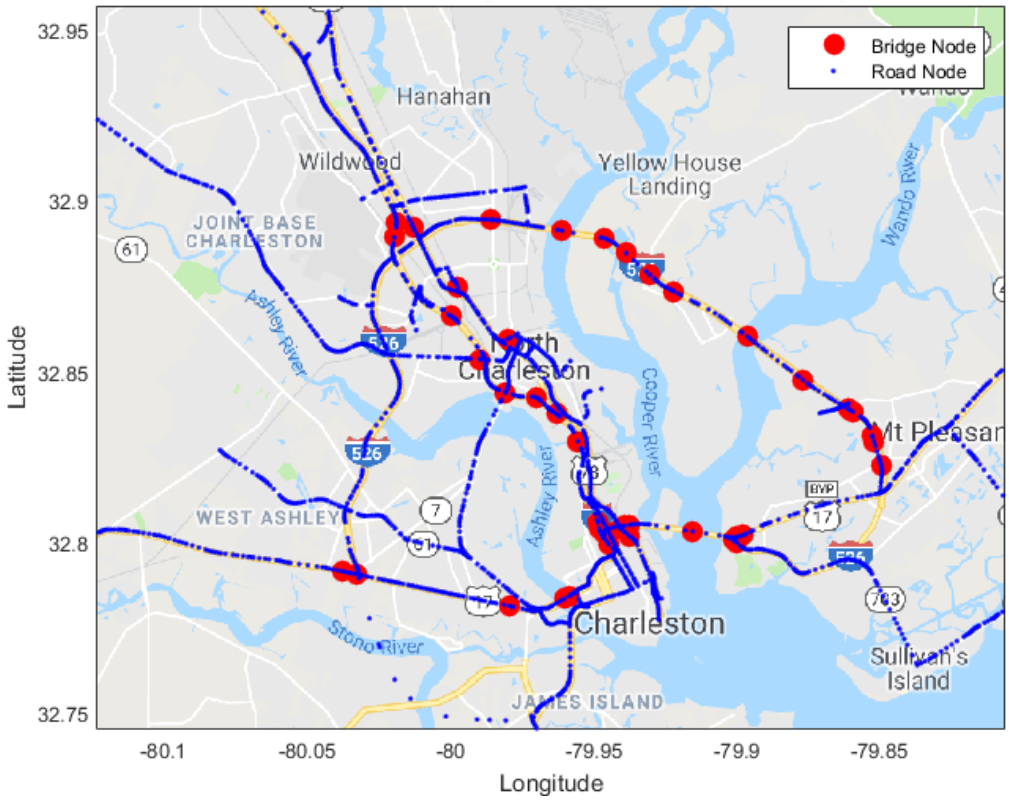


Figure 3.1: Charleston map in geographical coordinates

## 3.2 Modeling the Seismic Demand

There were two earthquake scenarios observed for the study case in this research: (1) M7.1 (32.936° N 80.015° W), and (2) M7.3 (32.900° N 80.000° W) (see Figures 3.2 and 3.3). For attaining the magnitude of the nodal seismic demand, XML's grid for the Peak Ground Acceleration (PGA) and Spectral Acceleration (Sa) at 0.3, 1.0, and 3.0 seconds from USGS was employed and coupled with the nearest neighbor search algorithm with respect to the modeled geospatial vector data. Lastly, a USGS's JSON text was translated into seismic contour graphical representation.

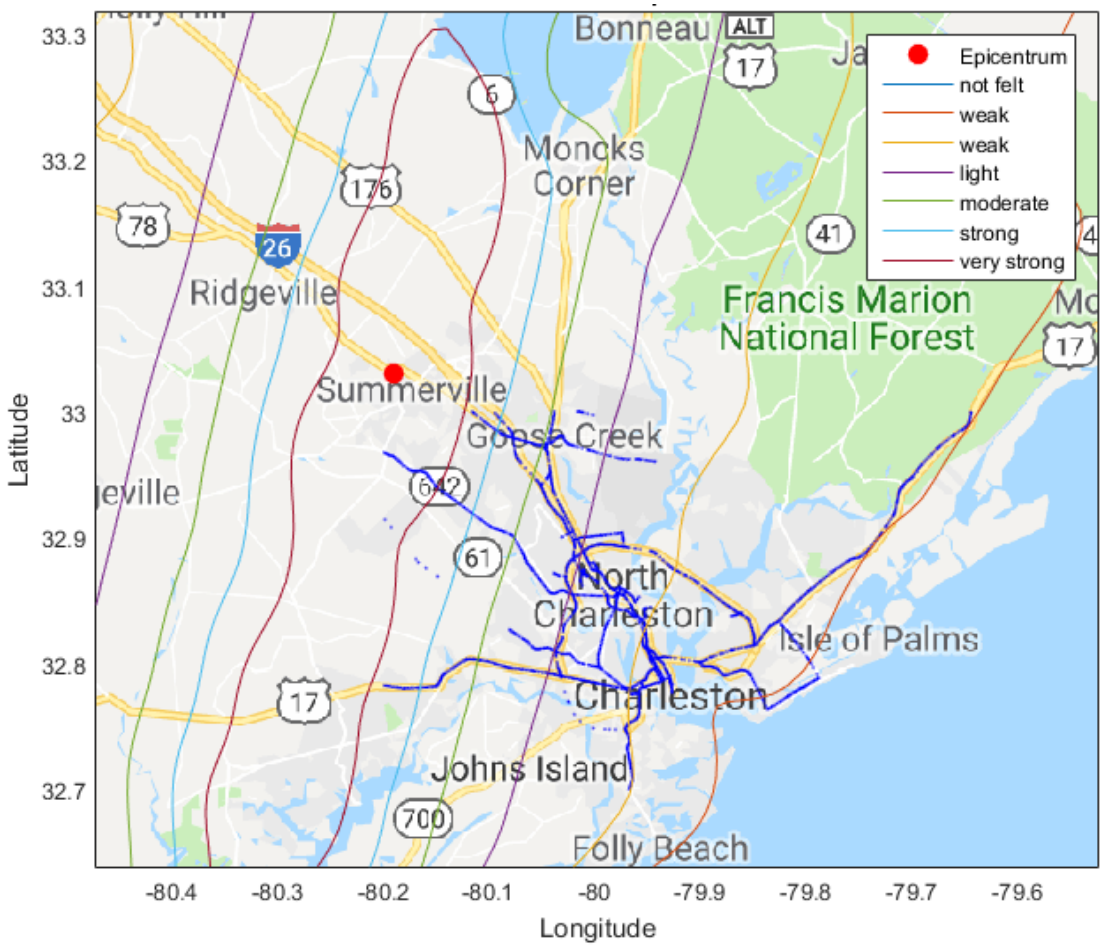


Figure 3.2: Matlab plot of seismic contour scenario M7.1 (32.936°N 80.015°W, depth 20.1 km) in geographical coordinates

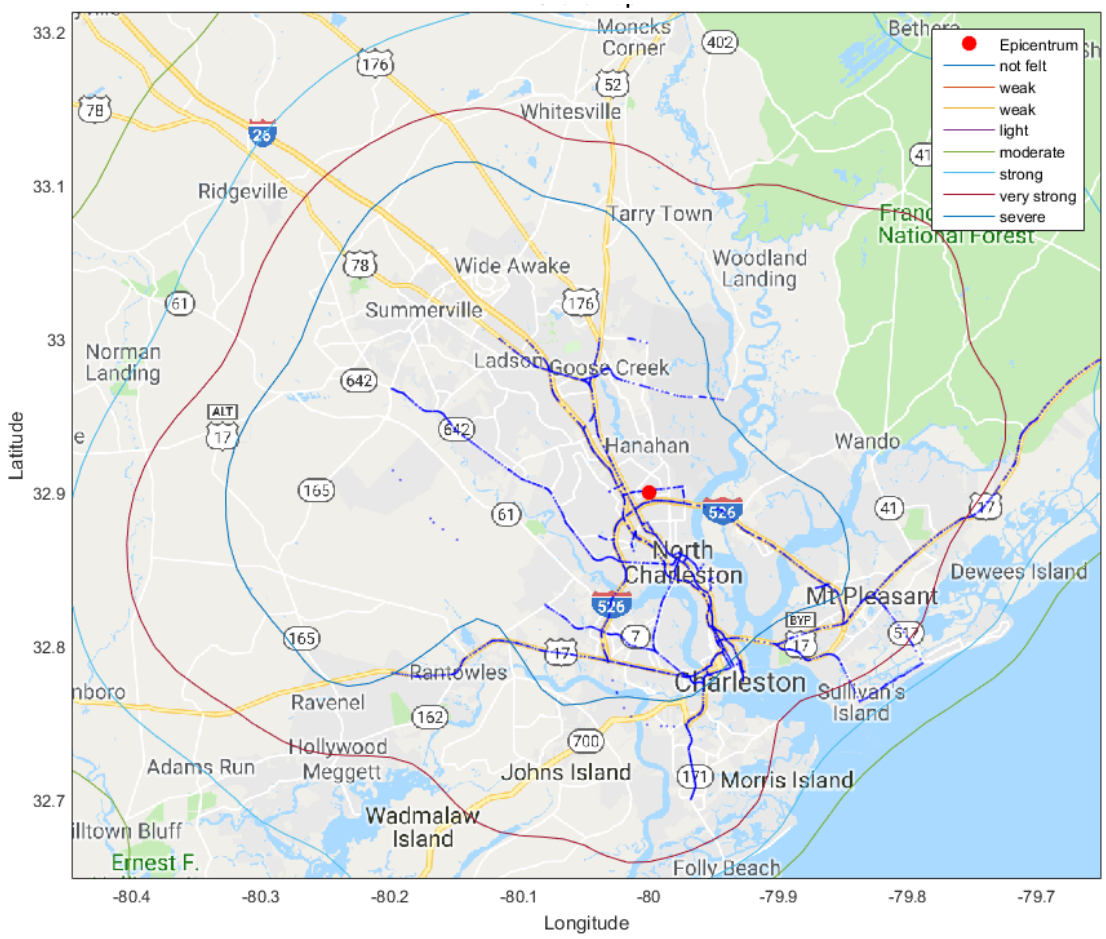


Figure 3.3: Matlab plot of seismic contour scenario M7.3 (32.900°N 80.000°W, depth 10.1 km) in geographical coordinates

Note that the perceived shaking from the USGS is based on Table 3.1.

Table 3.1: USGS perceived shaking and the equivalent peak acceleration (after USGS, 2018)

| Perceived Shaking | Peak Acceleration (g) |
|---|---|
| Not felt | < 0.00007 |
| Weak | 0.0008 |
| Light | 0.01 |
| Moderate | 0.05 |
| Strong | 0.088 |
| Very strong | 0.15 |
| Severe | 0.27 |
| Violent | 0.47 |
| Extreme | > 0.83 |

## 3.3 Incorporating NBI and Hazus Database

In the current state of the practice, the structural capacity of bridges with respect to seismic events is primarily based on the materiality, structural type, number of spans, and skew angles. The materiality and structural type in NBI are codified into digits that represent the material (predominantly concrete and steel) and structural system (box beams, frame, truss, etc.) employed in the bridge. Common bridge structural types in the NBI database have a direct correspondence to the bridge structural classification in the Hazus database, denoted as HWB. Unusual cases such as stayed girder structural systems are not provided in Hazus. Assumptions were made for these unusual cases. The nominal value of this structural capacity was factored to change the standard bridge fragility curves to a bridge-specific value for a given spectral acceleration. These were done through developing sets of routines that compute the $K_{3D}$ and $K_{skew}$ using NBI's data to account for number of spans, bridge skew angle, and spectra acceleration period (Table 3.2).

Table 3.2: The coefficient for evaluating $K_{3D}$
(after FEMA, 2013)

| Equation | A | B | K3D |
|---|---|---|---|
| 1 | 0.25 | 1 | 1+0.25/(N-1) |
| 2 | 0.33 | 0 | 1+0.33/N |
| 3 | 0.33 | 1 | 1+0.33/(N-1) |
| 4 | 0.09 | 1 | 1+0.09/(N-1) |
| 5 | 0.05 | 0 | 1+0.05/N |
| 6 | 0.20 | 1 | 1+0.2/(N-1) |
| 7 | 0.10 | 0 | 1+0.1/N |

Lines of scripts were then included in the development tool to map the structural type between the two databases. Once successfully mapped into Hazus each bridge had unique fragility curves that include four damage states at Sa (T = 1s).

Tables 3.3 and 3.4 show the NBI information extracted using the script within the tool. The translated structural category (HWB) in HAZUS was also included corresponding to the NBI data. The spectral acceleration for every bridge was also included.

## Table 3.3: NBI – HAZUS extracted and translated information with seismic demand (scenario M7.1)

| Database | NBI | | | | | | | | | Road | HAZUS | USGS |
|---|---|---|---|---|---|---|---|---|---|---|---|---|
| Index | StructNumber | YearBuilt | StructLength | DeckWidth | Material | StructType | Latitude | Longitude | ADT | ID | HWB | Sa (g) |
| 7857 | 8516 | 1992 | 5015.8 | 28.4 | 4 | 10 | 32531800 | 79574200 | 64400 | 10 | 16 | 0.369 |
| 7429 | 8062 | 1987 | 228.6 | 19.8 | 2 | 1 | 32525400 | 79565400 | 32200 | 13 | 10 | 0.328 |
| 7428 | 8061 | 1987 | 228.6 | 19.8 | 2 | 1 | 32525400 | 79563000 | 32200 | 20 | 10 | 0.336 |
| 7586 | 8227 | 1989 | 118.9 | 15.7 | 2 | 1 | 32524800 | 79554200 | 25800 | 27 | 10 | 0.317 |
| 7496 | 8134 | 1988 | 396.2 | 14.5 | 5 | 2 | 32522400 | 79551800 | 25800 | 40 | 17 | 0.305 |
| 7593 | 8235 | 1989 | 2407.9 | 14.4 | 6 | 21 | 32513600 | 79534800 | 26500 | 58 | 28 | 0.281 |
| 3914 | 4266 | 1964 | 70.7 | 45.7 | 3 | 2 | 32533600 | 80011200 | 66700 | 375 | 12 | 0.406 |
| 3915 | 4267 | 1964 | 97.5 | 45.7 | 3 | 2 | 32532400 | 80010600 | 66700 | 382 | 12 | 0.406 |
| 3708 | 4050 | 1963 | 252.4 | 28.3 | 3 | 2 | 32515400 | 80000000 | 87200 | 425 | 12 | 0.383 |
| 3917 | 4269 | 1964 | 100.6 | 30.2 | 3 | 2 | 32503000 | 79581200 | 84000 | 489 | 12 | 0.339 |
| 4341 | 4720 | 1966 | 237.4 | 30.2 | 3 | 2 | 32501200 | 79574800 | 83300 | 507 | 12 | 0.342 |
| 4556 | 4945 | 1967 | 527.6 | 30.2 | 3 | 2 | 32494200 | 79571800 | 83300 | 519 | 12 | 0.342 |
| 9119 | 9826 | 2005 | 1230.8 | 11.8 | 4 | 2 | 32481800 | 79565400 | 9100 | 580 | 16 | 0.307 |
| 9120 | 9827 | 2005 | 376.1 | 9.4 | 4 | 2 | 32481500 | 79565200 | 9300 | 581 | 16 | 0.307 |
| 9125 | 9832 | 2005 | 931.2 | 11.8 | 4 | 2 | 32475750 | 79564220 | 37750 | 594 | 16 | 0.308 |
| 7860 | 8519 | 1992 | 3235.5 | 15.5 | 4 | 2 | 32533600 | 79591200 | 39850 | 809 | 16 | 0.373 |
| 7500 | 8138 | 1988 | 91.4 | 14.8 | 1 | 1 | 32505400 | 79523600 | 26500 | 854 | 5 | 0.263 |
| 7677 | 8325 | 1990 | 75.3 | 16.8 | 3 | 2 | 32501800 | 79514200 | 26500 | 875 | 14 | 0.289 |
| 7678 | 8326 | 1990 | 64 | 14.3 | 2 | 1 | 32501200 | 79514200 | 22300 | 876 | 11 | 0.289 |
| 7682 | 8330 | 1990 | 64 | 14.3 | 1 | 1 | 32501200 | 79513600 | 22300 | 878 | 7 | 0.289 |
| 6841 | 7429 | 1981 | 117.3 | 14.6 | 2 | 1 | 32494800 | 79511800 | 22300 | 901 | 10 | 0.277 |
| 6842 | 7430 | 1981 | 42.1 | 14.3 | 3 | 2 | 32494200 | 79511800 | 22300 | 903 | 12 | 0.29 |
| 7765 | 8419 | 1991 | 49.1 | 20.2 | 6 | 2 | 32491800 | 79510600 | 22300 | 914 | 23 | 0.29 |
| 8974 | 9648 | 1982 | 11 | 45.7 | 1 | 19 | 32473600 | 80021800 | 40500 | 1107 | 28 | 0.399 |
| 8728 | 9402 | 1999 | 225.9 | 17.1 | 5 | 2 | 32472400 | 80020000 | 26300 | 1112 | 19 | 0.386 |
| 6517 | 7074 | 1978 | 178.9 | 10.2 | 3 | 2 | 32463600 | 79584800 | 10400 | 1181 | 12 | 0.337 |
| 166 | 228 | 1926 | 528.2 | 13.1 | 3 | 16 | 32470000 | 79573600 | 28200 | 1218 | 28 | 0.216 |
| 8467 | 9137 | 1997 | 274.9 | 16.9 | 4 | 2 | 32470000 | 79573000 | 28200 | 1219 | 16 | 0.216 |
| 9118 | 9825 | 2005 | 283.2 | 11.8 | 4 | 2 | 32480800 | 79564800 | 37750 | 1292 | 16 | 0.307 |
| 4827 | 5231 | 1968 | 1884.9 | 30.5 | 3 | 2 | 32481200 | 79564800 | 83300 | 1296 | 12 | 0.307 |
| 9131 | 9838 | 2005 | 243.2 | 9.4 | 6 | 2 | 32481770 | 79562000 | 7500 | 1315 | 23 | 0.307 |
| 9116 | 9823 | 2005 | 331 | 35.7 | 6 | 2 | 32481700 | 79561300 | 75500 | 1316 | 23 | 0.307 |
| 9117 | 9824 | 2005 | 2967.8 | 39.3 | 4 | 14 | 32480950 | 79545460 | 75500 | 1329 | 28 | 0.168 |
| 9130 | 9837 | 2005 | 499.9 | 11.8 | 6 | 2 | 32480500 | 79540060 | 21200 | 1340 | 23 | 0.261 |
| 9129 | 9836 | 2005 | 36.6 | 9.4 | 6 | 2 | 32480680 | 79535390 | 6000 | 1343 | 23 | 0.213 |
| 4111 | 4477 | 1965 | 13.7 | 18.7 | 1 | 1 | 32533600 | 80004200 | 25000 | 1932 | 28 | 0.406 |
| 5038 | 5478 | 2005 | 649.8 | 13.2 | 4 | 2 | 32480970 | 79561240 | 6700 | 2114 | 16 | 0.307 |
| 9115 | 9822 | 2005 | 676 | 21 | 6 | 2 | 32481500 | 79562600 | 75500 | 2121 | 23 | 0.307 |
| 3916 | 4268 | 1964 | 143 | 35.8 | 3 | 2 | 32503600 | 79585400 | 88700 | 2303 | 12 | 0.345 |
| 3282 | 3606 | 1961 | 67.1 | 28.3 | 3 | 2 | 32511200 | 79592400 | 87200 | 3053 | 12 | 0.345 |
| 9128 | 9835 | 2005 | 246.9 | 11.8 | 6 | 2 | 32480320 | 79540440 | 37750 | 3092 | 23 | 0.261 |
| 9123 | 9830 | 2005 | 388.6 | 11.8 | 4 | 2 | 32480000 | 79535800 | 75500 | 3096 | 16 | 0.261 |
| 7596 | 8238 | 1989 | 2407.9 | 14.4 | 6 | 21 | 32513000 | 79584800 | 26500 | 3460 | 28 | 0.368 |
| 607 | 714 | 1936 | 68.6 | 29.9 | 3 | 2 | 32523000 | 79594800 | 16300 | 3759 | 12 | 0.386 |

## Table 3.4: NBI – HAZUS extracted and translated information with seismic demand (scenario M7.3)

| Database | NBI | | | | | | | | | Road | HAZUS | USGS |
|---|---|---|---|---|---|---|---|---|---|---|---|---|
| Index | StructNumber | YearBuilt | StructLength | DeckWidth | Material | StructType | Latitude | Longitude | ADT | ID | HWB | Sa (g) |
| 7857 | 8516 | 1992 | 5015.8 | 28.4 | 4 | 10 | 32531800 | 79574200 | 64400 | 10 | 16 | 0.96 |
| 7429 | 8062 | 1987 | 228.6 | 19.8 | 2 | 1 | 32525400 | 79565400 | 32200 | 13 | 10 | 0.836 |
| 7428 | 8061 | 1987 | 228.6 | 19.8 | 2 | 1 | 32525400 | 79563000 | 32200 | 20 | 10 | 0.852 |
| 7586 | 8227 | 1989 | 118.9 | 15.7 | 2 | 1 | 32524800 | 79554200 | 25800 | 27 | 10 | 0.852 |
| 7496 | 8134 | 1988 | 396.2 | 14.5 | 5 | 2 | 32522400 | 79551800 | 25800 | 40 | 17 | 0.948 |
| 7593 | 8235 | 1989 | 2407.9 | 14.4 | 6 | 21 | 32513600 | 79534800 | 26500 | 58 | 28 | 0.818 |
| 3914 | 4266 | 1964 | 70.7 | 45.7 | 3 | 2 | 32533600 | 80011200 | 66700 | 375 | 12 | 0.859 |
| 3915 | 4267 | 1964 | 97.5 | 45.7 | 3 | 2 | 32532400 | 80010600 | 66700 | 382 | 12 | 0.845 |
| 3708 | 4050 | 1963 | 252.4 | 28.3 | 3 | 2 | 32515400 | 80000000 | 87200 | 425 | 12 | 0.839 |
| 3917 | 4269 | 1964 | 100.6 | 30.2 | 3 | 2 | 32503000 | 79581200 | 84000 | 489 | 12 | 0.956 |
| 4341 | 4720 | 1966 | 237.4 | 30.2 | 3 | 2 | 32501200 | 79574800 | 83300 | 507 | 12 | 0.826 |
| 4556 | 4945 | 1967 | 527.6 | 30.2 | 3 | 2 | 32494200 | 79571800 | 83300 | 519 | 12 | 0.948 |
| 9119 | 9826 | 2005 | 1230.8 | 11.8 | 4 | 2 | 32481800 | 79565400 | 9100 | 580 | 16 | 0.807 |
| 9120 | 9827 | 2005 | 376.1 | 9.4 | 4 | 2 | 32481500 | 79565200 | 9300 | 581 | 16 | 0.807 |
| 9125 | 9832 | 2005 | 931.2 | 11.8 | 4 | 2 | 32475750 | 79564220 | 37750 | 594 | 16 | 0.807 |
| 7860 | 8519 | 1992 | 3235.5 | 15.5 | 4 | 2 | 32533600 | 79591200 | 39850 | 809 | 16 | 0.757 |
| 7500 | 8138 | 1988 | 91.4 | 14.8 | 1 | 1 | 32505400 | 79523600 | 26500 | 854 | 5 | 0.72 |
| 7677 | 8325 | 1990 | 75.3 | 16.8 | 3 | 2 | 32501800 | 79514200 | 26500 | 875 | 14 | 0.916 |
| 7678 | 8326 | 1990 | 64 | 14.3 | 2 | 1 | 32501200 | 79514200 | 22300 | 876 | 11 | 0.916 |
| 7682 | 8330 | 1990 | 64 | 14.3 | 1 | 1 | 32501200 | 79513600 | 22300 | 878 | 7 | 0.916 |
| 6841 | 7429 | 1981 | 117.3 | 14.6 | 2 | 1 | 32494800 | 79511800 | 22300 | 901 | 10 | 0.784 |
| 6842 | 7430 | 1981 | 42.1 | 14.3 | 3 | 2 | 32494200 | 79511800 | 22300 | 903 | 12 | 0.784 |
| 7765 | 8419 | 1991 | 49.1 | 20.2 | 6 | 2 | 32491800 | 79510600 | 22300 | 914 | 23 | 0.777 |
| 8974 | 9648 | 1982 | 11 | 45.7 | 1 | 19 | 32473600 | 80021800 | 40500 | 1107 | 28 | 0.8 |
| 8728 | 9402 | 1999 | 225.9 | 17.1 | 5 | 2 | 32472400 | 80020000 | 26300 | 1112 | 19 | 0.8 |
| 6517 | 7074 | 1978 | 178.9 | 10.2 | 3 | 2 | 32463600 | 79584800 | 10400 | 1181 | 12 | 0.801 |
| 166 | 228 | 1926 | 528.2 | 13.1 | 3 | 16 | 32470000 | 79573600 | 28200 | 1218 | 28 | 0.926 |
| 8467 | 9137 | 1997 | 274.9 | 16.9 | 4 | 2 | 32470000 | 79573000 | 28200 | 1219 | 16 | 0.926 |
| 9118 | 9825 | 2005 | 283.2 | 11.8 | 4 | 2 | 32480800 | 79564800 | 37750 | 1292 | 16 | 0.807 |
| 4827 | 5231 | 1968 | 1884.9 | 30.5 | 3 | 2 | 32481200 | 79564800 | 83300 | 1296 | 12 | 0.807 |
| 9131 | 9838 | 2005 | 243.2 | 9.4 | 6 | 2 | 32481770 | 79562000 | 7500 | 1315 | 23 | 0.93 |
| 9116 | 9823 | 2005 | 331 | 35.7 | 6 | 2 | 32481700 | 79561300 | 75500 | 1316 | 23 | 0.93 |
| 9117 | 9824 | 2005 | 2967.8 | 39.3 | 4 | 14 | 32480950 | 79545460 | 75500 | 1329 | 28 | 0.924 |
| 9130 | 9837 | 2005 | 499.9 | 11.8 | 6 | 2 | 32480500 | 79540060 | 21200 | 1340 | 23 | 0.708 |
| 9129 | 9836 | 2005 | 36.6 | 9.4 | 6 | 2 | 32480680 | 79535390 | 6000 | 1343 | 23 | 0.708 |
| 4111 | 4477 | 1965 | 13.7 | 18.7 | 1 | 1 | 32533600 | 80004200 | 25000 | 1932 | 28 | 0.859 |
| 5038 | 5478 | 2005 | 649.8 | 13.2 | 4 | 2 | 32480970 | 79561240 | 6700 | 2114 | 16 | 0.93 |
| 9115 | 9822 | 2005 | 676 | 21 | 6 | 2 | 32481500 | 79562600 | 75500 | 2121 | 23 | 0.93 |
| 3916 | 4268 | 1964 | 143 | 35.8 | 3 | 2 | 32503600 | 79585400 | 88700 | 2303 | 12 | 0.745 |
| 3282 | 3606 | 1961 | 67.1 | 28.3 | 3 | 2 | 32511200 | 79592400 | 87200 | 3053 | 12 | 0.745 |
| 9128 | 9835 | 2005 | 246.9 | 11.8 | 6 | 2 | 32480320 | 79540440 | 37750 | 3092 | 23 | 0.708 |
| 9123 | 9830 | 2005 | 388.6 | 11.8 | 4 | 2 | 32480000 | 79535800 | 75500 | 3096 | 16 | 0.708 |
| 7596 | 8238 | 1989 | 2407.9 | 14.4 | 6 | 21 | 32513000 | 79584800 | 26500 | 3460 | 28 | 0.749 |
| 607 | 714 | 1936 | 68.6 | 29.9 | 3 | 2 | 32523000 | 79594800 | 16300 | 3759 | 12 | 0.839 |

# CHAPTER 4

# Monitoring Systems

## 4.1 Deployment of SHM System on a Bridge

Online monitoring systems provide remote internet connected services for daily summary reports and statistical data to observe the integrity and health of structures. Furthermore, online monitoring systems commonly provide alarm status information, parametric, and environmental data. One available online monitoring system is the Sensor Highway II data acquisition system from Physical Acoustics (Physical Acoustics, 2018) and this was employed in this portion of the investigation (Figure 4.1). It is designed for outside use and prepared with a weatherproof enclosure. Different types of sensors including AE, vibration, and strain are compatible with this system.

Other than the readily provided data for the bridges from NBI, additional data for the bridges within the case study domain was acquired to better understand the connection between acoustic emission data and ambient traffic loading. A video camera system was deployed during monitoring of a bridge in the Columbia, South Carolina area in combination with AE data (US-21, Wilson Blvd. over I-20 bridge). Classification approaches were utilized to guide the data assessment. Figure 4.2 shows the setup for vehicle vs. AE data recording. AE sensors were attached on the bridge deck and the interior girders. A video camera with high-resolution of 5 MP was employed to record the video.

Figure 4.1: Sensor Highway II – data acquisition system

(a) remote AE system

(b) AE sensors

(c) high resolution video camera

Figure 4.2: Vehicle vs. AE data recording setup

## 4.2 AE Data Activity

Figure 4.3 shows AE signal amplitude versus time and vehicular type passing over the bridge. Different AE activities, in terms of amplitude distributions and number of hits, were observed when different loads were applied, indicating the potential for this type of data to discriminate between different ambient events as well as events caused by activities not related to vehicular loading, such as seismic events.

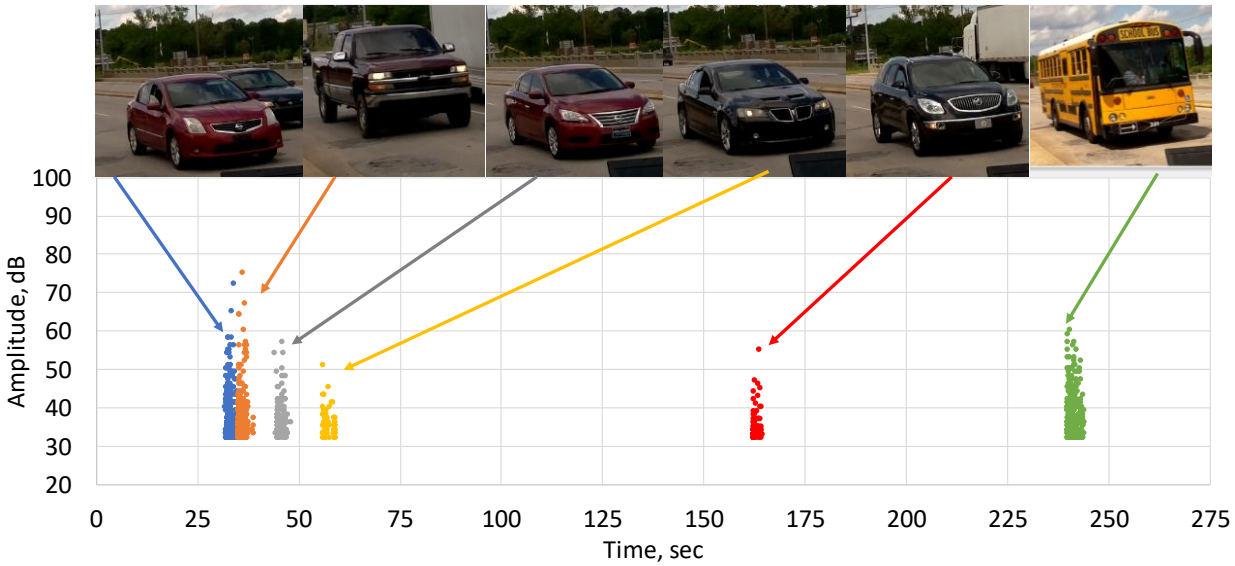


Figure 4.3: AE data caused by vehicular loading

# CHAPTER 5

## Fragility Curves

### 5.1 Hazus Fragility Curves

The construction of fragility curves for each bridge is based on the material structural type of that specific bridge. HAZUS's fragility curves assume the period of 1 second. $\xi_s$ is the median shift modification factor from (Padgett and DesRoches, 2009). The capacity curves were modeled based on the lognormal CDF curves. Let $S$ be a set of 8 retrofit strategies, N is the set of indices of the 4 damage state exceedance, and I is the set of indices for the bridges. The CDF equation for the bridges with retrofitting strategies, exceeding damage state N, is as follows:

$$F_n\left(D_{N_{i,s}} \geq D_n\right) = \Phi[z]_{i,s\,,D_n} = \int_{-\infty}^{z} \frac{1}{\sqrt{2\pi}}\, e^{[-0.5z^2]} dz \tag{5.1}$$

where,

$$s \in S, i \in I, n \in N.\ \mu_{Y_{i,s\,,D_n}} = \xi_{s_i} \mu_{Y_{i\,,D_n}} \tag{5.2}$$

$$Z = \frac{\ln(Sa_i) - \alpha_i \mu_{Y_{i,s,D_n}}}{\sigma_{Y_i}}\ , \tag{5.3}$$

$$, \mu_{Y_{i,D_n}} = \ln(M_{d_{i,D_n}}) \tag{5.4}$$

$D_n$: damage state, where n = 1: slight, n = 2: moderate, n = 3: extensive, and n = 4: complete.

$Sa_i$: Spectra acceleration for bridge i

$M_{d_{i\,,D_n}}$: Median spectra acceleration of natural period 1 second based on HAZUS structural type

The fragility curves were plotted in Matlab as shown below in Figure 5.1.

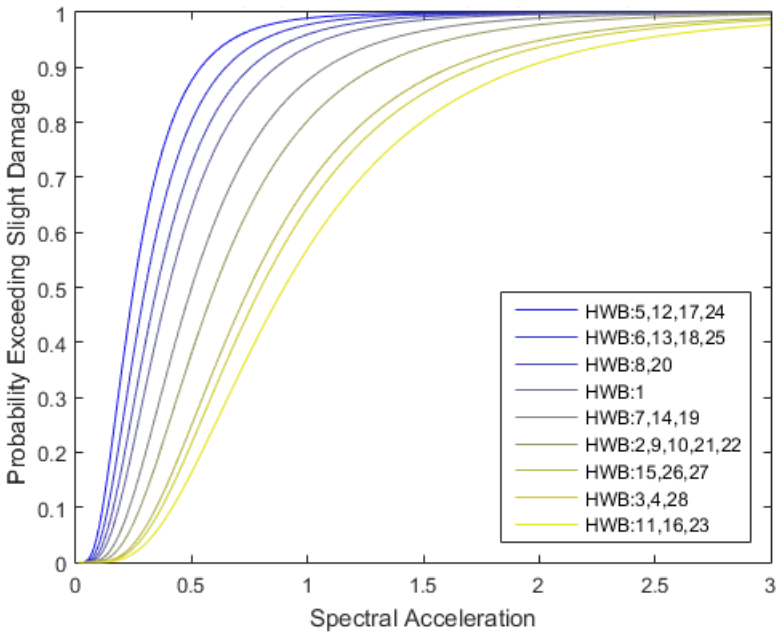


(a) exceeding slight damage

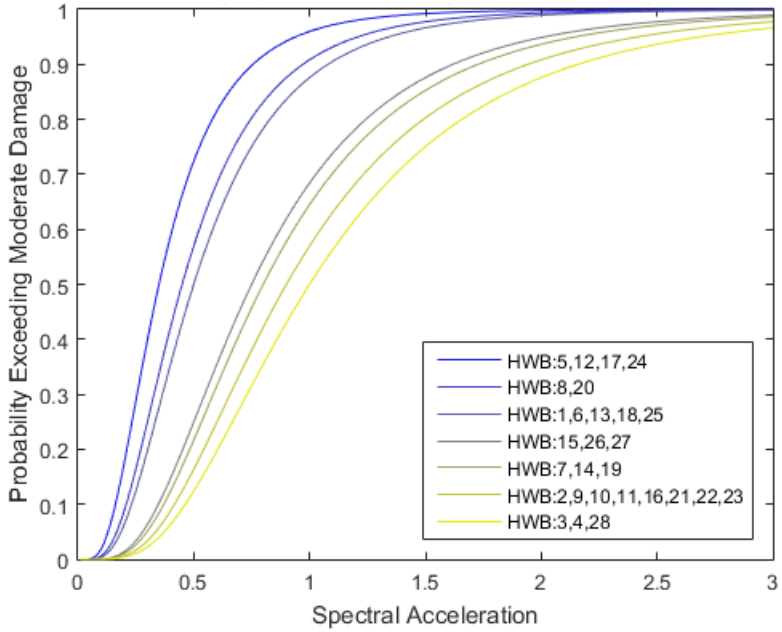


(b) exceeding moderate damage

Figure 5.1: Plots of HAZUS fragility curves

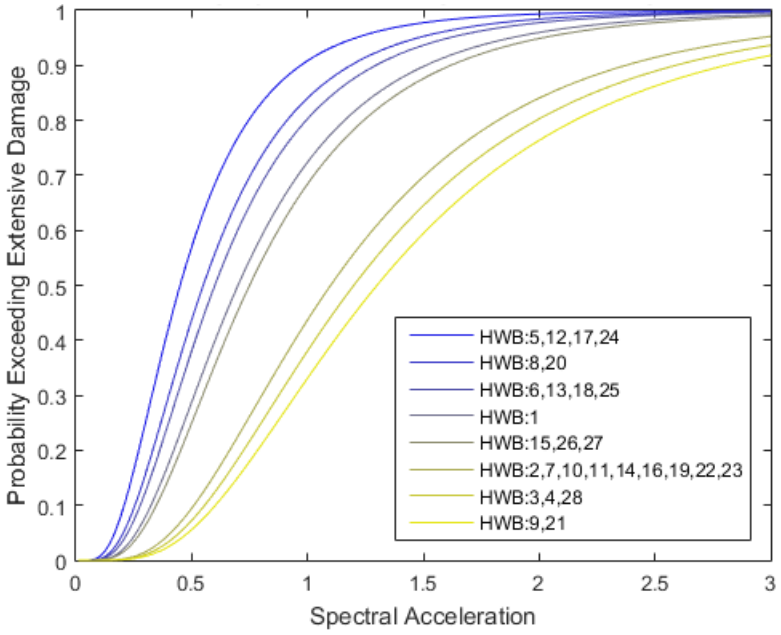


(c) exceeding extensive damage

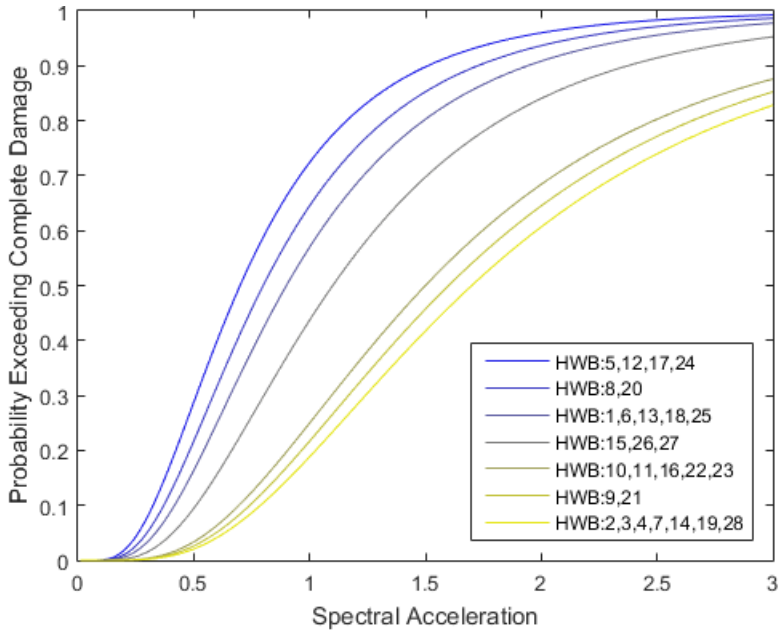


(d) exceeding complete damage

Figure 5.1: Plots of HAZUS fragility curves

## 5.2 Bridge Specific Fragility Curves

To convert the general HAZUS fragility curves into bridge specific fragility curves the equations and values in Table 3.2, adapted from FEMA (2013), are used along with the equations below:

$$\alpha_i = K_{skew_i} K_{3D_i} \text{ for } n \in N, i \in I \tag{5.5}$$

where,

$$K_{skew} = \sqrt{\sin(90 - \alpha)} \tag{5.6}$$

$$K_{3D} = 1 + A/(N - B) \tag{5.7}$$

The constants A and B are based on Table 3.2. To account for the effects of retrofitting, median shift modification factors from Padgett and DesRoches (2009) are used as the modification factor for the value of bridge-specific median. Figure 5.2 shows the fragility curve for an arbitrarily selected bridge (bridge NBI structural number 4477).

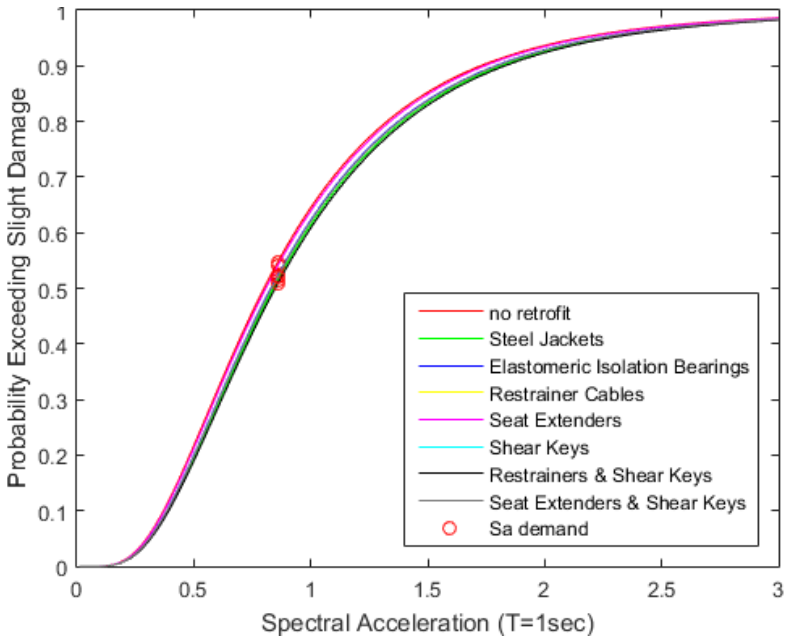


(a) exceeding slight damage

Figure 5.2: Example of fragility plots with and without retrofitting for bridge NBI structural number 4477 under event M7.3

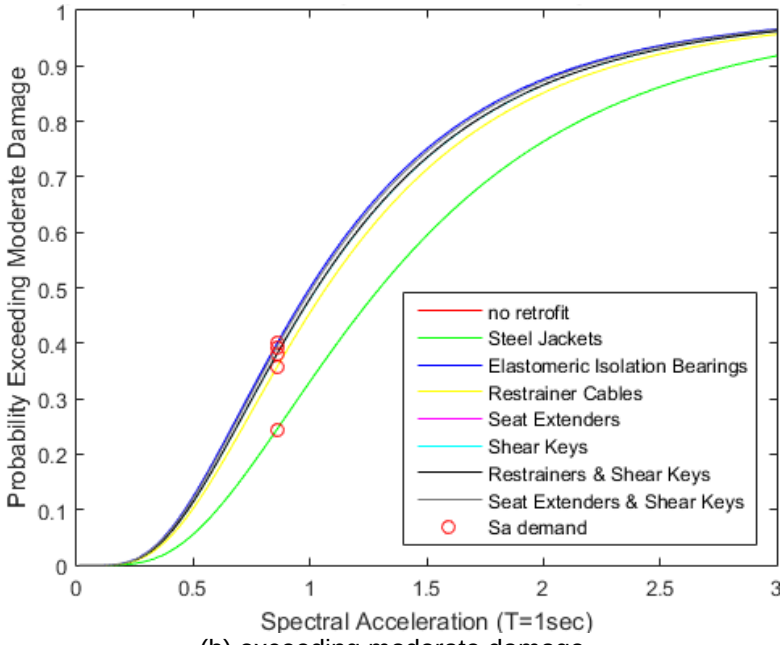


(b) exceeding moderate damage

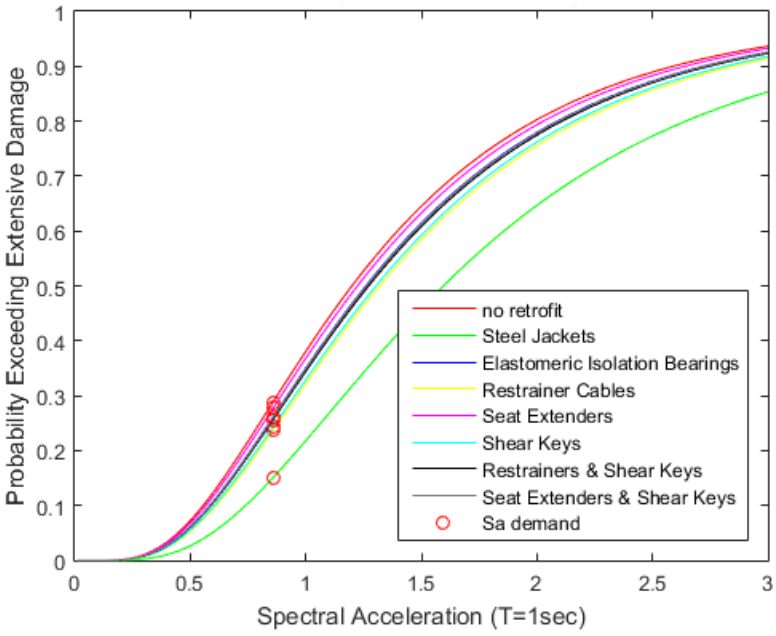


(c) exceeding extensive damage

Figure 5.2: Example of fragility plots with and without retrofitting for bridge NBI structural number 4477 under event M7.3

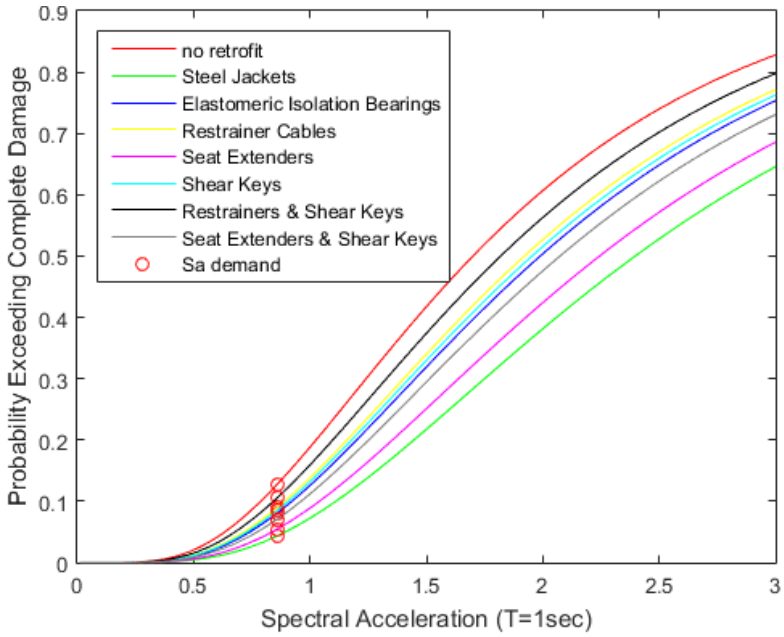


(d) exceeding complete damage

Figure 5.2: Example of fragility plots with and without retrofitting for bridge NBI structural number 4477 under event M7.3

From Table 3.4, the extracted information for bridge NBI structural number 4477 (Figure 5.3) under event M7.3 is shown in Table 5.1. An example of retrofitting strategy versus the probability of exceeding a damaged state for NBI structural number 4477 under event M7.3 is shown in Table 5.2.

Table 5.1: Data for bridge NBI structural number 4477 under event M7.3

| Database | NBI | | | | | | | | | Road | HAZUS | USGS |
|---|---|---|---|---|---|---|---|---|---|---|---|---|
| Index | StructNumber | YearBuilt | StructLength | DeckWidth | Material | StructType | Latitude | Longitude | ADT | ID | HWB | Sa (g) |
| 4111 | 4477 | 1965 | 13.7 | 18.7 | 1 | 1 | 32533600 | 80004200 | 25000 | 1932 | 28 | 0.859 |

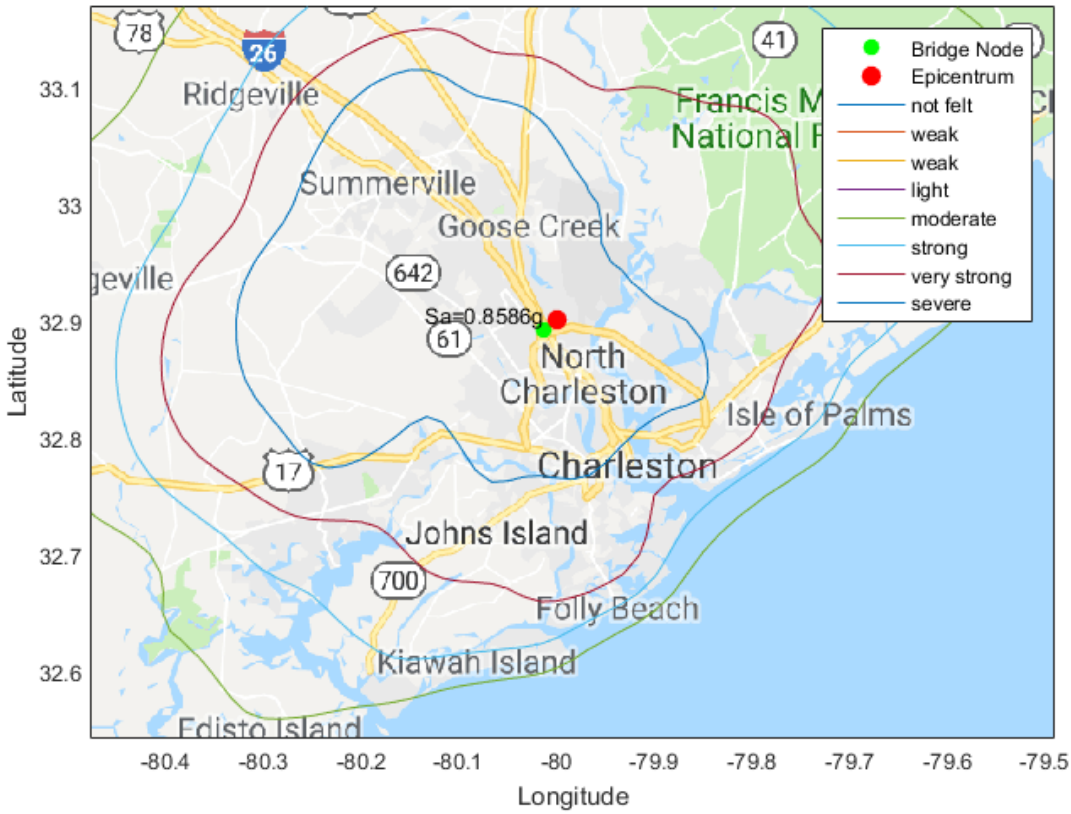


Figure 5.3: Geographical location of bridge 4477 and plot of seismic contour for event M7.3

Table 5.2: Example of retrofitting strategy vs. the probability of exceeding a damaged state for NBI structural number 4477 under event M7.3

| | The probability of exceeding a damaged state | | | |
|---|---|---|---|---|
| Strategy | slight | moderate | extensive | complete |
| 1 | 0.5469 | 0.3997 | 0.2884 | 0.1275 |
| 2 | 0.5146 | 0.2447 | 0.1507 | 0.0435 |
| 3 | 0.523 | 0.3997 | 0.2613 | 0.0807 |
| 4 | 0.5403 | 0.3569 | 0.2367 | 0.0898 |
| 5 | 0.5403 | 0.3808 | 0.2773 | 0.0547 |
| 6 | 0.5209 | 0.3802 | 0.2429 | 0.0853 |
| 7 | 0.5083 | 0.3808 | 0.2562 | 0.1054 |
| 8 | 0.5209 | 0.3933 | 0.26 | 0.0708 |

Since the developed tool was made to be versatile, the study domain can be broadened by simply configuring the boundary setups in the latitude and longitude inputs. In this case, there are 44 bridges under the study domain. In the later section, for the optimization, the values from those matrices will be connected to the developed Genetic Algorithm as design variables to estimate the failure probability of each bridge in each iteration.

## 5.3 Bent Capacity and Demand of Selected Bridges

### 5.3.1 Behavior of Pile to Bent Cap Connections under Seismic Forces

In addition to the failure probability approximated from fragility curves, experiments carried out at USC were utilized to better identify the probability of pile-to-bent cap connections. The ultimate lateral force capacity measured for the interior specimen (18 in. embedment) was 15 kips (Figure 5.4), and for the case of 2 in and 18 in embedment exterior specimen capacity was 5 kips and 7 kips, respectively (Figure 5.5).

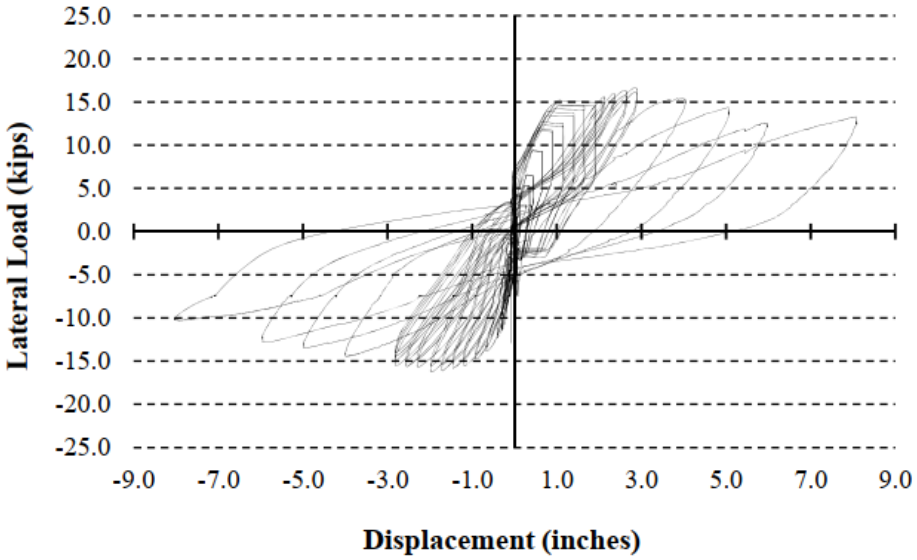


Figure 5.4: Lateral Force versus Displacement - Interior specimen (18 in embedment length) (Ziehl et al. 2012)

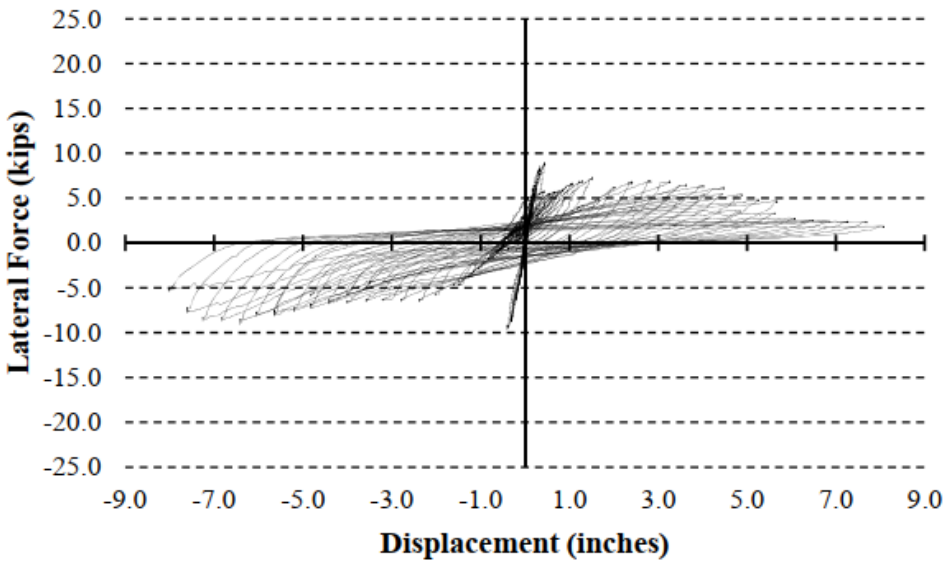


(a) 18 in embedment length

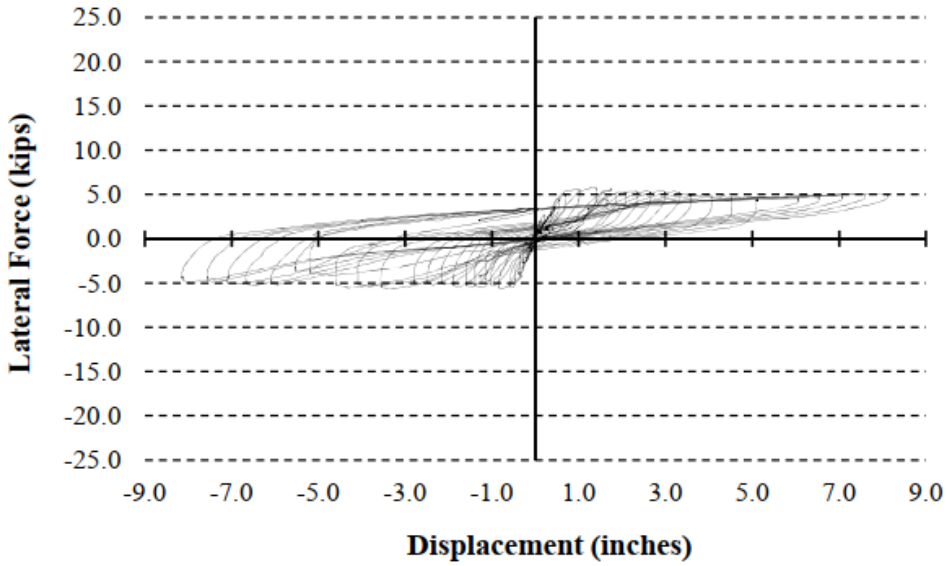


(b) 2 in embedment length

Figure 5.5: Lateral Force versus Displacement - Exterior specimen (Ziehl et al. 2012)

### 5.3.2 Ultimate Capacity of Pile to Bent Cap Connections of Bridges

Based on the experimental results, the ultimate and yield capacities of bents for selected bridges were estimated. Table 5.3 summarizes the results of 28 of 44 selected bridges from the network and Figure 5.6 shows examples of three different pile-to-bent cap connections.

Table 5.3 Ultimate bent capacity and demand of bent

| Bridge number | Latitude | Longitude | Total weight (bent), kips | No. of exterior piles (diameter range, in) | No. of interior piles (diameter range, in) | Ultimate bent capacity, kips | Demand, kips | Ratio of ultimate capacity/ Demand |
|---|---|---|---|---|---|---|---|---|
| 1 | 32.8888 | -79.946 | 1313 | 2 (26-40) | 2 (26-40) | 221-1480 | 1090 | 0.2-1.3 |
| 2 | 32.8845 | -79.9386 | 1927 | 2 (26-40) | 2 (26-40) | 221-1480 | 1599 | 0.1-0.9 |
| 3 | 32.8781 | -79.9303 | 435 | 2 (26-36) | 1 (26-36) | 138-585 | 361 | 0.3-1.6 |
| 4 | 32.8933 | -80.0189 | 1191 | 2 (26-36) | 11 (26-36) | 967-4099 | 988 | 0.9-4.1 |
| 5 | 32.8891 | -80.0196 | 1537 | 2 (26-30) | 13 (26-30) | 1133-2152 | 1275 | 0.8-1.6 |
| 6 | 32.8421 | -79.9698 | 97 | 2 (26-34) | 3 (26-34) | 304-1003 | 805 | 0.3-1.2 |
| 7 | 32.8373 | -79.9628 | 438 | 2 (26-30) | 4 (26-30) | 387-735 | 364 | 1.0-2.0 |
| 8 | 32.8294 | -79.9554 | 833 | 2 (26-34) | 2 (26-34) | 221-729 | 691 | 0.3-1.0 |
| 9 | 32.8055 | -79.9485 | 850 | 2 (26-32) | 3 (26-32) | 304-768 | 705 | 0.4-1.0 |
| 10 | 32.8039 | -79.948 | 745 | 2 (26-30) | 5 (26-30) | 469-892 | 618 | 0.7-1.4 |
| 11 | 32.7992 | -79.9447 | 745 | 2 (26-32) | 3 (26-32) | 304-768 | 618 | 0.4-1.2 |
| 12 | 32.8943 | -79.9861 | 243 | 2 (26-36) | N/A | 55-234 | 202 | 0.2-1.1 |
| 13 | 32.8388 | -79.8611 | 522 | 2 (26-32) | 2 (26-32) | 221-558 | 433 | 0.5-1.2 |
| 14 | 32.8308 | -79.8526 | 336 | 2 (26-30) | 2 (26-30) | 221-420 | 279 | 0.7-1.5 |
| 15 | 32.7905 | -80.0329 | 1080 | 2 (36-50) | N/A | 234-964 | 897 | 0.2-1.0 |
| 16 | 32.7833 | -79.96 | 782 | 2 (36-46) | N/A | 234-675 | 649 | 0.3-1.0 |
| 17 | 32.8022 | -79.9465 | 731 | 2 (26-32) | 3 (26-32) | 304-768 | 606 | 0.5-1.2 |
| 18 | 32.8046 | -79.9391 | 2160 | 2 (42-48) | 1 (42-48) | 1142-2025 | 1792 | 0.6-1.1 |
| 19 | 32.8013 | -79.8999 | 810 | 2 (42-48) | N/A | 457-810 | 672 | 0.6-1.2 |
| 20 | 32.8921 | -80.013 | 849 | 2 (42-48) | N/A | 457-810 | 705 | 0.6-1.1 |
| 21 | 32.8014 | -79.9372 | 1755 | 2 (50-56) | N/A | 963-1558 | 1456 | 0.3-1.0 |
| 22 | 32.8436 | -79.9808 | 691 | 2 (26-30) | 4 (26-30) | 387-734 | 573 | 0.6-1.2 |
| 23 | 32.8534 | -79.9899 | 633 | 2 (26-30) | 3 (26-30) | 304-577 | 525 | 0.5-1.0 |
| 24 | 32.8006 | -79.9012 | 723 | 2 (42-46) | N/A | 457-675 | 600 | 0.7-1.1 |
| 25 | 32.8744 | -79.9973 | 757 | 2 (20-24) | 15 (20-24) | 387-902 | 628 | 0.6-1.4 |


Figure 5.6: Examples of pile-to-bent cap connections

# CHAPTER 6

# Problem Formulation

## 6.1 Optimization Parameters

The optimization was modeled as a multi-objective integer programming problem. The tool can be used for two types of problems: (1) to maximize the score that indicates the priority of bridges that need to be retrofitted, and to minimize the retrofit cost, and (2) to minimize the failure probability of traveling with respect to the given seismic demand for an arbitrary traveling scenario, and to minimize the retrofit cost. The number of the design variables is equivalent to the number of bridges, and the range of values it can take is the number of retrofitting strategies provided - in this case 8 retrofitting strategies. In the case for 44 bridges, there is the total of $8^{44}$ retrofitting combinations. The total retrofit cost was calculated as follows:

$$TR = \sum_{i \in I} RC_i A_i P_i \tag{6.1}$$

And the allowable retrofit cost was calculated as follows:

$$ATR = \frac{1}{2} \sum_{i \in I} RC_i A_i c_2 \tag{6.2}$$

where,

$$P_i = \begin{cases} 0, s \in \{1\} \\ \frac{1}{n} \sum_{i=1}^{n} M_{1_{i,s}}, s \in \{4,5\} \\ \frac{1}{n} \sum_{i=1}^{n} M_{2_{i,s}}, s \in \{2,3,6,7,8\} \end{cases} \tag{6.3}$$

$RC_i$: cost replacement of bridge i per unit deck area.

$A_i$: the NBI deck area of bridge i

$M_k$: the set k of n random numbers following triangular PDF:

$$f(x|a_k, b_k, c_k) = \begin{cases} \frac{2(x - a_k)}{(c_k - a_k)(b_k - a_k)}, a_k \le x \le b_k \\ \frac{2(c - x)}{(c_k - a_k)(c_k - b_k)}, b_k \le x \le c_k \\ 0, x < a_k, x > c_k \end{cases} \tag{6.4}$$

where k ∈ {1, 2}, where 1 indicates a superstructure retrofitting index and 2 indicates superstructure and substructure retrofitting indices. The strategies are detailed as follows: s = 1: do nothing; s = 2: steel jackets; s = 3: elastomeric isolation bearings; s = 4: restrainer cables; s = 5: seat extenders; s = 6: shear keys; s = 7: restrainers and shear keys; s = 8: seat extenders and shear keys.

Note that the constraint for the allowable retrofit cost can be slightly adjusted after running several optimization routines for experimental purposes. The purpose of such adjustment is because knowing exactly whether the constraint is active or not is difficult without having a grasp about where the optimum may be located. If the problem was to be applied in a real case, a budget might be predetermined by government entities, such as the Department of Transportation. However, in this case, the work was considered still at the theoretical and experimental phase, and thus such value was considered adjustable for the sake of making the case interesting. Since the retrofit cost is one of the objective functions, one of the strategies to make the optimization case interesting is first to run a few optimization routines, see where the optimum may likely be located, then modify the constraint such that it is closed from the range of optima from the previous runs.

In the second model, the concern of the optimization is only the bridges that intersect with the shortest path at any arbitrary traveling path. For any given departure point and arrival point, there will be various options of traveling path, but only one shortest path. During pre-disaster planning, the traveling distance and the probability of failure of traveling can become the consideration of selecting which route is to be taken by the traveler.

In the first model, the concern of the optimization covers the entire highway bridge network under the study domain. The objective function concerning the bridge score has three categories affected by the failure probability, which results in the importance of the bridges in the network. The bridge that has the high score has the priority to be retrofitted compared to those with the low scores. The level of importance is based on expected failure probability, traffic capacity, historical significance, and centrality.

### 6.1.1 Expected Failure Probability

The failure probability is based on the fragility curve. The higher the probability of failure of a bridge, the higher the score, and therefore, the higher the priority for the bridge as a candidate for retrofitting. The extensive damage state exceedance in the constructed fragility curve was used as a criterion to determine the failure probability. Let $\beta_{i_{ns}}$ be a vector of the normally distributed random number of size $I$ by $\#\mathrm{PfSim}$, where $\#\mathrm{PfSim}$ is the desired number of Monte Carlo simulations, $S$ is a set of retrofit strategy indices, and $I$ is a set of bridge indices. The expected failure probability for every bridge was computed as follows:

$$\forall s \in S, \forall i \in I, \forall ns \in \{1, \dots, \#\text{PfSim}\}.$$

$$BC_{i,s,ns} = \begin{cases} 1, \Phi[z]_{i,s,D_3} \geq \beta_{i_{ns}} \\ 0, \Phi[z]_{i,s,D_3} < \beta_{i_{ns}} \end{cases} \quad (6.5)$$

$$Pf_{i,s} = \frac{\sum_{ns} BC_{i,s,ns}}{\#\text{PfSim}} \quad (6.6)$$

where

$BC_{i,s,ns}$: bridge condition with respect to using retrofitting strategy $s \in S$, represented as a matrix of binaries of the size of $I$ by $\#\text{PfSim}$.

For the Monte Carlo simulation, the binary 1 indicates failure and 0 indicates surviving. The failure probability of bridges with respect to applied retrofit strategies for event M7.1 and M7.3 are shown in Tables 6.1 and 6.2.

Table 6.1: Failure probability of bridges with respect to applied retrofit strategies for event M7.1

| | Retrofit Strategy | | | | | | | |
|---|---|---|---|---|---|---|---|---|
| Bridge ID | 1 | 2 | 3 | 4 | 5 | 6 | 7 | 8 |
| 8516 | 0.01815 | 0.01035 | 0.00695 | 0.0121 | 0.01945 | 0.01125 | 0.0085 | 0.011 |
| 8062 | 0.01905 | 0.00985 | 0.00995 | 0.0187 | 0.0222 | 0.0216 | 0.01865 | 0.0201 |
| 8061 | 0.0233 | 0.01155 | 0.00905 | 0.0213 | 0.0228 | 0.02295 | 0.02035 | 0.02195 |
| 8227 | 0.0186 | 0.0093 | 0.00845 | 0.01645 | 0.01765 | 0.0169 | 0.015 | 0.01715 |
| 8134 | 0.2568 | 0.12695 | 0.22905 | 0.205 | 0.247 | 0.2088 | 0.22625 | 0.23345 |
| 8235 | 0.00725 | 0.00165 | 0.00655 | 0.00505 | 0.0072 | 0.00625 | 0.00715 | 0.0064 |
| 4266 | 0.4204 | 0.37235 | 0.2283 | 0.39365 | 0.41625 | 0.40315 | 0.38875 | 0.41345 |
| 4267 | 0.46335 | 0.42245 | 0.2687 | 0.4338 | 0.4508 | 0.4481 | 0.4368 | 0.45585 |
| 4050 | 0.38635 | 0.338 | 0.2058 | 0.3647 | 0.388 | 0.37255 | 0.36055 | 0.3826 |
| 4269 | 0.3044 | 0.26675 | 0.1506 | 0.27655 | 0.3081 | 0.29045 | 0.2847 | 0.2999 |
| 4720 | 0.3429 | 0.30315 | 0.17045 | 0.3207 | 0.3413 | 0.3253 | 0.3173 | 0.3371 |
| 4945 | 0.4325 | 0.38675 | 0.245 | 0.4054 | 0.43095 | 0.40785 | 0.4004 | 0.42595 |
| 9826 | 0.01295 | 0.0074 | 0.00465 | 0.0082 | 0.01445 | 0.0081 | 0.0053 | 0.00745 |
| 9827 | 0.01385 | 0.00765 | 0.004 | 0.0082 | 0.01235 | 0.00735 | 0.00595 | 0.00715 |
| 9832 | 0.0156 | 0.008 | 0.0048 | 0.00885 | 0.0131 | 0.00855 | 0.0056 | 0.0076 |
| 8519 | 0.02615 | 0.01635 | 0.0092 | 0.0176 | 0.0268 | 0.0178 | 0.0111 | 0.0148 |
| 8138 | 0.17555 | 0.07855 | 0.1525 | 0.136 | 0.1664 | 0.13825 | 0.15195 | 0.1544 |
| 8325 | 0.0153 | 0.01105 | 0.00345 | 0.0132 | 0.01565 | 0.01445 | 0.01135 | 0.015 |
| 8326 | 0.00985 | 0.00605 | 0.00455 | 0.0112 | 0.01035 | 0.00965 | 0.00945 | 0.01 |
| 8330 | 0.00895 | 0.0033 | 0.0084 | 0.0067 | 0.0097 | 0.00765 | 0.00785 | 0.01015 |
| 7429 | 0.01005 | 0.0037 | 0.00335 | 0.009 | 0.01095 | 0.00815 | 0.0078 | 0.0093 |
| 7430 | 0.2331 | 0.19775 | 0.1043 | 0.2158 | 0.2316 | 0.22505 | 0.2112 | 0.22455 |
| 8419 | 0.0125 | 0.00335 | 0.01195 | 0.00705 | 0.01335 | 0.00975 | 0.01105 | 0.01105 |
| 9648 | 0.0329 | 0.0109 | 0.02905 | 0.02255 | 0.03165 | 0.02615 | 0.02705 | 0.02695 |
| 9402 | 0.03325 | 0.01025 | 0.02735 | 0.0226 | 0.0296 | 0.0232 | 0.02545 | 0.02955 |
| 7074 | 0.4094 | 0.3589 | 0.21745 | 0.3832 | 0.4096 | 0.3877 | 0.3773 | 0.4 |
| 228 | 0.0023 | 0.00055 | 0.002 | 0.00135 | 0.0024 | 0.0015 | 0.002 | 0.00215 |
| 9137 | 0.00295 | 0.0013 | 0.0007 | 0.0014 | 0.0026 | 0.0014 | 0.0014 | 0.00125 |
| 9825 | 0.01365 | 0.0073 | 0.00485 | 0.00685 | 0.0118 | 0.008 | 0.00575 | 0.0067 |
| 5231 | 0.36565 | 0.32375 | 0.18805 | 0.335 | 0.3632 | 0.3499 | 0.3364 | 0.3564 |
| 9838 | 0.01265 | 0.00345 | 0.01075 | 0.00855 | 0.01205 | 0.00875 | 0.0103 | 0.0112 |
| 9823 | 0.01425 | 0.0037 | 0.0097 | 0.01035 | 0.0126 | 0.01015 | 0.01115 | 0.01015 |
| 9824 | 0.0004 | 0.0002 | 0.00045 | 0.0006 | 0.0007 | 0.00065 | 0.0007 | 0.0008 |
| 9837 | 0.0063 | 0.0019 | 0.00605 | 0.0038 | 0.00705 | 0.0056 | 0.00545 | 0.0067 |
| 9836 | 0.00045 | 0.0002 | 0.0006 | 0.00065 | 0.0009 | 0.00065 | 0.00075 | 0.0009 |
| 4477 | 0.0338 | 0.0116 | 0.0281 | 0.023 | 0.0325 | 0.02555 | 0.02755 | 0.0306 |
| 5478 | 0.01625 | 0.0089 | 0.0044 | 0.01035 | 0.0148 | 0.00835 | 0.00645 | 0.0071 |
| 9822 | 0.01705 | 0.00525 | 0.0133 | 0.01295 | 0.0156 | 0.01115 | 0.01465 | 0.01355 |
| 4268 | 0.336 | 0.29715 | 0.16765 | 0.3096 | 0.3359 | 0.31915 | 0.3078 | 0.32975 |
| 3606 | 0.3289 | 0.28865 | 0.1695 | 0.31285 | 0.3348 | 0.3152 | 0.30715 | 0.3222 |
| 9835 | 0.00565 | 0.00135 | 0.0047 | 0.00375 | 0.0056 | 0.00465 | 0.0046 | 0.00495 |
| 9830 | 0.0022 | 0.0012 | 0.00065 | 0.00155 | 0.0022 | 0.0017 | 0.0012 | 0.0011 |
| 8238 | 0.02435 | 0.0069 | 0.0202 | 0.0191 | 0.02415 | 0.0178 | 0.0203 | 0.0182 |
| 714 | 0.48785 | 0.45085 | 0.2921 | 0.4685 | 0.4983 | 0.48375 | 0.4649 | 0.4839 |

Table 6.2: Failure probability of bridges with respect to applied retrofit strategies for event M7.3

| | Retrofit Strategy | | | | | | | |
|---|---|---|---|---|---|---|---|---|
| Bridge ID | 1 | 2 | 3 | 4 | 5 | 6 | 7 | 8 |
| 8516 | 0.31365 | 0.24175 | 0.1901 | 0.2584 | 0.3202 | 0.25055 | 0.2138 | 0.23395 |
| 8062 | 0.31645 | 0.22765 | 0.20665 | 0.30725 | 0.3155 | 0.3104 | 0.29905 | 0.3135 |
| 8061 | 0.32795 | 0.238 | 0.22475 | 0.32305 | 0.32775 | 0.32255 | 0.30175 | 0.32465 |
| 8227 | 0.3169 | 0.23695 | 0.2121 | 0.31465 | 0.32435 | 0.31565 | 0.29475 | 0.3169 |
| 8134 | 0.89215 | 0.77575 | 0.8787 | 0.86055 | 0.8892 | 0.8659 | 0.8704 | 0.87445 |
| 8235 | 0.2615 | 0.1346 | 0.2357 | 0.20865 | 0.25335 | 0.21295 | 0.23215 | 0.2362 |
| 4266 | 0.8498 | 0.8248 | 0.69365 | 0.83175 | 0.8469 | 0.84335 | 0.8371 | 0.84775 |
| 4267 | 0.8677 | 0.84385 | 0.7263 | 0.85525 | 0.8688 | 0.8611 | 0.8573 | 0.8664 |
| 4050 | 0.83935 | 0.82385 | 0.68525 | 0.8269 | 0.84665 | 0.8373 | 0.83005 | 0.8434 |
| 4269 | 0.8896 | 0.86485 | 0.7617 | 0.87955 | 0.88745 | 0.8802 | 0.87825 | 0.88775 |
| 4720 | 0.8483 | 0.8288 | 0.6971 | 0.8413 | 0.85465 | 0.84875 | 0.8406 | 0.8488 |
| 4945 | 0.9368 | 0.9198 | 0.8446 | 0.9278 | 0.9374 | 0.931 | 0.92775 | 0.93115 |
| 9826 | 0.28115 | 0.2129 | 0.1608 | 0.21845 | 0.2825 | 0.2103 | 0.18095 | 0.2084 |
| 9827 | 0.2763 | 0.1994 | 0.151 | 0.21425 | 0.26685 | 0.2052 | 0.1744 | 0.1937 |
| 9832 | 0.27845 | 0.20975 | 0.15985 | 0.22145 | 0.2744 | 0.21225 | 0.18215 | 0.2063 |
| 8519 | 0.22035 | 0.1594 | 0.11825 | 0.1775 | 0.2269 | 0.1686 | 0.13845 | 0.162 |
| 8138 | 0.77195 | 0.60215 | 0.73945 | 0.71935 | 0.7589 | 0.7273 | 0.7356 | 0.73515 |
| 8325 | 0.4025 | 0.35585 | 0.22125 | 0.37345 | 0.3943 | 0.38925 | 0.38085 | 0.39685 |
| 8326 | 0.3451 | 0.2564 | 0.2389 | 0.3395 | 0.3505 | 0.3411 | 0.3265 | 0.34335 |
| 8330 | 0.35545 | 0.1974 | 0.32395 | 0.29675 | 0.3418 | 0.30425 | 0.31995 | 0.32345 |
| 7429 | 0.27355 | 0.19275 | 0.1713 | 0.2678 | 0.2661 | 0.2648 | 0.24445 | 0.26185 |
| 7430 | 0.8195 | 0.7944 | 0.65915 | 0.80605 | 0.821 | 0.8119 | 0.80535 | 0.8205 |
| 8419 | 0.28345 | 0.1438 | 0.254 | 0.2348 | 0.2683 | 0.2383 | 0.2472 | 0.25345 |
| 9648 | 0.25095 | 0.1209 | 0.22605 | 0.20005 | 0.2416 | 0.2106 | 0.2236 | 0.2244 |
| 9402 | 0.26605 | 0.1346 | 0.2355 | 0.2123 | 0.25585 | 0.22135 | 0.2328 | 0.2339 |
| 7074 | 0.8837 | 0.86125 | 0.7572 | 0.8757 | 0.88145 | 0.8804 | 0.8747 | 0.8816 |
| 228 | 0.33615 | 0.18425 | 0.30905 | 0.2829 | 0.3196 | 0.2864 | 0.2932 | 0.299 |
| 9137 | 0.3534 | 0.2715 | 0.21335 | 0.29325 | 0.35235 | 0.27795 | 0.2442 | 0.27465 |
| 9825 | 0.2536 | 0.18755 | 0.1476 | 0.20395 | 0.2601 | 0.19455 | 0.16735 | 0.18875 |
| 5231 | 0.89565 | 0.87405 | 0.7756 | 0.884 | 0.89685 | 0.89065 | 0.8854 | 0.8894 |
| 9838 | 0.3512 | 0.19365 | 0.3226 | 0.29535 | 0.33645 | 0.2973 | 0.32125 | 0.319 |
| 9823 | 0.35655 | 0.20065 | 0.3275 | 0.3035 | 0.352 | 0.31205 | 0.32415 | 0.32755 |
| 9824 | 0.33085 | 0.1865 | 0.3061 | 0.28065 | 0.3164 | 0.27445 | 0.2954 | 0.2995 |
| 9837 | 0.22115 | 0.10135 | 0.19785 | 0.17405 | 0.2057 | 0.17525 | 0.1902 | 0.192 |
| 9836 | 0.1133 | 0.0451 | 0.1003 | 0.08705 | 0.10925 | 0.09085 | 0.09275 | 0.0984 |
| 4477 | 0.2835 | 0.15125 | 0.25805 | 0.23805 | 0.27545 | 0.24015 | 0.2568 | 0.2642 |
| 5478 | 0.3666 | 0.2829 | 0.2363 | 0.3026 | 0.3647 | 0.2966 | 0.25835 | 0.28135 |
| 9822 | 0.39585 | 0.2281 | 0.36415 | 0.3339 | 0.38385 | 0.34245 | 0.358 | 0.3578 |
| 4268 | 0.7991 | 0.77255 | 0.6258 | 0.78475 | 0.80365 | 0.7884 | 0.7944 | 0.79545 |
| 3606 | 0.8028 | 0.76925 | 0.6255 | 0.7844 | 0.79855 | 0.7944 | 0.78645 | 0.796 |
| 9835 | 0.19955 | 0.0912 | 0.1792 | 0.1546 | 0.1861 | 0.1646 | 0.17355 | 0.17425 |
| 9830 | 0.11305 | 0.07555 | 0.0542 | 0.07915 | 0.1145 | 0.0764 | 0.0638 | 0.0723 |
| 8238 | 0.21505 | 0.1027 | 0.1922 | 0.1736 | 0.2038 | 0.17925 | 0.18825 | 0.19465 |
| 714 | 0.8989 | 0.875 | 0.7754 | 0.8862 | 0.89805 | 0.89255 | 0.889 | 0.8982 |

### 6.1.2 Traffic Capacity

Traffic capacity is represented by the Average Daily Traffic (ADT). The higher the NBI-based ADT, the higher the priority for the bridge as a candidate for retrofitting. The value of ADT was acquired from the NBI database, NBI item 29 (see FHWA, 1995).

The bridge with the highest ADT in the study domain is the bridge with NBI structural number 4268 with ADT = 88,700 vehicles per day (the location of this bridge is shown in Figure 6.1 and the ADT is shown in Figure 6.2). Although this bridge has high ADT, it has very low centrality (centrality score=87) (see Appendix A for values of all bridges). This means this bridge has low influence with respect to the other vertices in the network.

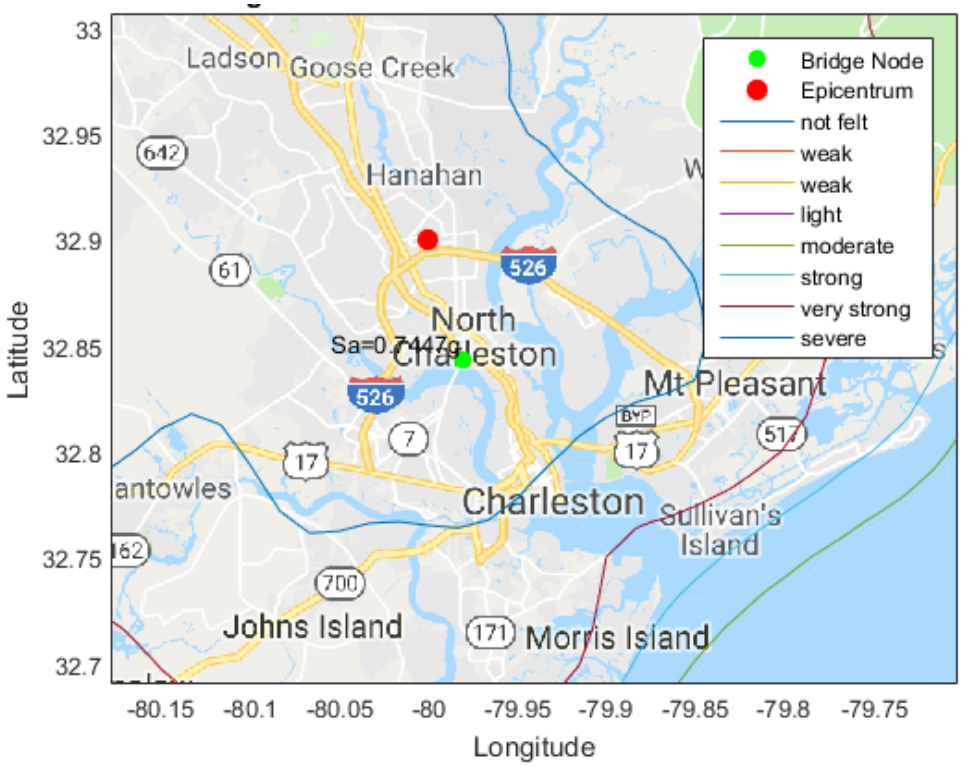


Figure 6.1: Location of bridge NBI structural number 4268 (seismic contour event M7.3)

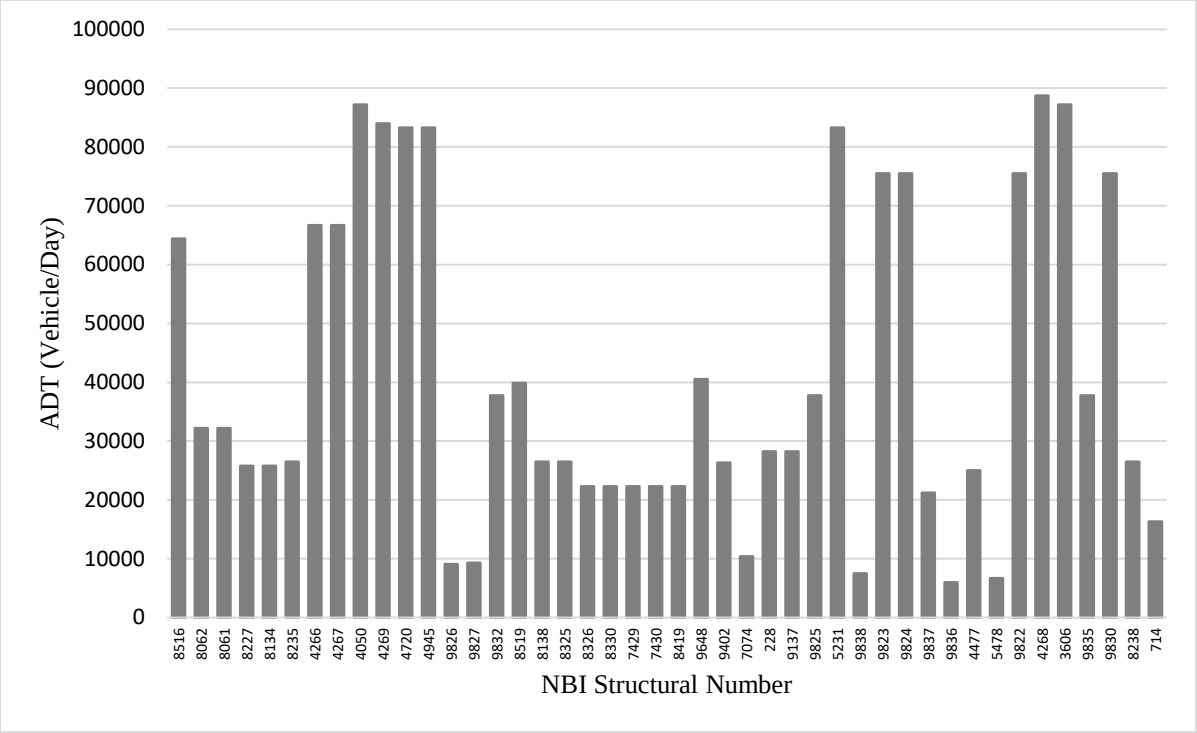


Figure 6.2: Traffic capacity of bridges

### 6.1.3 Centrality

Betweenness centrality: the higher the betweenness centrality, the more the bridge is passed by the number of shortest paths, and therefore, the higher the priority for the bridge as a candidate for retrofitting. Implementing the Dijkstra shortest path algorithm, the score for the betweenness centrality can be computed as follows:

$$\forall_{i \in I}, \forall_{j \in I.}$$

$$\tilde{\mathrm{I}}_{ij} = Dijkstra\ (i,j) \tag{6.7}$$

$$C_i = \begin{cases} C_i + 1, i \in \tilde{\mathrm{I}}_{ij} \\ C_i + 0, \ \ i \notin \tilde{\mathrm{I}}_{ij} \end{cases} \tag{6.8}$$

where,

$\tilde{\mathrm{I}}$ = index of the shortest path from point i to j.

The Dijkstra algorithm works by initially assigning the distance value of ∞ with the temporary state t, except the starting node. The algorithm then proceeds iteratively by finding the minimum distance between the current and other temporary nodes, minimizing the distance value $d_j$ of node $j$, i.e. $min_{j \in J} d_j = d_{j*}$ by updating $d_j = \min(d_j, d_i + c_{ij})$ where $c_{ij}$ is the cost of link $(i,j)$, and relabeling node $j^*$ to permanent (as current node) (details may be found in Rardin, 1997).

The bridge with the highest centrality in the study domain is the bridge with NBI structural number 9825 with centrality score = 825 (the location of this bridge is shown in Figure 6.3 and the centrality score is shown in Figure 6.4). This is to be expected since the bridge is located at the east end of I-26, intersecting with the major routes US 17 and close to US 54. However, the bridge has a relatively low ADT score as can be seen in Figure 6.3.

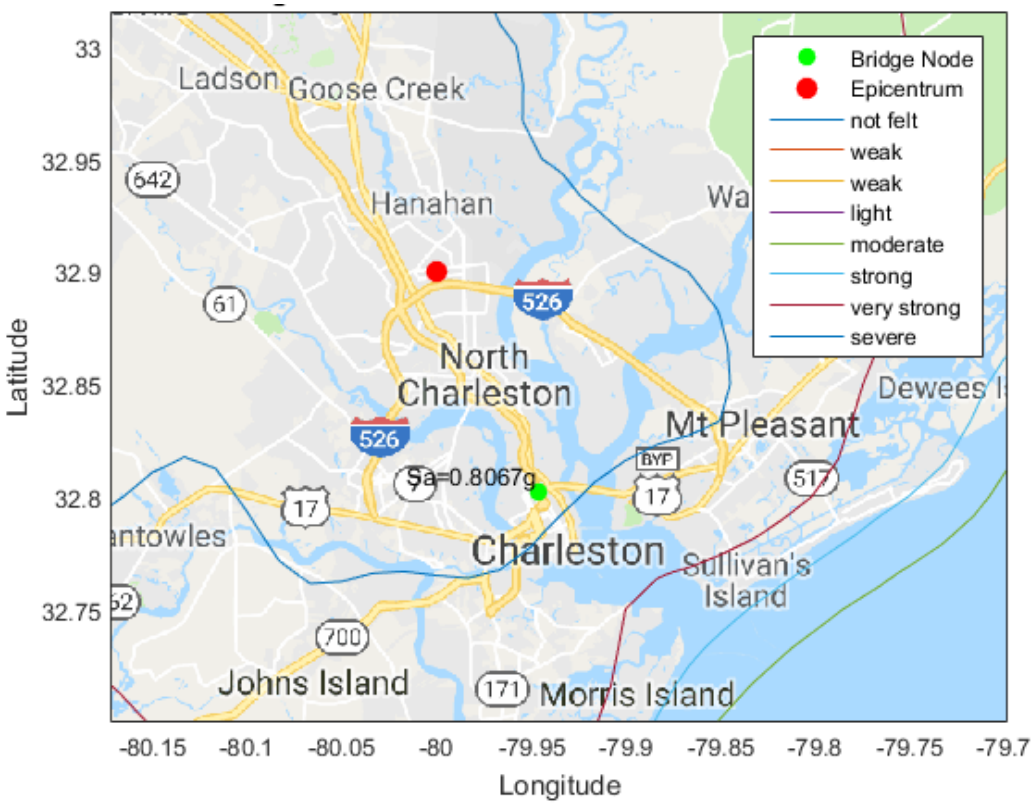


Figure 6.3: Location of bridge NBI structural number 9825 (seismic contour event M7.3)

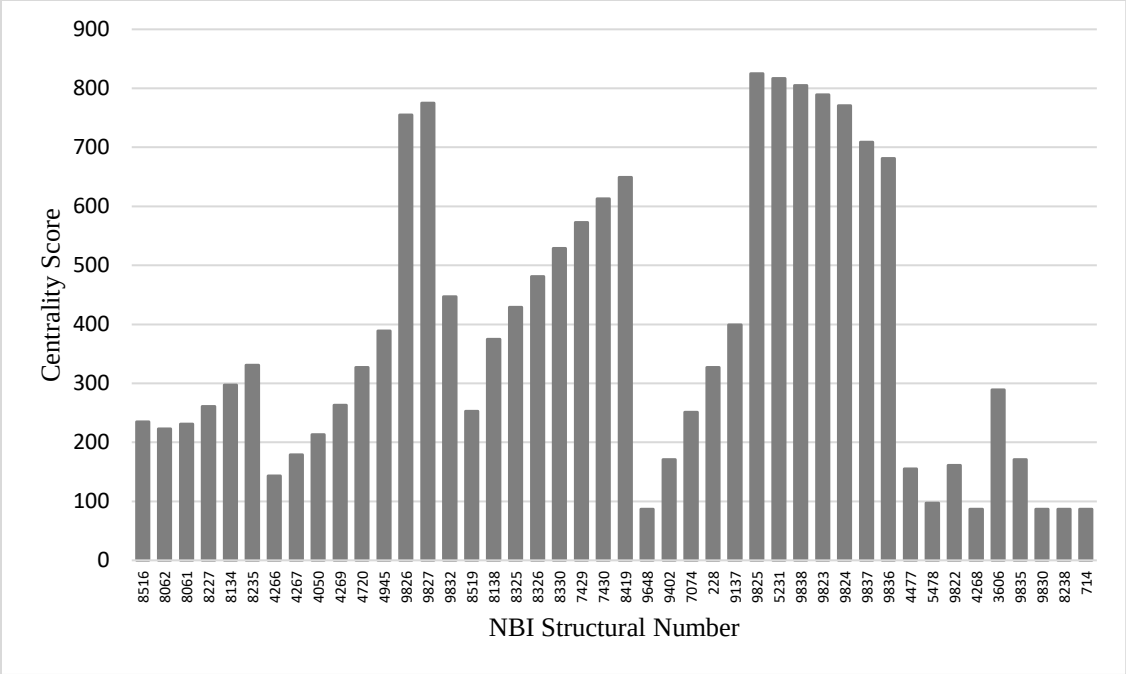


Figure 6.4: Centrality score of bridges

An example of a bridge that has both an above average centrality score and traffic capacity that is under the study domain is NBI structural number 9824, which is the Arthur Ravenel, Jr. Bridge crossing the Cooper River, built in 2005.

### 6.1.4 Centrality

The lower the NBI-based historical significance, the higher the priority for the bridge as a candidate for retrofitting. However, since later the optimization is modeled for maximization, the ranking system was reversed such that the value “5” indicates the highest score of historical significance, and “1” the lowest. The historical significance of bridges is included in NBI item 37, which indicates that a bridge might be associated with a historical property or area or could be derived from the fact that the bridge was associated with significant events or circumstances (see FHWA, 1995). This field gives the bridge with high historical significance to stand out since it is rare for bridges to have even a historical significance score of “3”. The bridge with the highest historical significance score in the study domain is the bridge with NBI structural number 228 with historical significance score = 5 (see Figures 6.5, and 6.6).

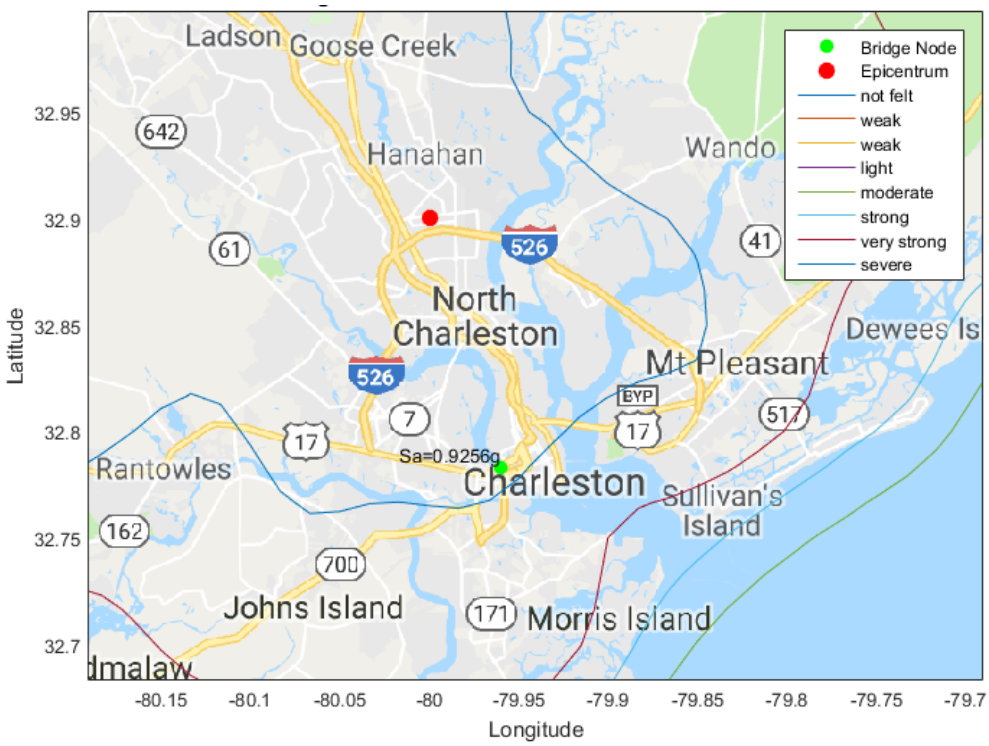


Figure 6.5: Location of bridge NBI structural number 228 (seismic contour event M7.3)

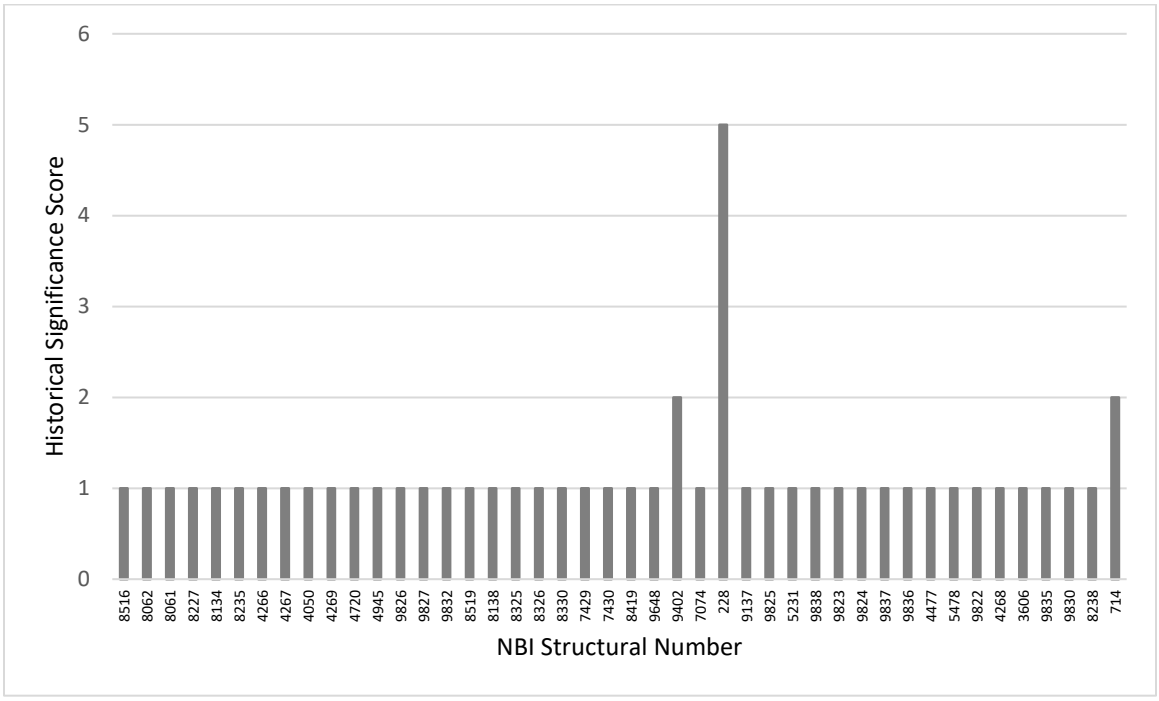


Figure 6.6: Historical significance score of bridges

## 6.2 Optimization Model 1

Optimization model 1 accounts for all bridges in the network under the study domain. Expected failure probability is calculated based on the probability of exceedance described previously. A Monte Carlo simulation was used by comparing the matrix generated from a random number generator and the probability of the bridge exceeding certain damage. This will also be the case for the second optimization case. An approximate ideal simulation number is set to be around 20,000 simulations under the consideration of both accuracy and computational cost. Having acquired the failure probability, the optimization model was formulated as follows:

maximize

$$w(SC) + \frac{1}{1 + (1 - w)3(TR_{norm})} \tag{6.9}$$

subject to

$$TR \leq ATR \tag{6.10}$$

where

$$SC = \sum_{i \in I} \left( \left(1 - Pf_{i,s}\right) \left( \frac{\lambda_1(ADT_i)}{\sum_{j \in I} ADT_j} + \frac{\lambda_2(HS_i)}{\sum_{j \in I} HS_j} + \frac{\lambda_3(C_i)}{\sum_{j \in I} C_j} \right) \right) \tag{6.11}$$

Parameters:

$w$: the weight of the objective function
$C_i$: the score of the betweenness centrality for bridge i$\in I$
$HS_i$: the score of the historical significance for bridge i$\in I$
$ADT_i$: the score of the average daily traffic for bridge i$\in I$
$Pf_i$: failure probability for bridge i$\in I$
$SC$: the sum of the total score for all bridges in $I$
$ATR$: allowable total retrofit cost
$TR_{norm}$: the normalized total retrofit cost
$\lambda_1$:weight for ADT
$\lambda_2$:weight for HS
$\lambda_3$:weight for centrality

Decision variables:

S = the retrofit strategy (s = 1: do nothing; s = 2: steel jackets; s = 3: elastomeric isolation bearings, s = 4: restrainer cables, s = 5: seat extenders; s = 6: shear keys; s = 7: restrainers and shear keys; s = 8: seat extenders and shear keys).

Note that $\lambda_1$, $\lambda_2$, and $\lambda_3$ defines the level of importance in each criterion: ADT, HS, and centrality, and each range between 0 to 3, but the sum should not be more than 3. In this investigation each of these three values is set to 1 as setting the proper value is highly subjective.

## 6.3 Optimization Model 2

Optimization model 2 accounts only for bridges that intersect the traveling $T$, a set of some possible paths from departure point $d$ to arrival point $a$. Also, the bridge nodal index $i$ only accounts for those that intersect the shortest path in $\tilde{I}_{ij}$, therefore the $Pf_i$ can be calculated using equation 5.5 and 5.6 with $i \in \tilde{I}_{ij}$. For a possible path $t \in T$, the optimization that minimizes the failure probability of traveling and retrofit cost was written as follows:

maximize

$$\frac{1}{1 + w(Pt) + (1 - w)(TR_{norm})} \tag{6.12}$$

subject to

$$TR \leq ATR \tag{6.13}$$

where

$$Pt = \sum_{i \in \tilde{I}_{ij}} \frac{Pf_{i,s}}{\#Ptsims} \tag{6.14}$$

Parameters

$\tilde{I}_{ij}$: The shortest path indices in $Dijkstra(d, a)$; $\#Ptsims$: the number of Monte Carlo simulations for failure probability of traveling; $Pt$: the failure probability of traveling from d to a.

Decision variables:

S = the retrofit strategy (s = 1: do nothing; s = 2: steel jackets; s = 3: elastomeric isolation bearings, s = 4: restrainer cables, s = 5: seat extenders; s = 6: shear keys; s = 7: restrainers and shear keys; s = 8: seat extenders and shear keys).

# CHAPTER 7

# Minimization of Retrofit Cost

## 7.1 Validation of Customized Genetic Algorithm

A customized stochastic optimization algorithm, Genetic Algorithm (GA), was programmed in Matlab to perform the optimization process. The developed GA was considered convenient since the problems, as formulated in the previous chapter, took the form of integer programming problems with the number of variables for retrofit strategy implementation equivalent to the number of bridges under the study domain (case 1) or intersecting the shortest path (case 2). GA is considered relatively powerful to deal with problems that are robust in nature.

The customized GA uses a binary encoding process and performs the selection procedure by using the roulette wheel selection based on the individuals' fitness value (see Mitchell, 1998). Two crossover methods are implemented into the customized GA including the single-point and uniform crossover. The crossover operation swaps bits of information, which is analogous to biological crossing over and recombination of chromosomes in cell meiosis. The operation creates two offspring. For instance, a single crossover method chooses a crossover point in a string of binaries in the parents and swaps the bits from the cutting point to an end between parents. In the uniform crossover, the swapping of bits is based on the swapping probability (for details, see Sastry et al., 2005).

The genetic operation for the mutation process uses the bit inversion technique with an adjustable rate of mutation. The user also has the option to activate elitism and to configure the rate of elitism to help ensure convergence. Elitism strategy is widely utilized to ensure improvement of the convergence in the individuals' fitness in each subsequent generation (Liang and Leung 2010). The process iteratively continues until reaching the termination criterion.

Three different test functions are used to validate the precision and robustness of the developed customized GA: (1) Booth function, (2) Levi function, and (3) Easom function.

The corresponding equation of the Booth function is as follows (Jamil and Yang, 2013):

$$f(\mathbf{x}) = (x_1 + 2x_2 - 7)^2 + (2x_1 + x_2 - 5)^2 \tag{7.1}$$

The optimum is at f = 0 and x* = [1,3]. Figure 7.1 shows that using a population size of 20 individuals and 20 generations, with the lower bound [0 0], and upper bound [10.1 10.1], the customized GA converges to the minimum f = 0.

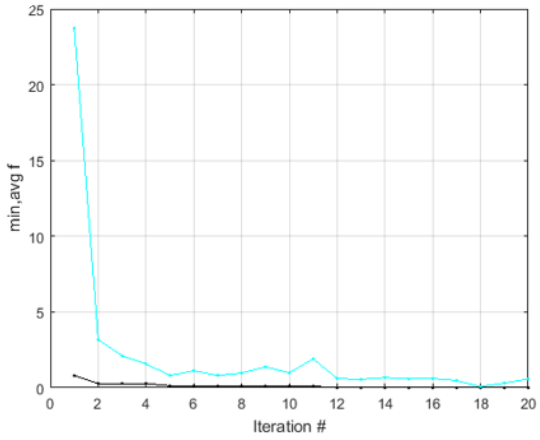


(a) Minimum value (black) and average value (light blue) of the fitness function vs. iteration number

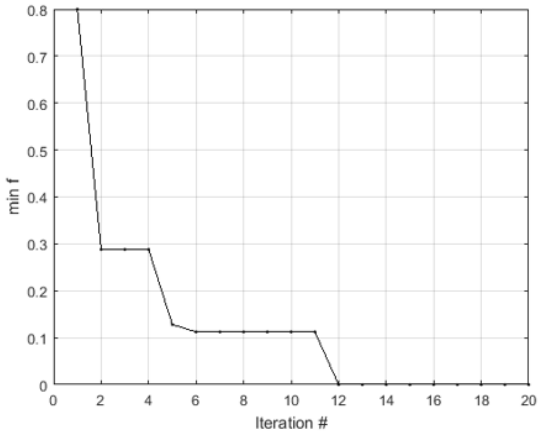


(b) Minimum value of the fitness function vs. iteration number

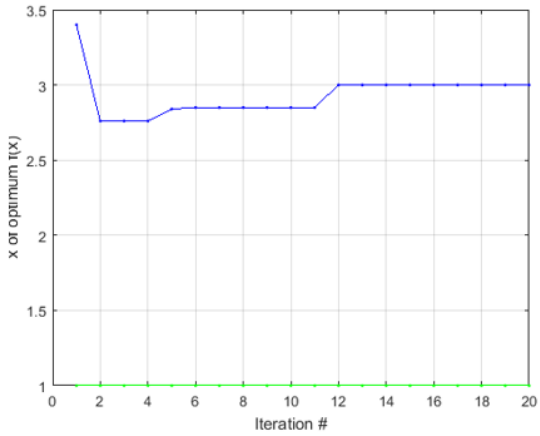


(c) Design variables of best individual vs. iteration number

Figure 7.1 Customized GA validation for the Booth function

The corresponding equation of the Levi function is as follows (Malherbe, Contal and Vayatis, 2016):

$$f(\mathbf{x}) = \sin^2(3\pi x_1) + (x_1 - 1)^2 \left[1 + \sin^2(3\pi x_2)\right] + (x_2 - 1)^2 \left[1 + \sin^2(2\pi x_2)\right] \quad (7.2)$$

The optimum is at f = 0 and x* = [1,1]. Figure 7.2 shows that using 20 individuals and 20 generations, with the lower bound [0 0], and upper bound [10.1 10.1], the customized GA converges to the minimum f = 0.

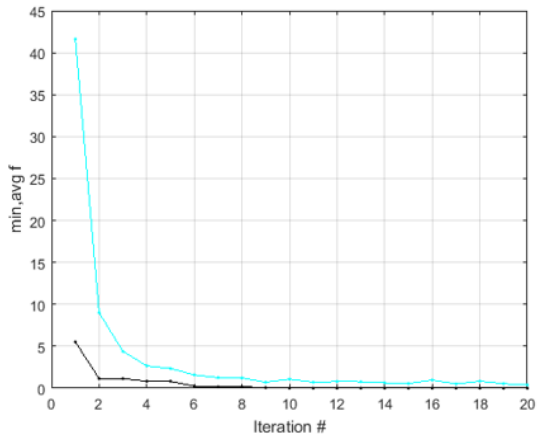


(a) minimum value (black) and the average value (light blue) of the fitness function vs. iteration number

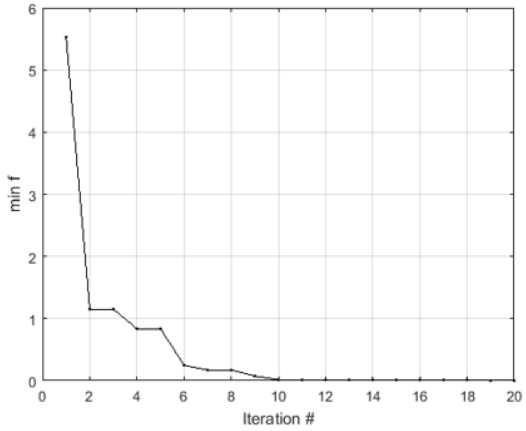


(b) minimum value of the fitness function vs. iteration number

Figure 7.2: Customized GA validation for Levi function

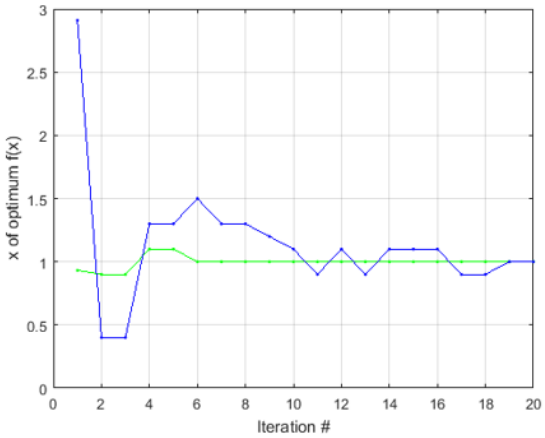


(c) design variables of best individual vs. iteration number

Figure 7.2: Customized GA validation for Levi function

The corresponding equation of the Easom function is as follows (Molga and Smutnicki, 2005):

$$f(\mathbf{x}) = -\cos(x_1)\cos(x_2)\exp\left(-(x_1-\pi)^2-(x_2-\pi)^2\right) \tag{7.3}$$

The optimum is at f = -1 and x* = [π, π]. Figure 7.3 shows that using 80 individuals and 30 generations, with the lower bound [0 0], and upper bound [50.11 50.11], the customized GA converges to the minimum f = -0.99489

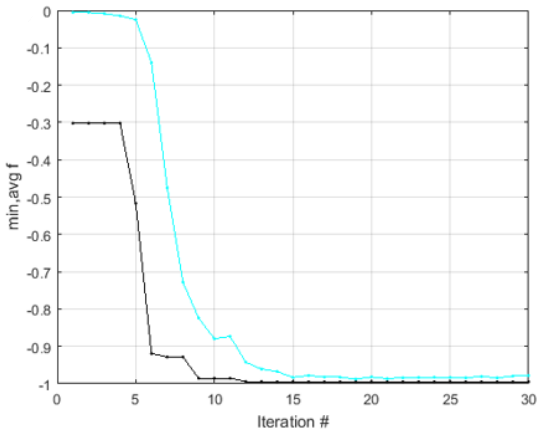


(a) Minimum value (black) and the average value (light blue) of the fitness function vs. iteration number

Figure 7.3: Customized GA validation for the Easom function

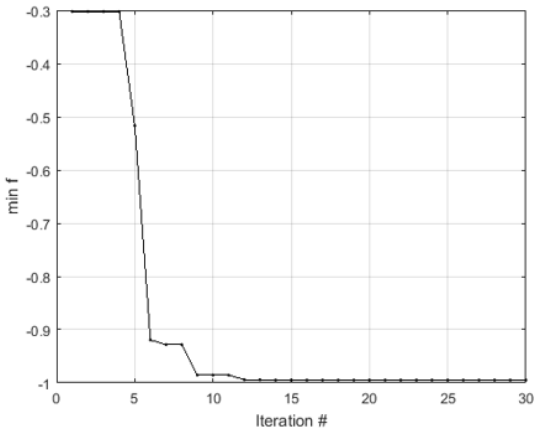


(b) Minimum value of the fitness function vs. iteration number

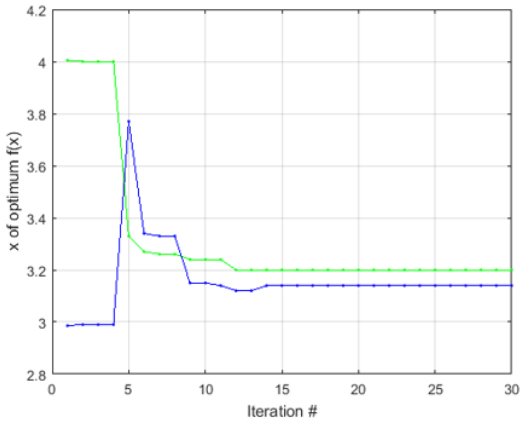


(c) Design variables of best individual vs. iteration number

Figure 7.3: Customized GA validation for the Easom function

An earlier version of the developed customized GA has been implemented for a structural shape optimization for a parametric twisted skyscraper design under both wind and dead loads as functions of the design variables. The problem was modeled as a mixed integer nonlinear programming problem and classified as a black-box simulation-based optimization problem (see Wonoto and Blouin, 2019, for details).

## 7.2 GA Implementation and Results on Optimization Model 1

### 7.2.1 Optimization Model 1 for Event M7.1

The optimization was run on the model shown in Figure 3.2 with the mathematical model as expressed in equations 6.8, 6.9 and 6.10. When all the design variables are set to 1, and the weight is set to 1, the objective function corresponded to the total retrofit cost will be neglected. A simple single run of this gave the score as follows (Table 7.1):

Table 7.1 Sum of scores and total retrofit cost for all strategies are set as “do nothing” (opt. model= 1, event M7.1)

| ADT score | HS score | Centrality score | Sum of score | TotalRetrofitCost |
|---|---|---|---|---|
| 0.8283 | 0.8827 | 0.9065 | 2.6756 | 0 |

Note that the maximum sum of the score is 3. Also, the values shown in Table 7.1 is always different for every run of Monte Carlo simulation due to probabilistic effect in the simulation. In this case, 20,000 simulations were used. Table 7.1 shows that when the retrofit strategy is set as “do nothing” gives the sum of the score of 2.7656, which is quite high. As can be seen, the reason for this phenomenon to occur is because the failure probability is rather low for this specific scenario M7.1 (20.1 km depth) for the given distance to the earthquake epicenter (in Summerville, 37.13 km linear distance to Charleston). Note that the sum of score SC, i.e., the first objective function, can range from 0 (when all bridges fail, i.e., when all $Pf_i = 1$) to 3 (when all bridges have 0 failure probability, which is unlikely in the case of an earthquake such as that studied). As opposed to an exhaustive search, a more cultivated approach is to employ an optimization method to configure the retrofit strategy combination that allows the sum of score approach 3, i.e., the one that maximizes score of ADT, HS, and centrality factored by the failure probability.

Note that GA starts with only requiring the lower and upper bounds, unlike an optimization algorithm such as the Sequential Quadratic Programming (SQP) that conventionally requires an initial point with lower and upper bounds of the optimization. Figure 7.4 shows GA with 120 iterations for optimization model 1. Table 7.2 shows improved sum of scores when neglecting total retrofit cost (event. = M7.1, opt. model = 1, w = 1, max. gen. = 120, pop. = 10), and Table 7.3 shows GA retrofit combinations (event. = M7.1, opt. model = 1, w = 1, max. gen. = 120, pop. = 10).

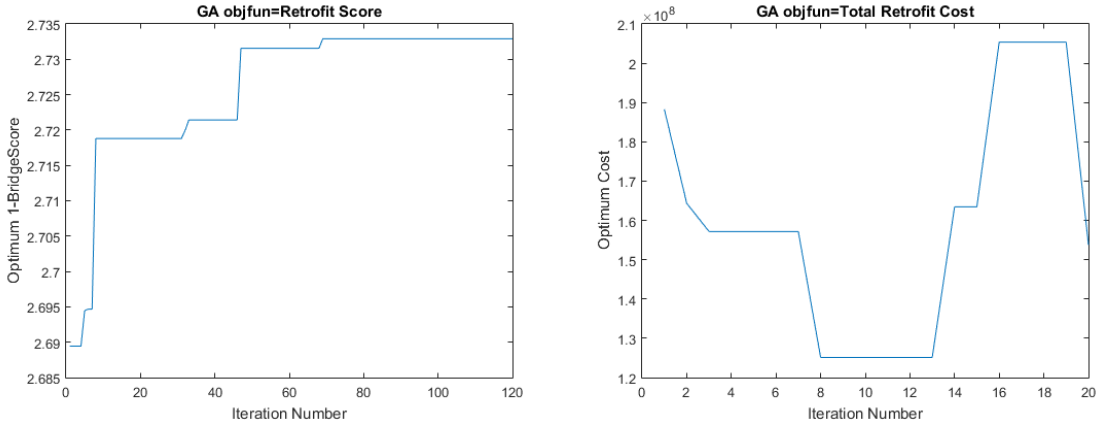


Figure 7.4: GA iteration for maximizing the sum of score and neglecting the retrofit cost (event M7.1)

Table 7.2: Improved sum of scores when neglecting total retrofit cost
(event. = M7.1, opt. model= 1, w=1, max. gen. =120, pop. =10)

| ADT score | HS score | Centrality score | Sum of score | TotalRetrofitCost |
|---|---|---|---|---|
| 0.8838 | 0.9185 | 0.9307 | 2.7329 | 1.565e+08 |

Table 7.3: GA retrofit combinations
(event. = M7.1, opt. model= 1, w=1, max. gen. =120, pop. =10)

| BridgeID | 8516 | 8062 | 8061 | 8227 | 8134 | 8235 | 4266 | 4267 | 4050 |
|---|---|---|---|---|---|---|---|---|---|
| Retrofit | 3 | 3 | 4 | 6 | 2 | 3 | 1 | 3 | 3 |
| BridgeID | 4269 | 4720 | 4945 | 9826 | 9827 | 9832 | 8519 | 8138 | 8325 |
| Retrofit | 3 | 3 | 3 | 1 | 3 | 1 | 5 | 6 | 5 |
| BridgeID | 8326 | 8330 | 7429 | 7430 | 8419 | 9648 | 9402 | 7074 | 228 |
| Retrofit | 1 | 7 | 4 | 2 | 1 | 4 | 3 | 6 | 5 |
| BridgeID | 9137 | 9825 | 5231 | 9838 | 9823 | 9824 | 9837 | 9836 | 4477 |
| Retrofit | 2 | 5 | 2 | 7 | 1 | 1 | 4 | 7 | 7 |
| BridgeID | 5478 | 9822 | 4268 | 3606 | 9835 | 9830 | 8238 | 714 | |
| Retrofit | 7 | 2 | 3 | 6 | 5 | 1 | 3 | 3 | |

### 7.2.2 Optimization Model 1 for Event M7.3

For case M7.3, as shown in Figure 3.3, when each retrofit strategy is set as “do-nothing”, and neglecting the total retrofit cost, the maximization of the sum of score will result as shown in Table 7.4.

Table 7.4: Sum of scores and total retrofit cost for all strategies are set as “do nothing” (opt. model= 1, event M7.3)

| ADT score | HS score | Centrality score | Sum of score | TotalRetrofitCost |
|---|---|---|---|---|
| 0.4507 | 0.5367 | 0.5619 | 1.5493 | 0 |

The sum of score of for event M7.3 is much smaller compared to event M7.1 since the failure probability of the bridges for M7.3 is much higher (see equation 5.11). Here the constraint for the allowable retrofit cost (ATR) is set US $257.52 million, which is half of the highest possible random value (US $515 million) in the triangular CDF. For an experiment, the ATR will be reduced to US $122 million to be more restrictive, which is when the allowable total retrofit cost was all based on the percent replacement cost of 15.4%. The first observation was to see how the two objective functions (the sum of score and total retrofit cost) behave with the constraint that was relaxed. Setting the GA maximum iteration to 120 and number of populations to 8 will give the combination of retrofitting strategies as follows (Table 7.5):

Table 7.5: GA retrofit combinations
(event. = M7.3, opt. model= 1, w=1, max. gen. =120, pop. =8)

| BridgeID | 8516 | 8062 | 8061 | 8227 | 8134 | 8235 | 4266 | 4267 | 4050 |
|---|---|---|---|---|---|---|---|---|---|
| Retrofit | 3 | 5 | 2 | 7 | 2 | 2 | 6 | 4 | 3 |
| BridgeID | 4269 | 4720 | 4945 | 9826 | 9827 | 9832 | 8519 | 8138 | 8325 |
| Retrofit | 3 | 3 | 6 | 3 | 1 | 2 | 5 | 2 | 5 |
| BridgeID | 8326 | 8330 | 7429 | 7430 | 8419 | 9648 | 9402 | 7074 | 228 |
| Retrofit | 7 | 4 | 7 | 6 | 2 | 6 | 6 | 6 | 3 |
| BridgeID | 9137 | 9825 | 5231 | 9838 | 9823 | 9824 | 9837 | 9836 | 4477 |
| Retrofit | 3 | 6 | 3 | 8 | 1 | 2 | 3 | 5 | 2 |
| BridgeID | 5478 | 9822 | 4268 | 3606 | 9835 | 9830 | 8238 | 714 | |
| Retrofit | 2 | 2 | 3 | 3 | 5 | 4 | 8 | 7 | |

The corresponding improved sum of score is as follows (Table 7.6):

Table 7.6: Improved sum of scores when neglecting total retrofit cost (event. = M7.3, opt. model= 1, w=1, max. gen. = 120, pop. = 8, ATR = US $257.52)

| ADT score | HS score | Centrality score | Sum of score | TotalRetrofitCost |
|---|---|---|---|---|
| 0.5347 | 0.6000 | 0.6274 | 1.7621 | 1.9072e+08 |

Note that the total retrofit cost is relatively far below the allowable retrofit cost of US $257.52 million. Thus, the constraint with the allowable retrofit cost (ATR) of US $257.52 million is most likely inaccurate. As can be seen in Table 7.7, setting the GA maximum iteration to 200 and number of populations to 20 will give the combination retrofit strategy as follows:

Table 7.7: GA retrofit combinations when neglecting total retrofit cost
(event. = M7.3, opt. model = 1, w = 1, max. gen. = 200, pop. = 20, ATR = US $257.52)

| BridgeID | 8516 | 8062 | 8061 | 8227 | 8134 | 8235 | 4266 | 4267 | 4050 |
|---|---|---|---|---|---|---|---|---|---|
| Retrofit | 3 | 4 | 5 | 6 | 8 | 3 | 1 | 4 | 4 |
| BridgeID | 4269 | 4720 | 4945 | 9826 | 9827 | 9832 | 8519 | 8138 | 8325 |
| Retrofit | 2 | 3 | 3 | 3 | 2 | 7 | 4 | 2 | 3 |
| BridgeID | 8326 | 8330 | 7429 | 7430 | 8419 | 9648 | 9402 | 7074 | 228 |
| Retrofit | 8 | 2 | 2 | 3 | 2 | 3 | 7 | 1 | 2 |
| BridgeID | 9137 | 9825 | 5231 | 9838 | 9823 | 9824 | 9837 | 9836 | 4477 |
| Retrofit | 1 | 2 | 3 | 1 | 2 | 1 | 4 | 4 | 7 |
| BridgeID | 5478 | 9822 | 4268 | 3606 | 9835 | 9830 | 8238 | 714 | |
| Retrofit | 6 | 2 | 3 | 3 | 3 | 4 | 2 | 1 | |

The corresponding improved sum of score is as follows (Table 7.8 and Figure 7.5):

Table 7.8: Improved sum of scores when neglecting total retrofit cost
(event. = M7.3, opt. model = 1, w = 1, max. gen. = 200, pop. = 20, ATR = US $257.52)

| ADT score | HS score | Centrality score | Sum of score | TotalRetrofitCost |
|---|---|---|---|---|
| 0.5302 | 0.6116 | 0.6399 | 1.7818 | 1.6666e+08 |

The corresponding GA iteration is as follows:

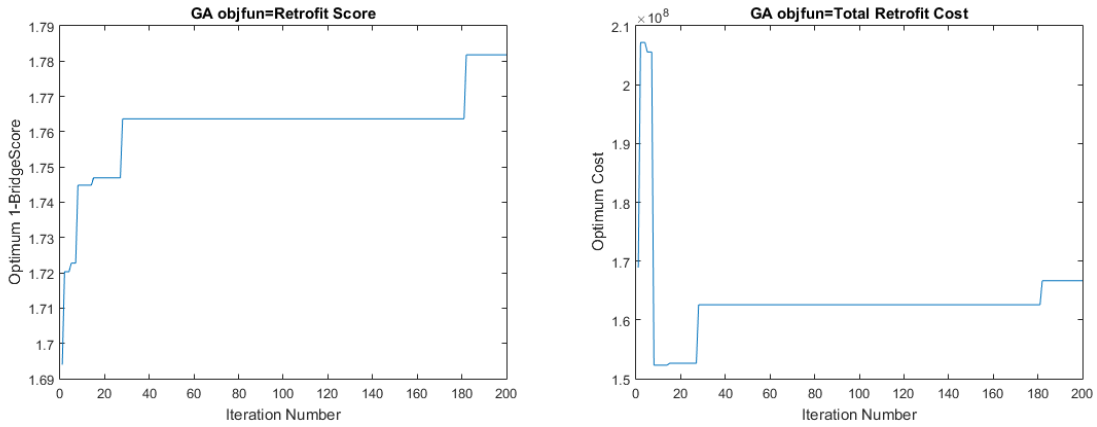


Figure 7.5 GA iteration for improving sum of score and neglecting the retrofit cost (event. = M7.3, opt. model= 1, w=1, max. gen. =200, pop. =20, ATR= US$257.52 million)

For the case M7.3, setting the GA maximum iteration to 200 and number of populations to 20, neglecting the sum of score, the minimization of total retrofit cost gives the combination retrofit strategy as follow (Table 7.9).

Table 7.9: GA retrofit combinations when neglecting sum of scores (event. = M7.3, opt. model = 1, w = 0, max. gen. = 200, pop. = 20, ATR = US $257.52 million)

| BridgeID | 8516 | 8062 | 8061 | 8227 | 8134 | 8235 | 4266 | 4267 | 4050 |
|---|---|---|---|---|---|---|---|---|---|
| Retrofit | 1 | 7 | 8 | 2 | 1 | 1 | 8 | 3 | 4 |
| BridgeID | 4269 | 4720 | 4945 | 9826 | 9827 | 9832 | 8519 | 8138 | 8325 |
| Retrofit | 5 | 4 | 6 | 8 | 6 | 4 | 4 | 4 | 4 |
| BridgeID | 8326 | 8330 | 7429 | 7430 | 8419 | 9648 | 9402 | 7074 | 228 |
| Retrofit | 4 | 2 | 7 | 8 | 6 | 4 | 4 | 1 | 7 |
| BridgeID | 9137 | 9825 | 5231 | 9838 | 9823 | 9824 | 9837 | 9836 | 4477 |
| Retrofit | 8 | 1 | 1 | 6 | 7 | 4 | 7 | 3 | 3 |
| BridgeID | 5478 | 9822 | 4268 | 3606 | 9835 | 9830 | 8238 | 714 | |
| Retrofit | 4 | 5 | 1 | 8 | 4 | 8 | 1 | 6 | |

Note that increasing the maximum generation and population, even more, will help the retrofit cost to approach 0 (when all strategies are “do-nothing”). The corresponding GA iteration is as follows (Figure 7.6):

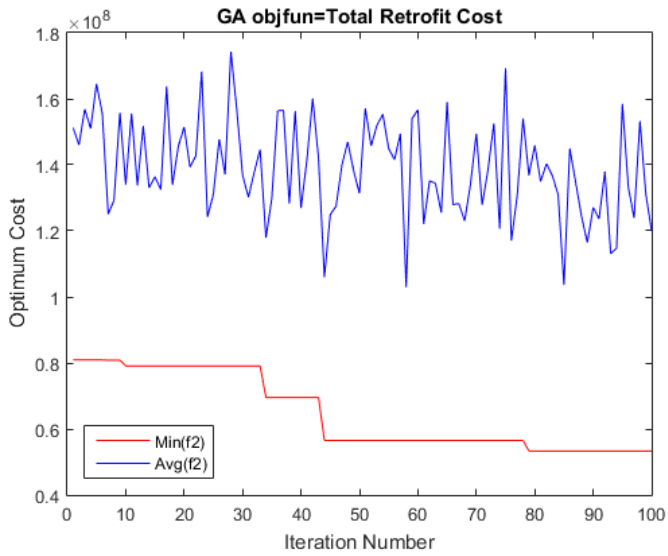


Figure 7.6: GA iteration for improving total retrofit cost and neglecting sum of score (event. = M7.3, opt. model = 1, w = 0, max. gen. = 200, pop. = 20, ATR = US $257.52 million)

Varying the weights of the two objective functions above give the Pareto frontier as shown in Figure 7.7. The two objective functions, as can be seen from the optimization model and the plots at Figure 7.7, are not conflicting. As the sum of score gets larger, the total retrofit cost gets larger as well because retrofitting the bridges tends to decrease the failure probability of the bridge and therefore increase the score of ADT, HS, and centrality, which will give the higher sum of score and total cost at the same time. The node labeling sorts the data based on the sum of score.

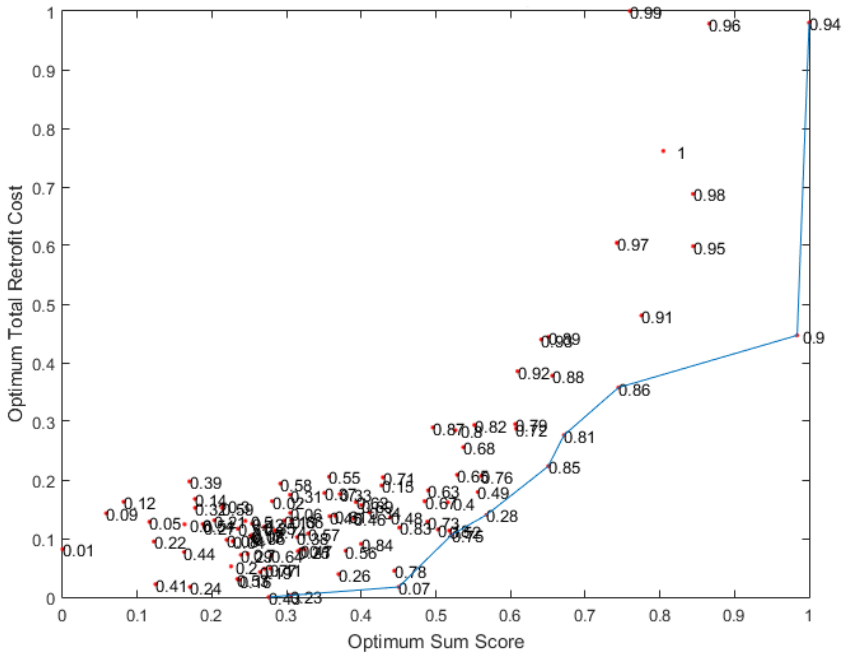


(a) Points labeled with objective function's weight w

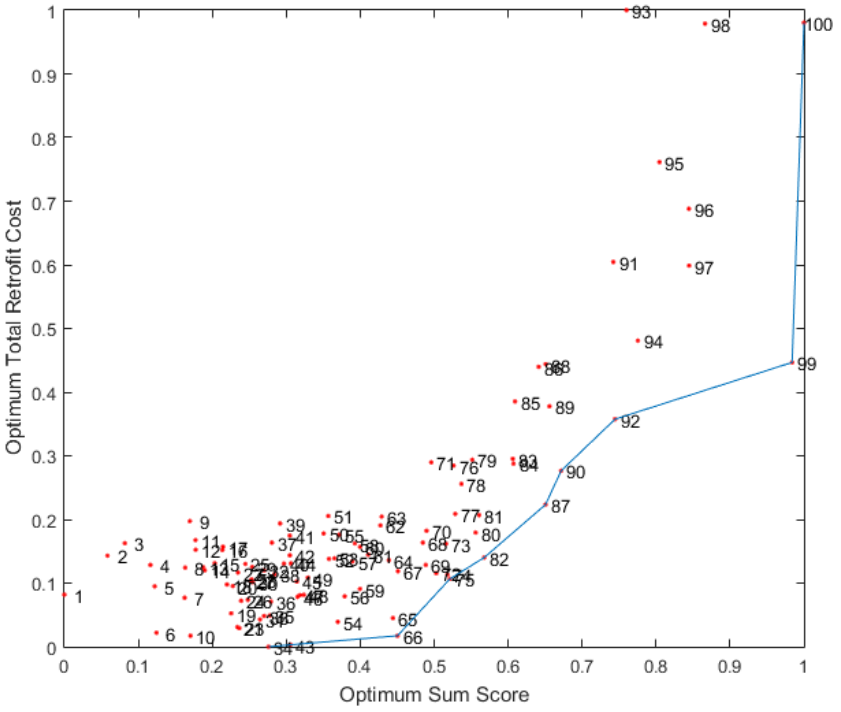


(b) Points labeled based on increasing optimum sum of score in Pareto iterations

Figure 7.7: Pareto front for maximizing sum of score and minimizing total cost (event. = M7.3, opt. model = 1, Pareto points = 100, w = varied, max. gen. = 50, pop. = 10, ATR = US $257.52)

One of the suggested optimum from the Pareto frontier, if one desires to maximize the sum of score as a priority while still having reasonable total cost please refer to Table 7.10.

Table 7.10: GA retrofit combinations for improving sum of score and total retrofit cost (event. = M7.3, opt. model = 1, w = 0.9, max. gen. = 50, pop. = 10, ATR = US $257.52)

| BridgeID | 8516 | 8062 | 8061 | 8227 | 8134 | 8235 | 4266 | 4267 | 4050 |
|---|---|---|---|---|---|---|---|---|---|
| Retrofit | 5 | 5 | 6 | 7 | 3 | 5 | 5 | 2 | 8 |
| BridgeID | 4269 | 4720 | 4945 | 9826 | 9827 | 9832 | 8519 | 8138 | 8325 |
| Retrofit | 3 | 3 | 5 | 2 | 8 | 3 | 5 | 6 | 3 |
| BridgeID | 8326 | 8330 | 7429 | 7430 | 8419 | 9648 | 9402 | 7074 | 228 |
| Retrofit | 3 | 2 | 4 | 3 | 2 | 5 | 4 | 4 | 2 |
| BridgeID | 9137 | 9825 | 5231 | 9838 | 9823 | 9824 | 9837 | 9836 | 4477 |
| Retrofit | 1 | 5 | 3 | 2 | 2 | 8 | 5 | 1 | 2 |
| BridgeID | 5478 | 9822 | 4268 | 3606 | 9835 | 9830 | 8238 | 714 | |
| Retrofit | 3 | 4 | 3 | 7 | 4 | 3 | 1 | 3 | |

The corresponding improved sum of score and total retrofit cost are as follows (Table 7.11):

Table 7.11: Improved sum of scores and total retrofit cost (event. = M7.3, opt. model = 1, w = 0.9, max. gen. = 50, pop. = 10, ATR = US $257.52)

| ADT score | HS score | Centrality score | Sum of score | TotalRetrofitCost |
|---|---|---|---|---|
| 0.5150 | 0.6104 | 0.6354 | 1.7608 | 1.1696e+08 |

Note that the total retrofit cost in Table 7.11 is below US $122 million, but not the result in Table 7.8. This indicates that setting the allowable retrofit cost as US $122 million would likely make the constraint active. This estimation that makes the constraint active would be difficult to be known without first running the GA for multiple times to have the grasp where the optimum may be located. The result in Table 7.11 reduces the sum of score by 1% from the result in Table 7.8 but improves the total retrofit cost by 30%. Appendix A shows the details of the improved ADT, HS, centrality, failure probability, and the retrofit cost for each bridge.

For instance, the bridge NBI structural number 228 (Ashley Memorial Bridge) receives a retrofitting strategy 2, i.e. steel jacketing retrofit. This is to be expected because the bridge is categorized as MSC steel, and the bridges' failure probability was calculated based on the extensive damage simulations, therefore implementing the modification factor for the median shift in Padgett and DesRoches, 2009, steel jacketing retrofit gives the highest factor. As can be seen in the appendix, using the chosen optimum from Pareto frontier, the failure probability of the bridge was reduced by 49% as compared to do nothing. This then improves the ADT, HS, and centrality as compared to do nothing, which is shown in detail in Appendix A.

After knowing the value that would likely make the constraint active, one additional attempt to optimization model 1 event M7.3 was to put a more restrictive constraint, i.e., reducing the amount of allowable retrofit cost to US $122 million. This gives (Table 7.12):

Table 7.12 GA retrofit combinations for improving sum of score and total retrofit cost (event. = M7.3, opt. model = 1, w = 1, max. gen. = 80, pop. = 20, ATR = US $122 million)

| BridgeID | 8516 | 8062 | 8061 | 8227 | 8134 | 8235 | 4266 | 4267 | 4050 |
|---|---|---|---|---|---|---|---|---|---|
| Retrofit | 4 | 7 | 5 | 5 | 6 | 5 | 4 | 5 | 3 |
| BridgeID | 4269 | 4720 | 4945 | 9826 | 9827 | 9832 | 8519 | 8138 | 8325 |
| Retrofit | 3 | 2 | 2 | 7 | 8 | 2 | 4 | 7 | 7 |
| BridgeID | 8326 | 8330 | 7429 | 7430 | 8419 | 9648 | 9402 | 7074 | 228 |
| Retrofit | 3 | 1 | 4 | 7 | 1 | 2 | 6 | 1 | 2 |
| BridgeID | 9137 | 9825 | 5231 | 9838 | 9823 | 9824 | 9837 | 9836 | 4477 |
| Retrofit | 4 | 7 | 4 | 3 | 7 | 4 | 1 | 3 | 2 |
| BridgeID | 5478 | 9822 | 4268 | 3606 | 9835 | 9830 | 8238 | 714 | |
| Retrofit | 7 | 2 | 6 | 3 | 6 | 5 | 2 | 3 | |

The corresponding improved sum of score and total retrofit cost is as follows (Table 7:13):

Table 7.13: Improved sum of scores (event. = M7.3, opt. model = 1, w = 1, max. gen. = 80, pop. = 20, ATR = US $122 million)

| ADT score | HS score | Centrality score | Sum of score | TotalRetrofitCost |
|---|---|---|---|---|
| 0.5105 | 0.6016 | 0.6099 | 1.7221 | 1.1042e+08 |

Note that the result in Table 7.13 shows the total retrofit cost that is closed to the constraint when ATR= US $122 million. Therefore, in this case, it is considered that the result from the Pareto front for the weight of 0.9 is the best-improved candidate for event M7.3 with optimization model 1 based on the Pareto frontier and several runs of GA.

### 7.2.3 Optimization Model 1 for Event M7.3 for Pile-to-Bent Connection

Twenty-five bridges were used for the optimization for the pile-to-bent connection with the failure probability estimated using the data from the investigations performed at U. South Carolina. Here, instead of eight strategies, only two retrofitting strategies were used for the optimization (Figures 7.8 - 7.10 and Table 7.14).

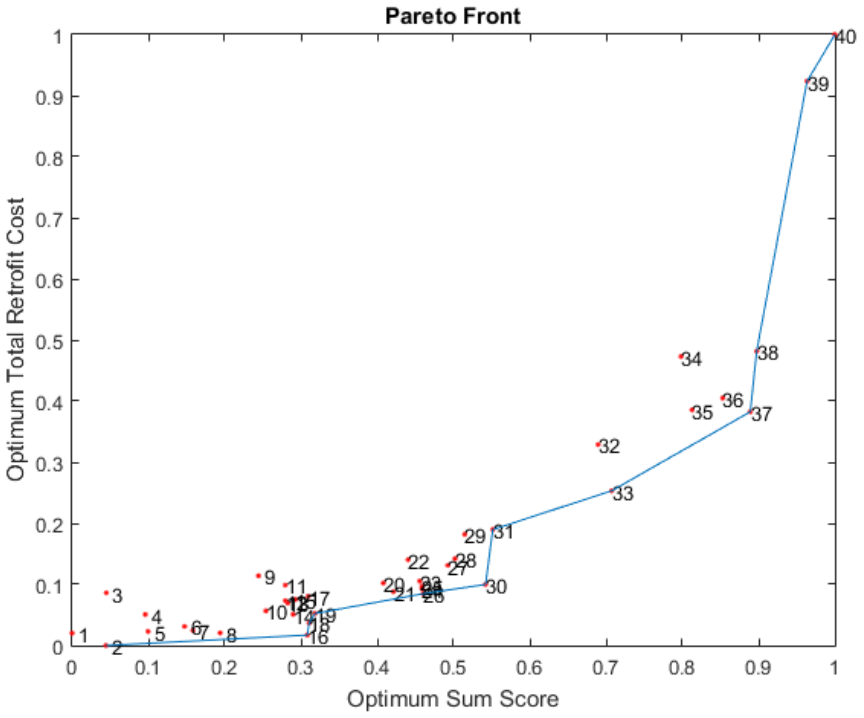


(a) Points labeled with objective function's weight w

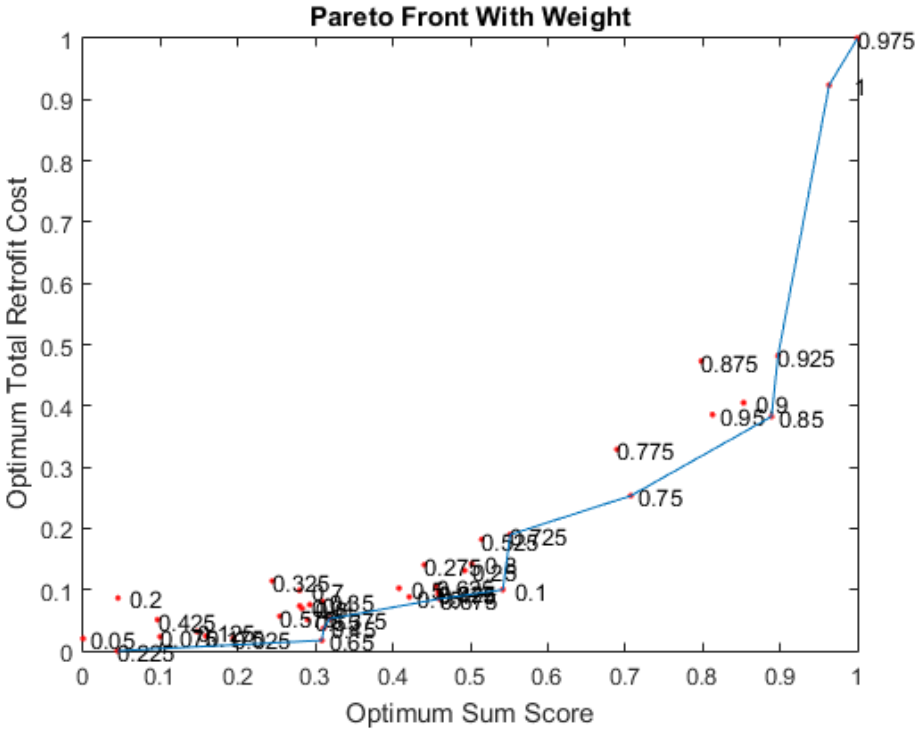


(b) Points labeled based on increasing optimum sum of score in Pareto iterations

Figure 7.8: Pareto front for maximizing sum of score and minimizing total cost of the pile-to-bent connections (event. = M7.3, opt. model = 1, Pareto points = 100, w = varied, max. gen. = 50, pop. = 10, ATR = US $257.52)

Table 7.14: GA retrofit combinations for improving sum of score, failure probability of pile-to-bent connection, and total retrofit cost based on the opted candidate from the Pareto frontier

| **BridgeID** | 8062 | 8061 | 8227 | 4266 | 4267 | 4269 | 4720 | 4945 |
|---|---|---|---|---|---|---|---|---|
| **Retrofit** | 1 | 2 | 2 | 2 | 1 | 1 | 2 | 2 |
| **BridgeID** | 9826 | 9827 | 9832 | 8519 | 8325 | 7429 | 9402 | 228 |
| **Retrofit** | 2 | 1 | 2 | 1 | 1 | 2 | 2 | 2 |
| **BridgeID** | 9825 | 9838 | 9837 | 4477 | 5478 | 4268 | 3606 | 9835 |
| **Retrofit** | 2 | 2 | 2 | 2 | 2 | 2 | 1 | 1 |
| **BridgeID** | 714 | | | | | | | |
| **Retrofit** | 1 | | | | | | | |

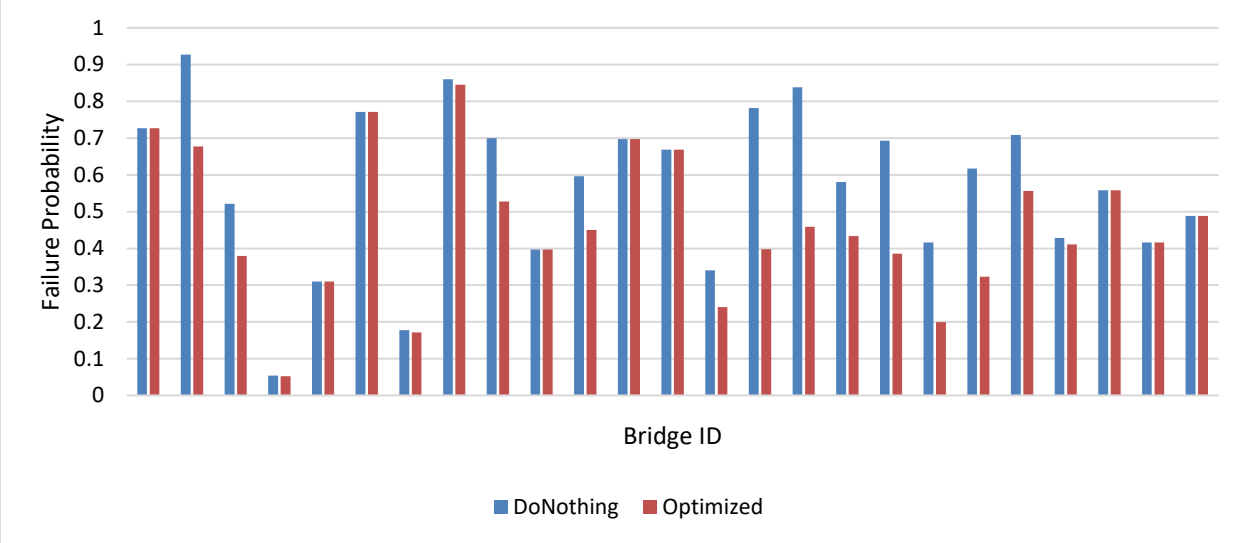


Figure 7.9: Improved failure probability from the opted Pareto frontier solution as compared to do nothing

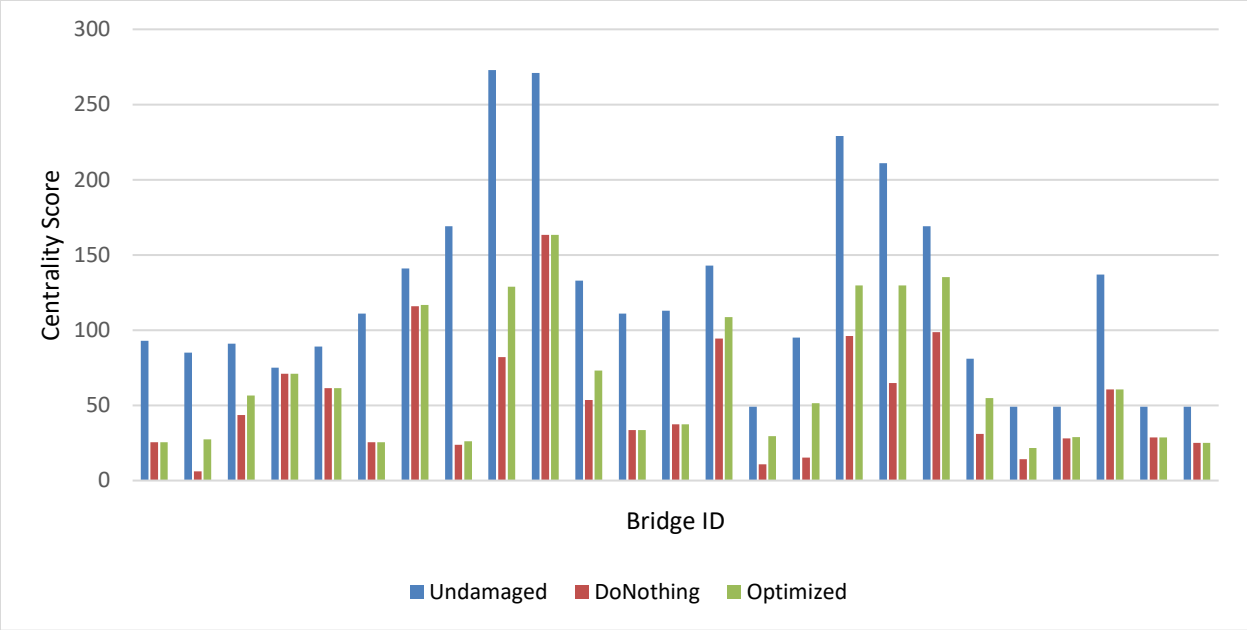


Figure 7.10: Improved centrality score from the opted Pareto frontier solution as compared to do nothing

## 7.3 GA Implementation and Results on Optimization Model 2

Another application of the developed tool is to optimize a set of bridges that intersects with the traveling path based on an arbitrary traveling scenario. Given the focus is to retrofit the route that connects between departure and arrival points, the tool gives several scenarios of traveling paths. These traveling paths are presented as plots with the traveling distances shown. Through these images, the users (e.g., Department of Transportation) can choose the travel routes to focus on for retrofitting purposes based on the distance and number of bridges intersected by the traveling path. Optimization model 2 is based on equations 6.11, 6.12, and 6.13 presented in chapter 6.

Figure 7.11 shows the three traveling scenarios generated by the tool for the given arbitrary departure and arrival points.

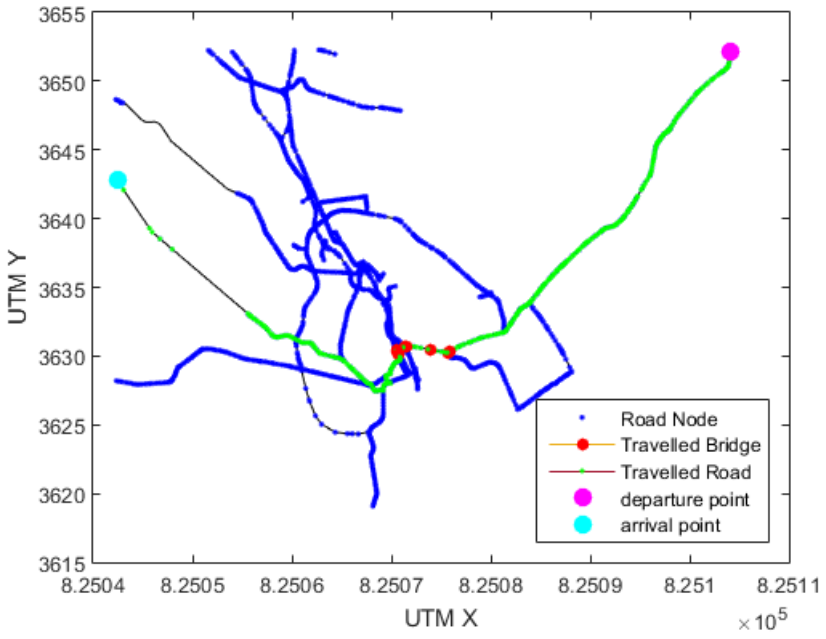


(a) 79 km travel distance

Figure 7.11: Arbitrary traveling scenarios

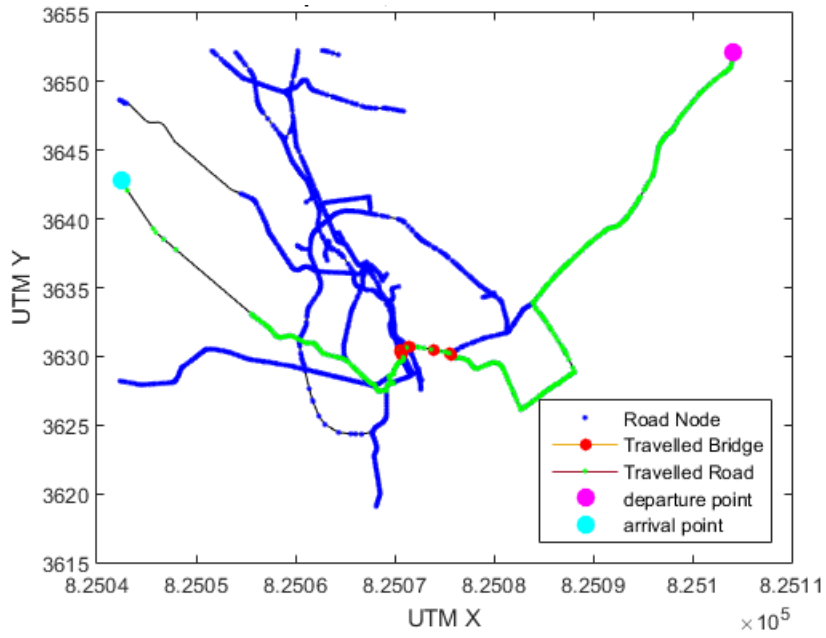


(b) 92 km travel distance

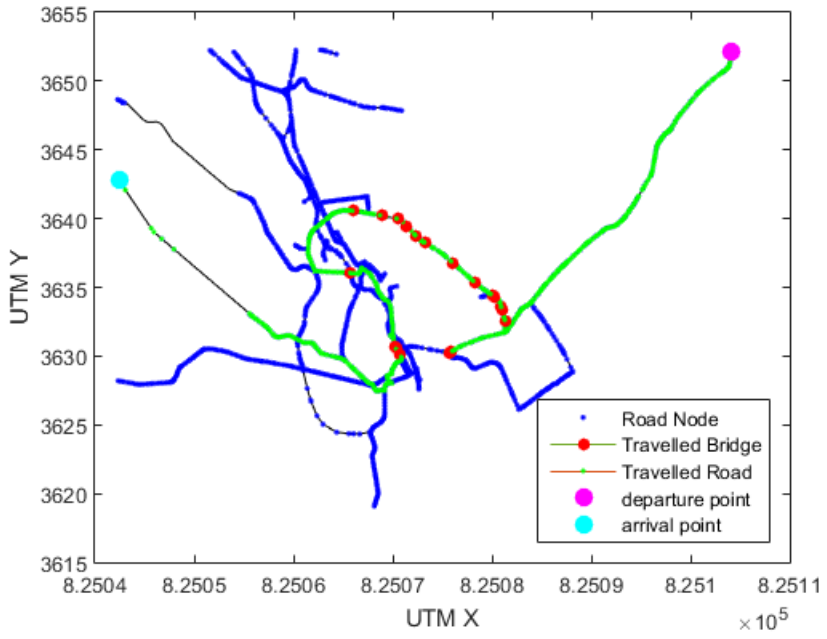


(c) 120 km travel distance

Figure 7.11: Arbitrary traveling scenarios

Traveling scenario “a” (79 km travel distance) was taken for the optimization case due to its shortest travel distance. The constraint for the allowable retrofit cost, based on equation 5.13, was US $71.085 million.

### 7.3.1 Optimization Model 2 for Event M7.1

For event M7.1, given that all strategies for the bridges are set to “do-nothing,” the failure probability for traveling and the total retrofit cost are as follows (Table 7.15):

Table 7.15: Failure probability of traveling and total retrofit cost for all strategies are set as “do nothing” (opt. model = 2, event M7.1)

| Pf travel | TotalRetrofitCost |
|---|---|
| 0.0530 | 0 |

Setting the GA maximum iteration to 80 and number of populations to 10, neglecting the retrofit cost, the GA results and iterations is shown as in Figure 7.12 and Table 7.16.

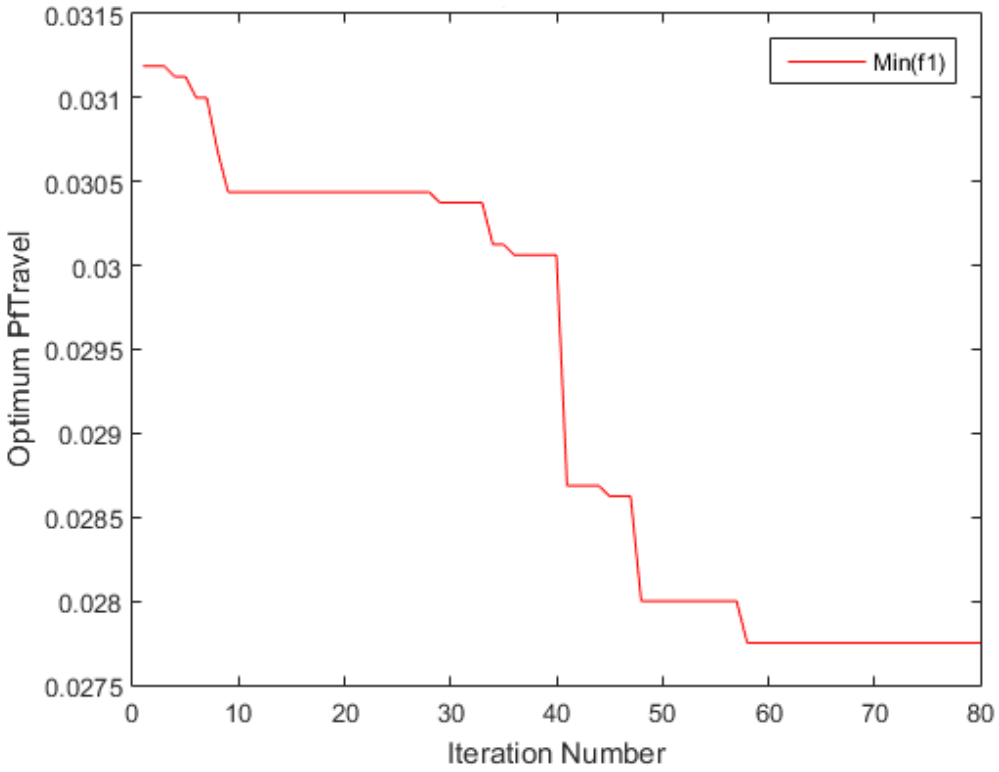


Figure 7.12: GA iteration for improving failure probability of travelling and neglecting total retrofit cost (event. = M7.1, opt. model = 2, w = 1, max. gen. = 80, pop. = 10, ATR = US $71.085 million)

Table 7.16 Improved sum of scores
(event. = M7.1, opt. model = 2, w = 1, max. gen. = 80, pop. = 10, ATR = US $71.085 million)

| Pf travel | TotalRetrofitCost |
|---|---|
| 0.02775 | US$54.8 million |

Based on the epicenter and magnitude of the earthquake for M7.1, the estimated failure probability of traveling is small even without any implementation for the retrofits. Therefore, event M7.3 is the focus of these study cases.

### 7.3.2 Optimization Model 2 for Event M.7.3

For case M7.3, given all strategies for the bridges are set to “do-nothing,” the failure probability for traveling and the total retrofit cost are as follows (Table 7.17):

Table 7.17: Failure probability of traveling and total retrofit cost for all strategies are set as “do nothing” (opt. model = 2, event M7.3)

| Pf travel | TotalRetrofitCost |
|---|---|
| 0.3501 | 0 |

Setting the GA maximum iteration to 500 and number of populations to 20, neglecting the retrofit cost, the minimization of failure probability of traveling cost gives the combination retrofit strategy as follows (Table 7.18):

Table 7.18: GA retrofit combinations for improving failure probability of travelling and total retrofit cost (event. = M7.3, opt. model = 2, w = 1, max. gen. = 500, pop. = 20, ATR = US $71.085 million)

| BridgeID | 9832 | 9825 | 5231 | 9838 | 9823 | 9824 | 9837 | 9836 |
|---|---|---|---|---|---|---|---|---|
| Retrofit | 7 | 8 | 3 | 2 | 2 | 4 | 2 | 4 |

The corresponding improved failure probability of traveling, neglecting the total retrofit cost is as follows (Table 7.19):

Table 7.19: Improved failure probability of travelling (event. = M7.3, opt. model = 2, w = 1, max. gen. = 500, pop. = 20, ATR = US $71.085 million)

| Pf travel | TotalRetrofitCost |
|---|---|
| 0.2504 | 4.4467e+07 |

As can be seen in Table 7.19, the total retrofit cost is far below ATR. Thus, the constraint is most likely inactive.

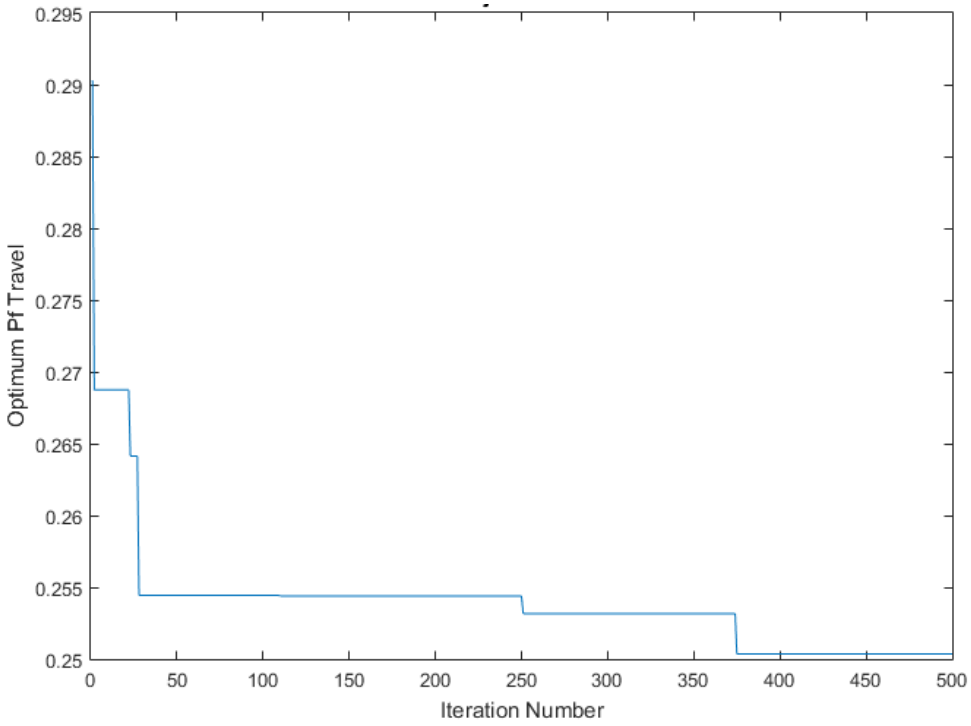


Figure 7.13: GA iteration for improving failure probability of travelling and neglecting total retrofit cost (event. = M7.3, opt. model = 2, w = 1, max. gen. = 500, pop. = 20, ATR = US $71.085 million)

Setting w = 0 (to minimize the cost), a simple GA run shows how the two objective functions contradict.

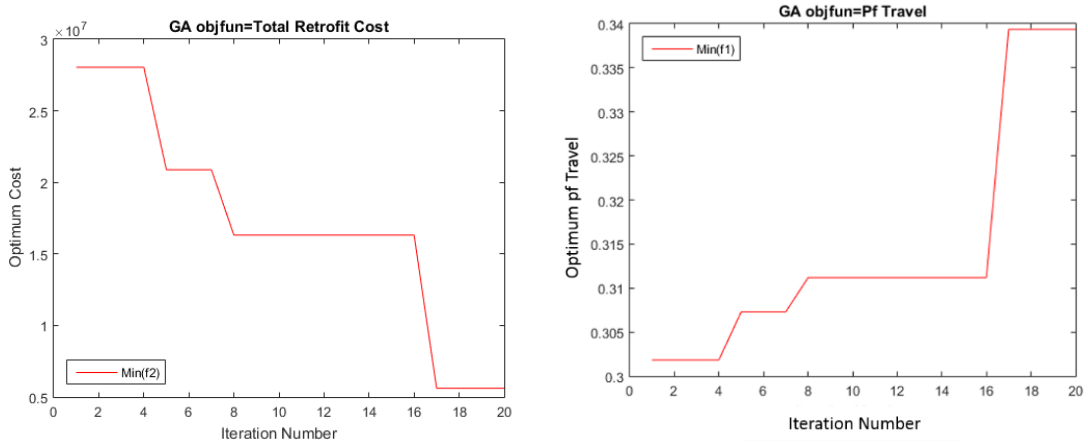


Figure 7.14: GA iteration for improving total retrofit cost neglecting failure probability of travelling (event. = M7.3, opt. model = 2, w = 0, max. gen. = 20, pop. = 5, ATR = US $71.085 million)

Varying the weights of the two objective functions above give the Pareto front as shown in Figure 7.15. Note that the node labeling is based on the failure probability of traveling or X-axis. The two objective functions, as can be seen from the optimization model and the plots, are conflicting. As the failure probability of traveling gets larger, the total retrofit cost gets smaller, indicating less effort is put into retrofitting the bridges.

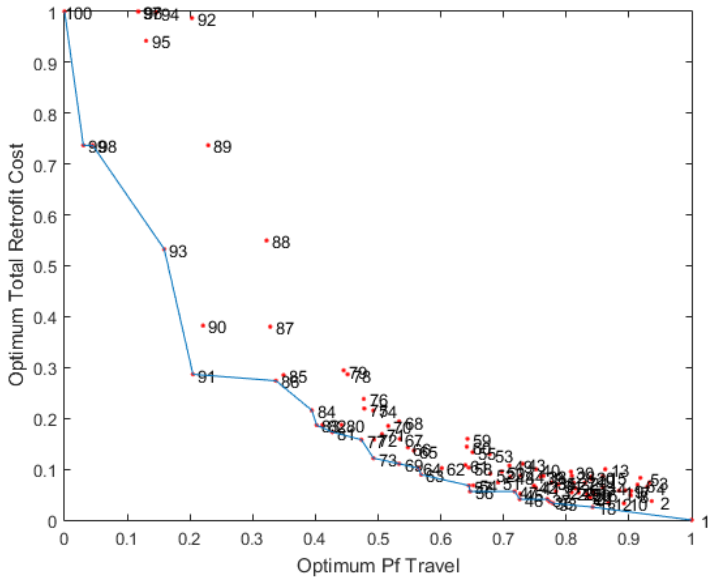


(a) Points labeled with objective function's weight w

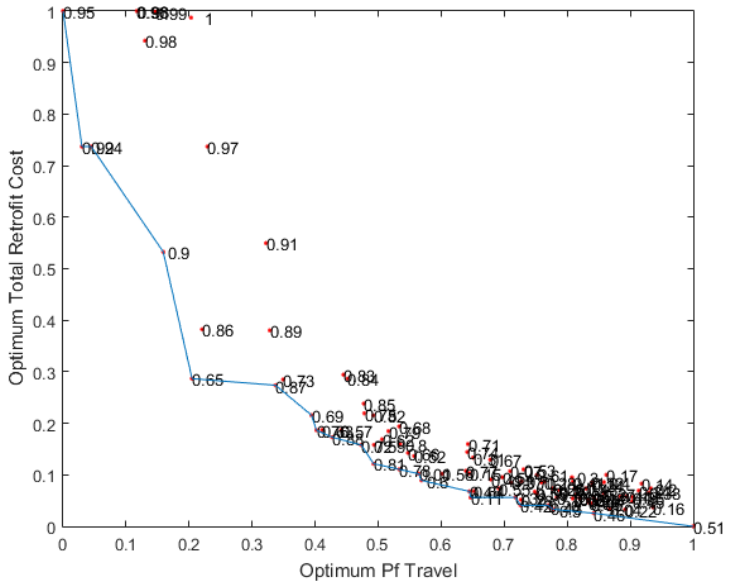


(b) Points labeled based on decreasing optimum failure probability in Pareto iterations

Figure 7.15: Pareto front for minimizing failure probability of travelling and minimizing total cost (event. = M7.3, opt. model = 2, Pareto points = 100, w = varied, max. gen. = 100, pop. = 10, ATR= US $71.085 million)

One of the suggested optimums from the Pareto frontier, if one desires to minimize the failure probability of traveling while still having reasonable total cost, is point 91 with the weight w = 0.65 shown in Figure 6.10. This gives a 5% increase in the failure probability of traveling from the previous result, but reduces the total retrofit cost by 61%.

Table 7.20: Improved failure probability and retrofit cost (event. = M7.3, opt. model = 2, w = 0.65, max. gen. = 100, pop. = 20, ATR = US $71.085 million)

| Pf travel | TotalRetrofitCost |
|---|---|
| 0.2631 | 1.7444+07 |

The corresponding retrofit combination is as follows (Table 7.21):

Table 7.21: GA retrofit combinations for improving failure probability of travelling and total retrofit cost (event. = M7.3, opt. model = 2, w = 0.65, max. gen. = 100, pop. = 20, ATR = US $71.085 million)

| BridgeID | 9832 | 9825 | 5231 | 9838 | 9823 | 9824 | 9837 | 9836 |
|---|---|---|---|---|---|---|---|---|
| Retrofit | 3 | 3 | 1 | 2 | 2 | 4 | 6 | 2 |

The allowable constraint retrofitting cost US $71.085 million (50% of maximum possible retrofit cost) is far from being active. One can try to use percent replacement cost 15.4% as the constraint which gives the allowable retrofit cost of US $16.894 million, which makes the result in Table 7.20 violate the constraint by 3% above the ATR.

However, since the Pareto frontier has given several options that are below US $16.894 million, and since US $17.444 million does not differ much from US $16.894 million relative to the observed range of cost and Pf travel around the suspected optimum, point 91 in the Pareto frontier was then taken as the best-improved candidate in this experiment.

# CHAPTER 8

## Technology Transfer

### 8.1 Usability

Since this investigation is partially funded through the USDOT C2M2 (Center for Connected Multimodal Mobility), one of the issues that was addressed during the research was technological transfer, with Departments of Transportation as target users. The tool strives to account for efficiency and usability. Many methods discussed in other research require the use of several tools to perform network modeling, visualization, analysis and optimization for retrofitting bridges, such as coupling HAZUS (running on top of a software: ESRI GIS ArcMap) and AMPL, an optimization software. This often raises problems in software accessibility, usability (having to learn the utilization of many platforms), and inefficiency (computational time). The tool developed in this investigation aimed to replace the need to use multi-platform with a single tool for modeling the network, seismic demand, and performing an optimization for developing retrofitting programs. Visualizations including geographical locations, seismic contours, bridge specific fragility curves, and optimization results are generated through plots, which makes the tool operate as an efficient and effective optimization system for developing new retrofitting programs.

To account for the usability aspect, a Graphical User Interface was programmed in Matlab. A GUI negates the need for the user to be familiar with the technical detail of the programming flow and syntax behind the developed tool, while still having controls on the modeling, analysis, and optimization tasks. The GUI was designed as a multi-window GUI, which appears one after another each time necessary information is generated from each routine, with most queried data presented as graphical representations. The multi-windows GUI allows the user to work progressively while having a clear picture regarding how the program works based on the guideline attached in each GUI.

### 8.2 Graphical User Interface

*ModelingNetworkANDDemand_GUI* shown in Figure 8.1 requires the input of geographical coordinate limits and center of network to define the study domain. The ADT target parameter filters the bridges to select only major bridges with high traffic capacity, which further narrows down the study domain. EQ event defines the earthquake scenario. *ModelingNetworkANDDemand_GUI* generates plots such as shown in Figures 3.2 and 3.3, and tables such as shown in Table 3.3 and Table 3.4. A plot showing the indices of the roads is also generated for the user to choose the arrival and departure point for the optimization case where minimizing the traveling failure probability becomes the main interest.

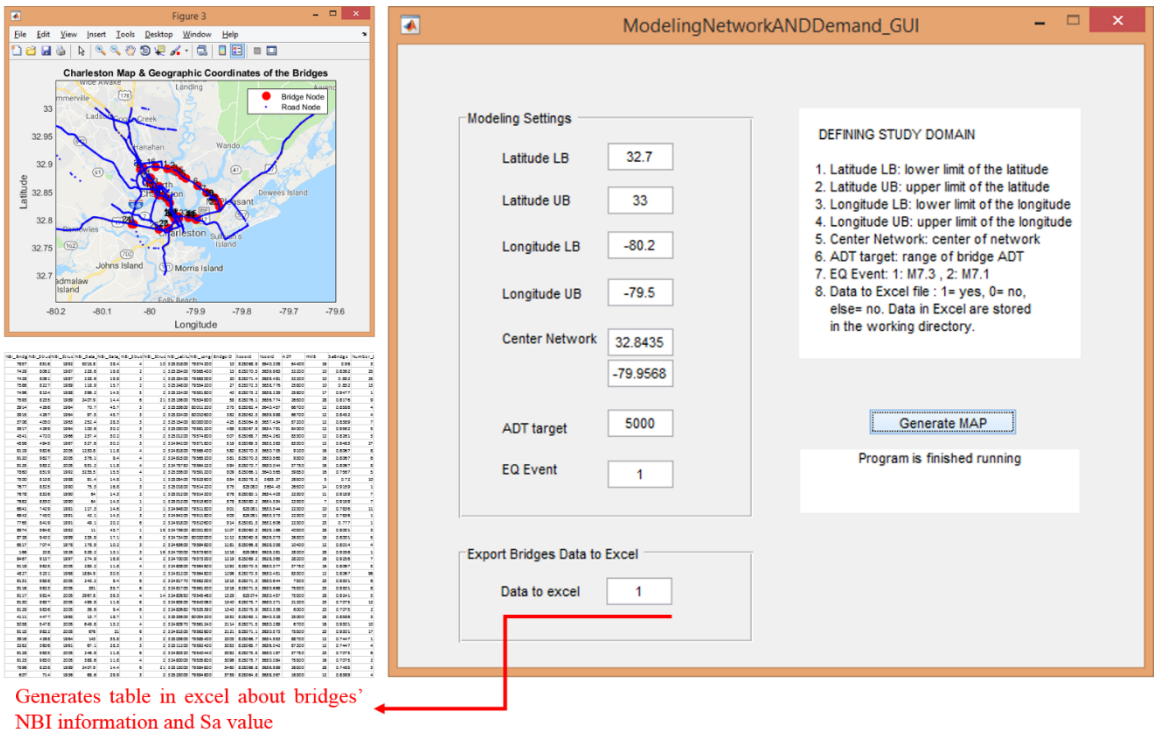


Figure 8.1: GUI to visualize the transportation network and seismic contour

The *GenerateBridgeFragilityCurves_GUI* appears only after *ModelingNetworkANDDemand_GUI* has finished running. *GenerateBridgeFragilityCurves_GUI* only has one field to be filled, which is the ID of the bridge. Bridge specific fragility curves and location of the selected bridge will be shown in plots based on user input. *GenerateBridgeFragilityCurves_GUI* generates plots such as shown in Figure 5.2.

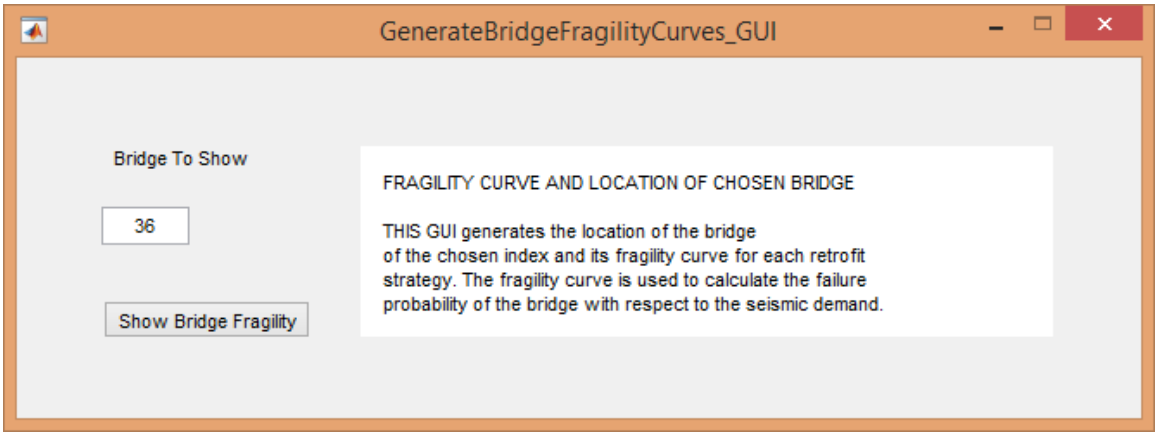


Figure 8.2: GUI to generate fragility curves

*SelectOptimizationModel_GUI* appears only after *GenerateBridgeFragilityCurves_GUI* has finished running. *SelectOptimizatioModel_GUI*

only has one field to be filled, which presently has two options for selecting the optimization model.

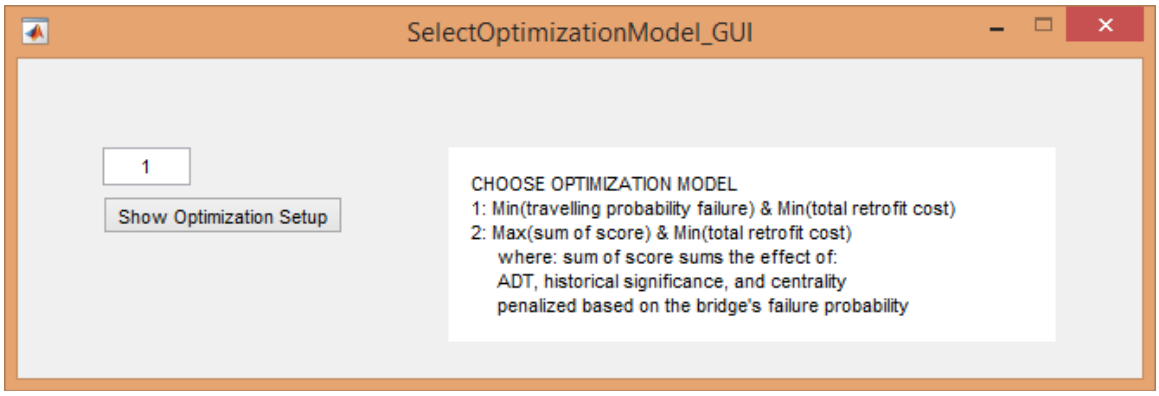


Figure 8.3: GUI to select an optimization model

Depending on the user input on the field in *SelectOptimizatioModel_GUI,* either the interface *CalculateBridgeConditionANDCost_GUI* (Figure 8.4) or *Calculate_PfTravel_Cost_GUI* (Figure 8.5) will appear. If the optimization model was set to 2, *CalculateBridgeConditionANDCost_GUI* will appear. *CalculateBridgeConditionANDCost_GUI* has two fields to be filled by the user. Both fields are related to the number of simulations required to calculate the failure probability of each bridge under the study domain and the retrofitting cost for each bridge.

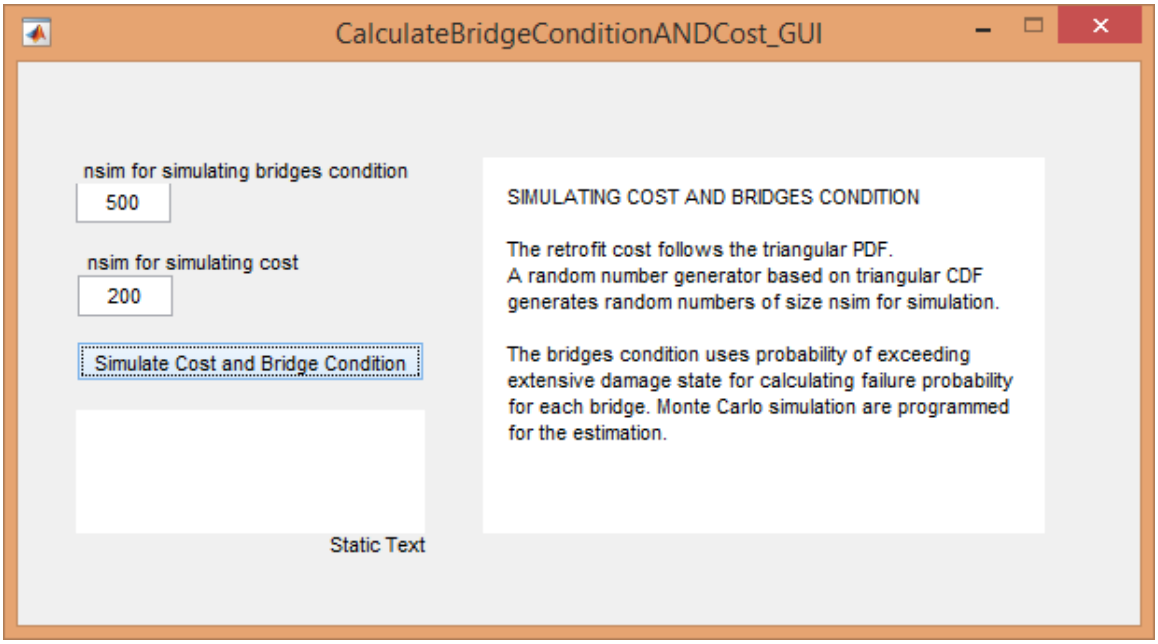


Figure 8.4: GUI to calculate bridge condition and retrofitting cost

*Calculate_PfTravel_Cost_GUI* has several fields to be filled by the user to calculate retrofitting cost, configure and visualize traveling paths with bridges intersecting the traveling paths, and choose the path to optimize. *Calculate_PfTravel_Cost_GUI* generates plots such as those shown in Figure 7.11.

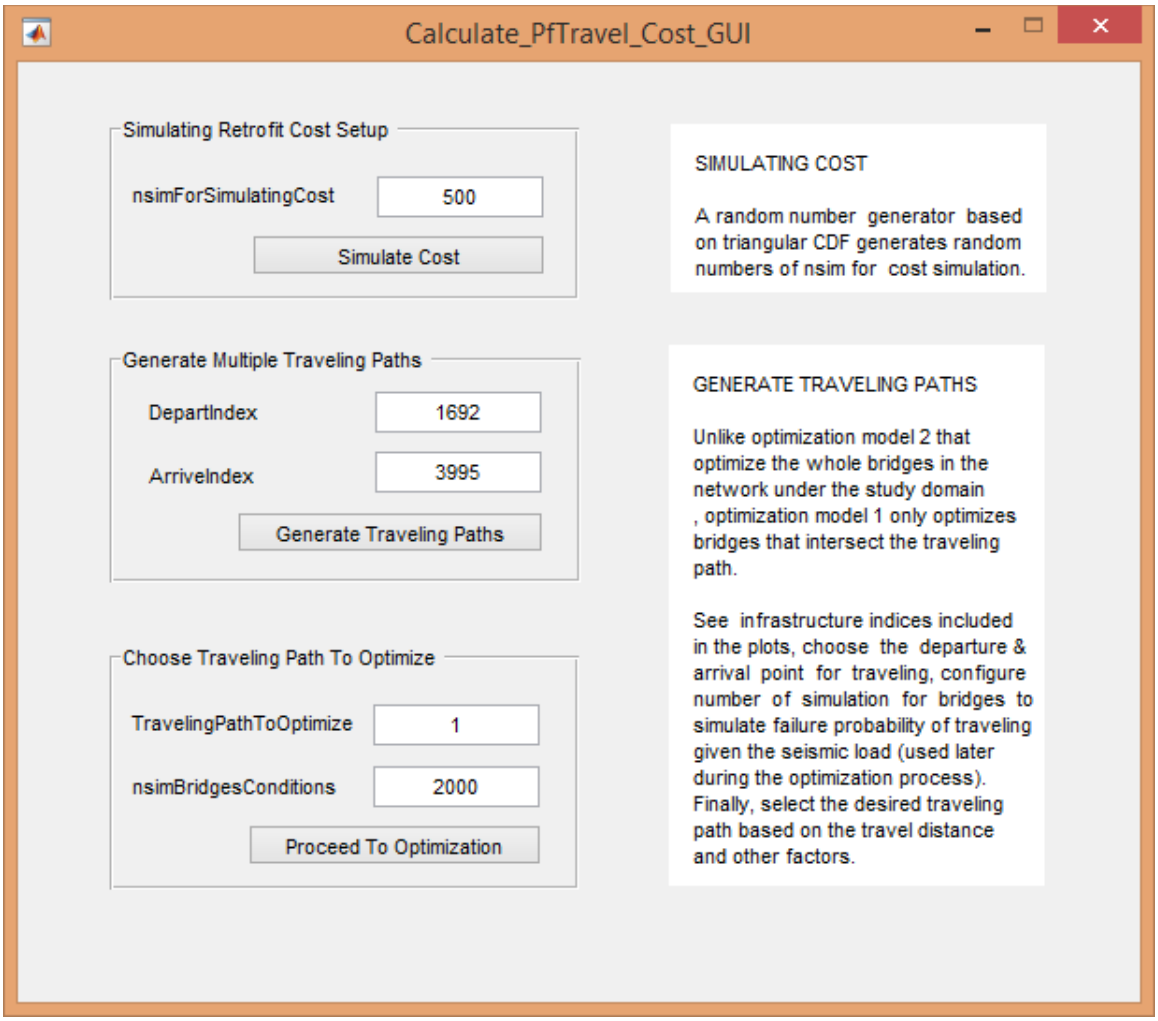


Figure 8.5: GUI to calculate retrofitting cost for each bridge, configure and visualize traveling paths, and choose traveling path to optimize

Both *CalculateBridgeConditionANDCost_GUI* and *Calculate_PfTravel_Cost_GUI* eventually converge to the final GUI, i.e., *Optimization_GUI*, which appears only after the previous GUI has finished running. *Optimization_GUI* has several fields to be filled by the user. In the first task, the user can input an arbitrary retrofitting combination and run the objective function one time to see the result of the desired combination. A field called "DataToExcel" generates a table in an Excel file that consists of detail comparative data between the undamaged, damaged (do nothing), and damaged (use optimized retrofit combination) of all bridge failure probability, ADT, HS, and centrality with the corresponding retrofitting cost. After acquiring a better grasp of the range of values that the objective function can take, the user can then proceed to the second task, that is to

run the optimization. The optimization reports the result via a text field. Copying and pasting this result, the user has the option to return to the first task to validate the optimization result with a one-time-run of the objective function. In the case for maximizing sum of score and minimizing retrofit cost, the user can have the option to configure the level of importance of ADT, HS, and centrality. The previous chapters assume these values to be unity, i.e., having the same importance, since the combinations are infinite and subjective in the sense that the importance of each of those parameters depends entirely on the judgement of the users, i.e., Departments of Transportation, under the consideration of certain time periods. However, using the GUI, these parameters are configurable, and thus turn the problem into a weighted sum of four objective functions problem, with three of them compacted into a single category, i.e., the bridge importance. *Optimization_GUI generates* plots such as shown in Figure 7.6, Figure 7.7, Figure 7.14, and Figure 7.15.

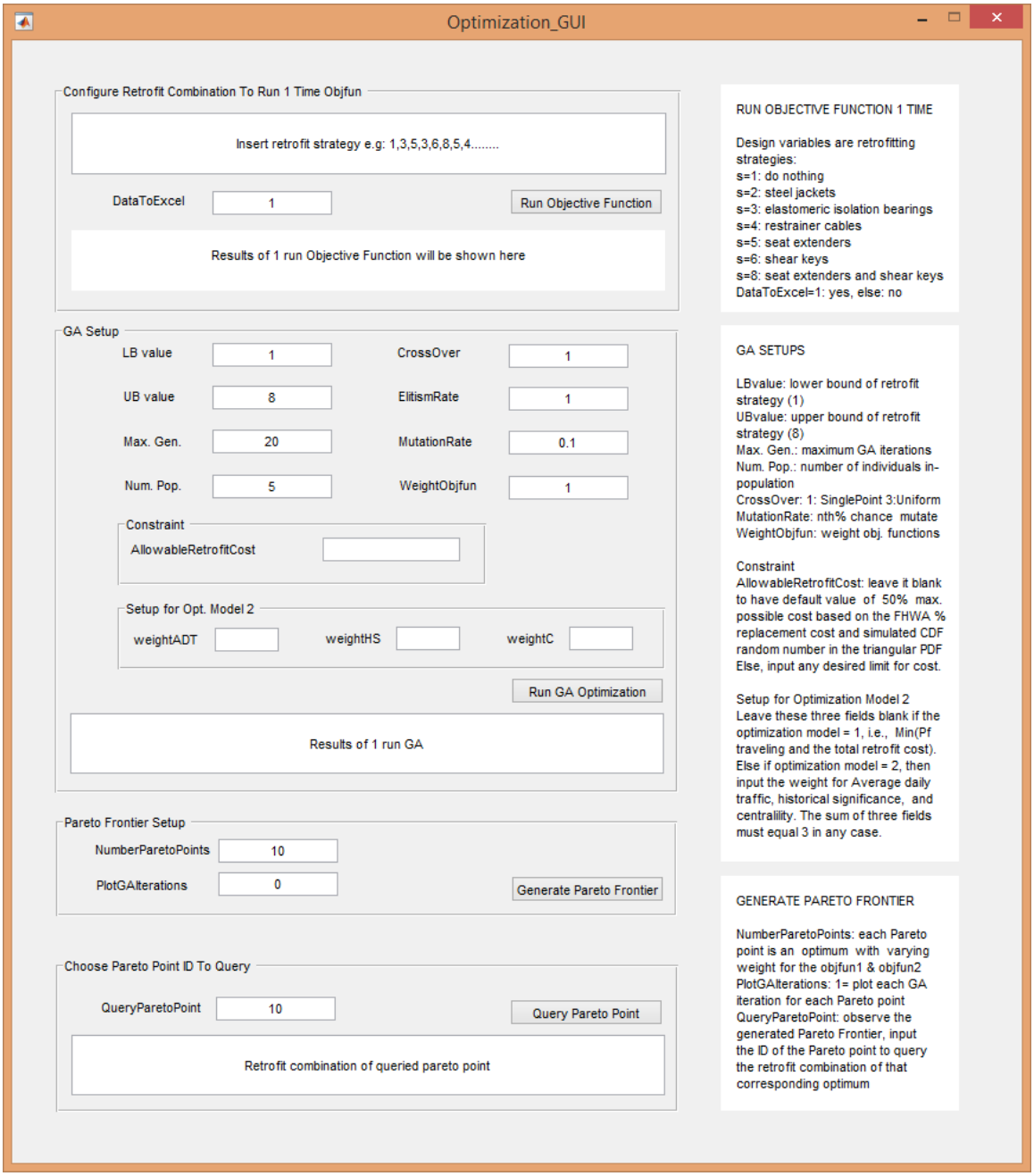


Figure 8.6: Default setups in optimization GUI

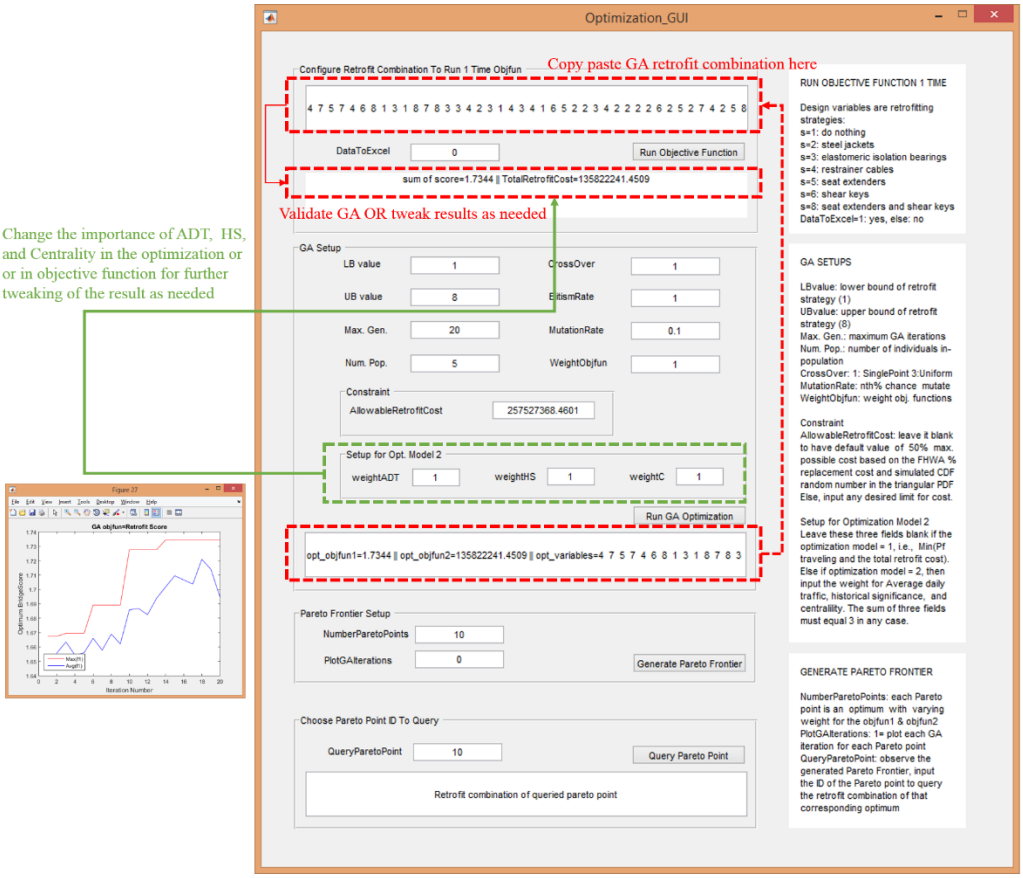


Figure 8.7: Optimization GUI when running GA

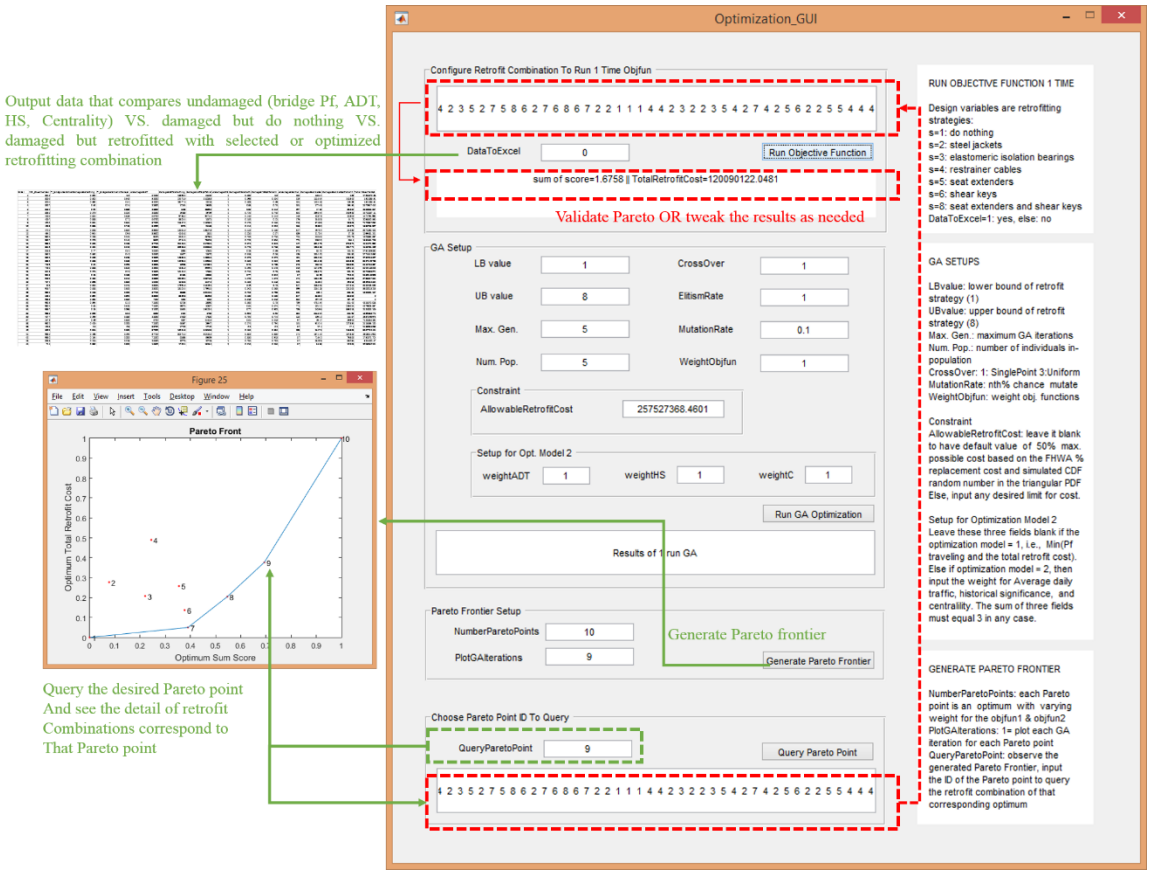


Figure 8.8: Optimization GUI when generating Pareto frontier

Re-running the Monte Carlo simulation with 20,000 simulations for retrofitting combinations shown in Table 7.10 and using the GUI, the results (Figure 8.9) are very close to the previous run as shown in Table 7.11. The sum of score is only reduced by 0.02% and the total retrofit cost differs by 2%. This is to be expected due to the probabilistic effect in the calculation of bridge failure and total retrofit cost. Setting the "DataToExcel= 1" gives the table as shown in the appendix A.

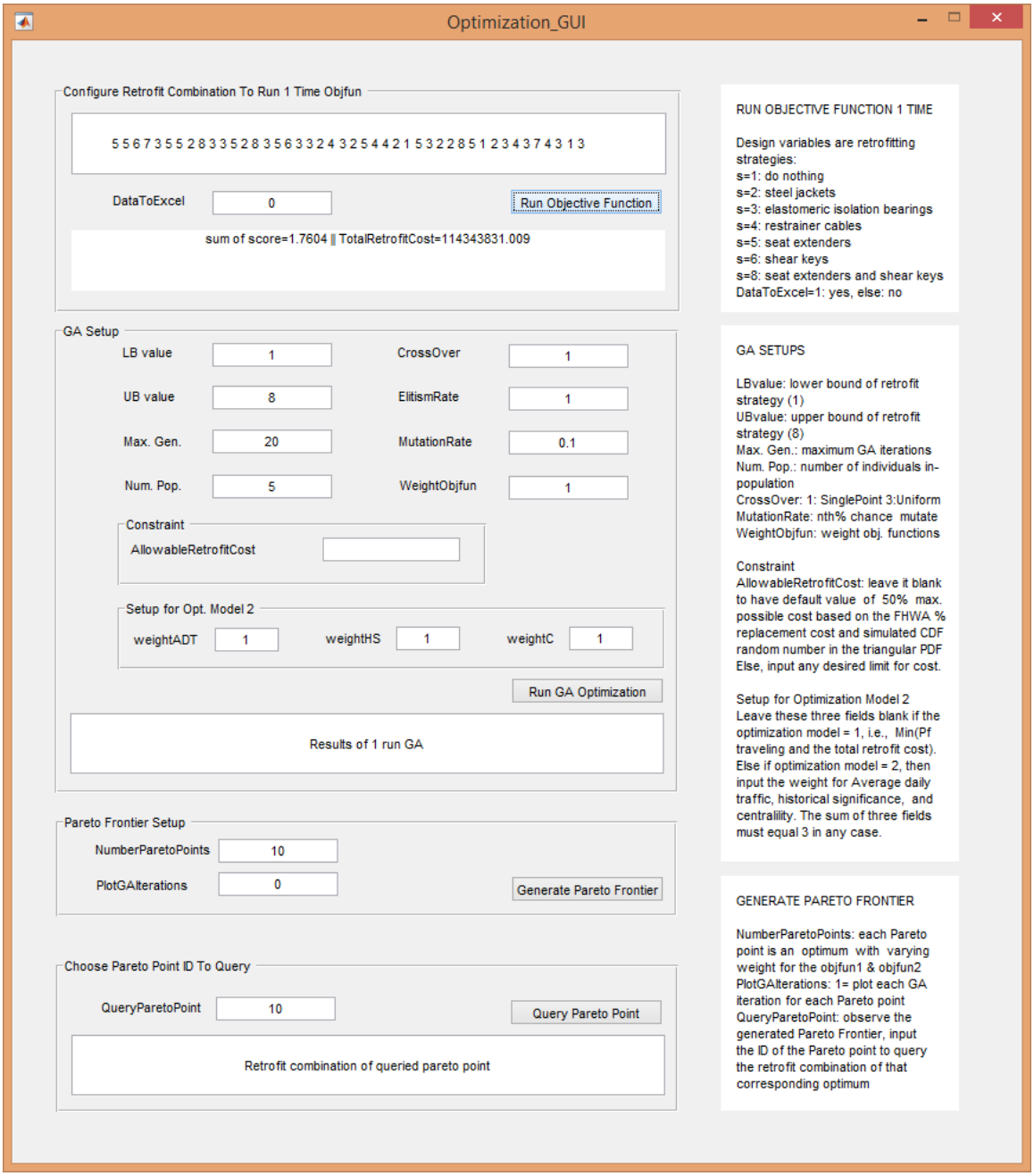


Figure 8.9: Run objective function using GUI for the same combination as in Table 7.10

# CHAPTER 9

## Summary and Conclusion

### 9.1 Summary

A significant number of bridges in the Southeastern and Central region of United States have been designed and constructed according to outdated seismic provisions. Recent studies have investigated potential damage in Charleston, however, most of these investigations do not account for important aspects of bridge importance simultaneously (such as centrality, historical significance, and traffic capacity). Furthermore, these prior investigations do not consider the actual detailing of structural connections, such as the critical pile-to-bent cap connection.

Full-scale experimental studies performed at the University of South Carolina were used to assess projected performance of such connections in a seismic event. This project develops a new tool that is informed with realistic structural behavior gained through full-scale experimental investigations and combines centrality, historical significance, and traffic capacity to assess expected damage. The results are useful for informing placement of monitoring systems, identification of potential retrofit strategies, and optimizing network performance.

This report presents results and discussion regarding the tool developed which can be used for optimizing the performance of a transportation network under seismic demand. The tool was designed to be versatile by employing SCDOT and USGS databases. NBI and Hazus databases were linked to the program to develop bridge-specific fragility curves. Monte Carlo simulations were implemented for calculating failure probability. Both the retrofit cost and fragility curves for the seven retrofit strategies were estimated based on the literature review in Chapter 2. The generation of Pareto frontier was coupled with the developed GA, which results in a range of optimal solutions, allowing the user to adjust them as desired. Finally, a multi-window GUI was developed to account for usability in technological transfer, with representatives of Departments of Transportation as potential users.

The optimization was implemented for events M7.1 and M7.3 for the Charleston network. The M7.3 simulated the 1886 Charleston earthquake with the same epicenter and become the focus of the studies. Two optimization models were formulated: (1) maximize the sum of score for ADT, HS, and centrality factored by bridge failure probability while minimizing total retrofit cost, and (2) minimizing failure probability of traveling while minimizing total retrofit cost. Both are modeled as integer programming problems.

From the Pareto frontier, the result of optimization model 1 gives improved candidates that increase the ADT, HS, and centrality for the 44 bridges as shown in Appendix A. It was found from the Pareto frontier that relaxing the constraint to allow retrofit US $257.52 million resulted in one of the optimum candidates with the sum of

score of 1.7608 and total retrofit cost of US $116.96 million. Pushing the total retrofit cost to US $122 million gave the sum of score of 1.7221 with total retrofit cost of US $110.42 million, indicating that the optimum for balancing retrofit cost and sum of score approaches the constraint of allowable retrofit cost US $122 million. The result with the sum of score 1.7608 from the Pareto frontier was the best candidate which balances those two aspects.

The results for the optimization model 2 have a conflicting objective function, which is shown by the Pareto frontier that decreases in the total retrofit cost as the failure probability of traveling increases. A solution from one of the improved candidates in the Pareto frontier was picked which balances the minimization of the failure probability of traveling and cost with the weight w = 0.65 in the second optimization model.

## 9.2 Conclusion

A significant number of bridges in the Southeastern and Central region of United States have been designed with insufficient seismic consideration. It has been estimated that close to 800 bridges would be closed if the Charleston event M7.3 (1886) was to reoccur. In anticipation of this potential consequence, this investigation develops a new tool that is informed with actual structural behavior gained through full-scale experimental investigations and combines centrality, historical significance, and traffic capacity to assess expected damage. The results are useful for informing placement of monitoring systems, identification of potential retrofit strategies, and optimizing network performance.

Many methods discussed in other investigations require the use of several tools to for optimization of retrofitting bridges, such as using Hazus (running on top of ESRI GIS ArcMap) coupled with AMPL, an optimization software. This raises issues in software accessibility, usability (having to become familiar with many platforms), and inefficiency (computational time). However, the tool developed in this research aimed to replace the need to use multiple platforms by a single tool. A multi-window GUI was developed to guide the user in the modeling, analysis, and optimization process for developing an optimized monitoring, and potentially, retrofitting program. With few changes in parameters in the GUI, the tool can be used to adjust the study domain and run different optimization scenarios. Several representations were generated in a single run to observe the study domain, seismic contours, and bridge-specific fragility curves with respect to various retrofitting strategies, and ranges of optimized retrofit programs with respect to bridge failure probability, traffic capacity, centrality, historical significance, and retrofit cost. In addition, results and other information are automatically generated and tabulated in Excel for users to readily post-process, observe the improvements, select the retrofitting programs, or make other adjustments as desired.

This investigation addresses efficiency in the decision-making process through a single platform tool having multiple solutions. The tool couples GA and the generation of a Pareto frontier to provide ranges of improved candidates, as a single optimum is likely to be unrealistic for implementation. There are always many aspects that are not cannot

be accounted for in any optimization model. The solution must provide a range of improved candidates as opposed to a single optimum, leaving the potential for external aspects to be considered during the decision-making process.

## 9.3 Future Research

The present work relies on the USGS shake map for generating seismic scenarios. Although two scenarios are used in the research, M7.1 and M7.3, only the 1886 M7.3 event was investigated in detail due to its historically known severe impact and estimated future damage if the event was to reoccur. The earthquake parameters and the spectra acceleration induced by the earthquake are based on the USGS database which relates to the actual event. An alternative option to create richer variation of scenarios is to use Hazus, such as using the same epicenter but modifying the attenuation function, the moment magnitude, depth, orientation of fault rupture, dip angle and so forth. However, a proper setup of the parameters for generating the scenarios can only be achieved through consultations with experts in geology. As the goal of this investigation is to create a tool that produces schematic plans for monitoring and/or retrofitting programs, incorporating other software would reduce efficiency in terms of software accessibility and usability, and therefore is outside the focus of the present research. The current investigation addresses the actual behavior of pile-to-bent cap connections, and therefore represents a significant improvement over the simplified approach to fragility curves, more work is needed in identification of the actual structural details used for the bridges included in the study including dimensional information, pile embedment depth in the bent cap, detailing of steel reinforcement in this region, and the point of fixity of the pile below grade.

# REFERENCES

AMPL Optimization Inc. (2013). *AMPL: Streamlined modeling for real optimization.* Retrieved May 2, 2018, from http://ampl.com/

Anay, R., Cortez, T. M., Jáuregui, D. V., ElBatanouny, M. K., and Ziehl, P. (2015) On-site acoustic-emission monitoring for assessment of a prestressed concrete double-tee-beam bridge without plans. *Journal of Performance of Constructed Facilities*, 30(4), pp. 04015062-1-9.

Anay, R., Soltangharaei, V., Assi, L., Devol, T., Ziehl, P., (2018) Identification of Damage Mechanisms in Cement Paste Based on Acoustic Emission, *Construction and Building Materials*, Vol. 164, 10, pp. 286-296.

ASTM. (2014). "Standard terminology for nondestructive examinations." E1316, West Conshohocken, PA

Billah, M., Bhuiyan, A., & Alam, S. (2013) Fragility analysis of retrofitted multi-column bridge bent subjected to near-fault and far field ground motion. *Journal of Bridge Engineering, 18*, 992-1004.

Bollinger, G. A., Johnston, A. C., Talwani, P., Long, L. T., Shedlock, K. M., Sibol, M. S., et al. (1991) Seismicity of the southeastern united States1698 to 1986. In D. B. Slemmons, E. R. Engdahl, M. D. Zoback & D. and Blackwell (Eds.), *Neotectonics of North America, Geological Society of America* (Decade Map Volume I ed., pp. 291-308)

Cartz, L. (1995) *Nondestructive Testing*. U.S. Department of Energy Office of Scientific and Technical Information, https://www.osti.gov/biblio/260617.

Chen, L. (2013). Quantifying annual bridge cost by overweight trucks in South Carolina. (M.S. Civil Engineering, Clemson University). *Tigerprints,*

Dutton, C. E. (1889) *The Charleston earthquake of august 31, 1886* No. 9) U.S. Geological Survey.

Emergency Management Division. (2012) *South Carolina earthquake guide.*

Federal Emergency Management Agency. (2013) *Hazus - MH 2.1: Technical manual*

Federal Highway Administration. (1995) *Recording and coding guide for the structure inventory and appraisal of the nation's bridges* No. FHWA-PD-96-001). Washington, D.C.: U.S. Department of Transportation.

Federal Highway Administration. (2006) *Seismic retrofitting manual for highway structures: Part 1- bridges*

Golaski, L., Gebski, P., and Ono, K. (2002) Diagnostics of reinforced concrete bridges by acoustic emission. *Journal of acoustic emission*, 20, pp. 83-89.

Hadzor, T. J. (2011) Acoustic Emission Testing of Repaired Prestressed Concrete Bridge Girders. *Master Thesis, Auburn University*, pp. 1-182.

Hedar, A. *Booth function.* Retrieved May 1, 2017, from http://www-optima.amp.i.kyoto-u.ac.jp/member/student/hedar/Hedar_files/TestGO_files/Page816.htm

Hedar, A. *Easom function.* Retrieved May 1, 2017, from http://www-optima.amp.i.kyoto-u.ac.jp/member/student/hedar/Hedar_files/TestGO_files/Page1361.htm

Ironistic. (2018). *2017 infrastructure report card.* Retrieved Augustus/20, 2018, from https://www.infrastructurereportcard.org/cat-item/bridges/

Jamil, M., & Yang, X. (2013). A literature survey of benchmark functions for global optimization problems. *Int. Journal of Mathematical Modelling and Numerical Optimization, 4*(2), 150-194.

Jeremic, B. (2004) A brief overview of the NEESgrid simulation platform OpenSEES: Application to the Soil–Foundation–Structure interaction problems. *Third UJNR Workshop on Soil–Structure Interaction,* California. *, 3.*

Joel. (2008). *Photograph of Ashley memorial bridge.* Retrieved August/28, 2018, from https://www.flickr.com/photos/8x7/2262069802/

Johnston, A. C. (1996) Seismic moment assessment of earthquakes in stable continental regions, III, New Madrid 1811-1812, charleston 1886 and Lisbon 1755, *Geophysical Journal International, 126*, 314-344.

Larosche, A., Cukrov, M., Sanders, D., and Ziehl, P., (2014a) Prestressed Pile to Bent Cap Connections: Seismic Performance of a Full-Scale Three-Pile Specimen. *ASCE Journal of Bridge Engineering*, Vol.19 (3), 04013012: pp. 1-10.

Larosche, A., Ziehl, P., ElBatanouny, M., and Caicedo, J., (2014b) Plain Pile Embedment for Exterior Bent Cap Connections in Seismic Regions. *Journal of Bridge Engineering*, Vol. 19, No. 4, 04013016: pp. 1-12.

Larosche, A., Ziehl, P., Mangual, J., and ElBatanouny, M., (2015) Damage Evaluation of Prestressed Pile to Bent Cap Connections with Acoustic Emission. *Engineering Structures*, Vol. 84, pp. 184-194.

Larson, H. (2000) *Seismic retrofit techniques.* Retrieved August/16, 2018, from http://www.loc.gov/pictures/item/ca2189.sheet.00002a/

Malherbe, C., Contal, E., & Vayatis, N. (2016) A ranking approach to global optimization. *Proceedings of the 33st International Conference on Machine Learning (ICML),*

Mitchell, M. (1998) *An introduction to genetic algorithms* MIT Press.

Molga, M., & Smutnicki, C. (2005) *Test functions for optimization needs.* Retrieved May 1, 2017, from http://www.zsd.ict.pwr.wroc.pl/files/docs/functions.pdf

Nuttli, O., Bollinger, G. A., & Hermann, R. (1986). *The 1886 Charleston, South Carolina, earthquake, A 1986 perspective* No. 985). Denver: U.S. GEOLOGICAL SURVEY CIRCULAR.

Padgett, J., & DesRoches, R. (2009) Retrofitted bridge fragility analysis for typical classes of multi-span bridges. *Earthquake Spectra, 25*(1), 117-141.

Padgett, J., Dennemann, K., & Ghosh, J. (2010) Risk-based seismic life-cycle cost–benefit (LCC-B) analysis for bridge retrofit assessment. *Structural Safety, 32*, 165.

Parmelee, S. (2013) Optimal retrofit strategy design for highway bridges under seismic hazards: A case study of charleston. (M.S. Civil Engineering, Clemson University). *Tigerprint,*

Rardin, R. (1997) *Optimization in operations research*. Prentice Hall: Pearson.

Roberts, J. (1996) US perspectives on seismic design of bridges. *Eleventh World Conference on Earthquake Engineering,* Sacramento. *, 11.* (2109)

Sastry, K., Goldberg, D., & Kendall, G. (2005) Genetic algorithms. In E. K. Burke, & G. Kendall (Eds.), *Search methodologies*. Boston, MA: Springer.

Shinozuka, M., Kim, S., Kushiyama, S., & Yi, J. -. (2002) Fragility curves of concrete bridges retrofitted by column jacketing. *Earthquake Eng. Vib., 1*, 195-205.

Soltangharaei, V., Anay, R., Hayes, N., Assi, L., Le Pape, Y., Ma, Z., and Ziehl, P. (2018) Damage Mechanism Evaluation of Large-Scale Concrete Structures Affected by Alkali-Silica Reaction Using Acoustic Emission. *Applied Sciences*, 8(11), pp. 1-19.

South Carolina Department of Transportation. (2018). *gis/mapping.* Retrieved May/20, 2018,
from http://info2.scdot.org/sites/GIS/SitePages/GISFiles.aspx?MapType=Shape

Stover, C. W., & Coffman, J. L. (1993) *Seismicity of the United States, 1568-1989 (revised)* No. 1527)U.S. Geological Survey Professional.

Surjavonic, S., & Bingham, D. (2015) *Levy function N.13.* Retrieved May 1, 2017, from https://www.sfu.ca/~ssurjano/levy13.html

Świt, G. (2018) Acoustic Emission Method for Locating and Identifying Active Destructive Processes in Operating Facilities. *Journal of Applied Sciences*, 8(8), 1295, pp.1-20.

Takamine, H., Watabe, K., Miyata, H., Asaue, H., Nishida, T., and Shiotani, T. (2018) Efficient damage inspection of deteriorated RC bridge deck with rain-induced elastic wave. *Construction and Building Materials*, 162, pp. 908-913.

The MathWorks. (2017) *Matlab: The language of technical computing.* Retrieved January 10, 2018, from https://www.mathworks.com/products/matlab.html

TRIPmedia. (2018) *Charleston road map.* Retrieved Augustus/20, 2018, from https://www.tripinfo.com/maps/SC-Charleston.htm

USGS. (2018) *Scenario catalogs.* Retrieved Augustus/20, 2018, from https://earthquake.usgs.gov/scenarios/catalog/

Wilson, N., & Ryan, K. (2009) *Seismic retrofit guidelines for Utah highway bridges* No. UT-09.06). Salt Lake City: Utah Department of Transportation.

Wipf, T. J., Klaiber, F. W., & and Russo, F. M. (1997) *Evaluation of seismic retrofit methods for reinforced concrete bridge columns* No. NCEER-97-0016). University at Buffalo: National Center for Earthquake Engineering Research.

Wong, I., Bouabid, J., Graf, W., Huyck, C., Porush, A., Silva, W., et al. (2005) Potential losses in a repeat of the 1886 charleston. *Earthquake. SCEMD,*

Wonoto, N., & Blouin, V. (2019) Integrating grasshopper and Matlab for shape optimization and structural form-finding of buildings. *Computer-Aided Design and Applications, 16*(1), 1-12.

Ziehl, P. H., Caicedo, J. M., Rizos, D., Mays, T., Larosche, A., ElBatanouny, M. K., and Mustain, B. (2012) Behavior of pile to bent cap connections subjected to seismic forces. *Rep. No. FHWA-SC-12-03, South Carolina DOT, Columbia, SC,* pp. 1-268.

# APPENDICES

## Appendix A

Optimum from 1 run GA
Case: Event M7.3
Optimization: Model 1, w = 1
GA maximum generation = 200
GA population = 20
Strategy:

| | | | | | | | | | |
|---|---|---|---|---|---|---|---|---|---|
| BridgeID | 8516 | 8062 | 8061 | 8227 | 8134 | 8235 | 4266 | 4267 | 4050 |
| Retrofit | 3 | 4 | 5 | 6 | 8 | 3 | 1 | 4 | 4 |
| BridgeID | 4269 | 4720 | 4945 | 9826 | 9827 | 9832 | 8519 | 8138 | 8325 |
| Retrofit | 2 | 3 | 3 | 3 | 2 | 7 | 4 | 2 | 3 |
| BridgeID | 8326 | 8330 | 7429 | 7430 | 8419 | 9648 | 9402 | 7074 | 228 |
| Retrofit | 8 | 2 | 2 | 3 | 2 | 3 | 7 | 1 | 2 |
| BridgeID | 9137 | 9825 | 5231 | 9838 | 9823 | 9824 | 9837 | 9836 | 4477 |
| Retrofit | 1 | 2 | 3 | 1 | 2 | 1 | 4 | 4 | 7 |
| BridgeID | 5478 | 9822 | 4268 | 3606 | 9835 | 9830 | 8238 | 714 | |
| Retrofit | 6 | 2 | 3 | 3 | 3 | 4 | 2 | 1 | |

Total retrofit cost at optimum = US $166.7 million

Comparison of average daily traffic:

| BridgeID | UndamagedADT | ADT_Damaged & do-nothing | ADT_Damaged & opt. |
|---|---|---|---|
| 8516 | 64400 | 44200.94 | 52157.56 |
| 8062 | 32200 | 22010.31 | 22306.55 |
| 8061 | 32200 | 21640.01 | 21646.45 |
| 8227 | 25800 | 17623.98 | 17656.23 |
| 8134 | 25800 | 2782.53 | 3239.19 |
| 8235 | 26500 | 19570.25 | 20253.95 |
| 4266 | 66700 | 10018.34 | 10018.34 |
| 4267 | 66700 | 8824.41 | 9654.825 |
| 4050 | 87200 | 14008.68 | 15094.32 |
| 4269 | 84000 | 9273.6 | 11352.6 |
| 4720 | 83300 | 12636.61 | 25231.57 |
| 4945 | 83300 | 5264.56 | 12944.82 |
| 9826 | 9100 | 6541.535 | 7636.72 |
| 9827 | 9300 | 6730.41 | 7445.58 |
| 9832 | 37750 | 27238.5125 | 30873.8375 |
| 8519 | 39850 | 31069.0525 | 32776.625 |
| 8138 | 26500 | 6043.325 | 10543.025 |
| 8325 | 26500 | 15833.75 | 20636.875 |
| 8326 | 22300 | 14604.27 | 14643.295 |
| 8330 | 22300 | 14373.465 | 17897.98 |
| 7429 | 22300 | 16199.835 | 18001.675 |
| 7430 | 22300 | 4025.15 | 7600.955 |
| 8419 | 22300 | 15979.065 | 19093.26 |
| 9648 | 40500 | 30336.525 | 31344.975 |
| 9402 | 26300 | 19302.885 | 20177.36 |
| 7074 | 10400 | 1209.52 | 1209.52 |
| 228 | 28200 | 18720.57 | 23004.15 |
| 9137 | 28200 | 18234.12 | 18234.12 |
| 9825 | 37750 | 28176.6 | 30669.9875 |
| 5231 | 83300 | 8692.355 | 18692.52 |
| 9838 | 7500 | 4866 | 4866 |
| 9823 | 75500 | 48580.475 | 60350.925 |
| 9824 | 75500 | 50520.825 | 50520.825 |
| 9837 | 21200 | 16511.62 | 17510.14 |
| 9836 | 6000 | 5320.2 | 5477.7 |
| 4477 | 25000 | 17912.5 | 18580 |
| 5478 | 6700 | 4243.78 | 4712.78 |
| 9822 | 75500 | 45613.325 | 58278.45 |
| 4268 | 88700 | 17819.83 | 33191.54 |
| 3606 | 87200 | 17195.84 | 32656.4 |
| 9835 | 37750 | 30216.9875 | 30985.2 |
| 9830 | 75500 | 66964.725 | 69524.175 |
| 8238 | 26500 | 20801.175 | 23778.45 |
| 714 | 16300 | 1647.93 | 1647.93 |

Comparison of historical significance values:

| BridgeID | UndamagedHS | HS_damaged_doNothing | HS_damaged_opt |
|---|---|---|---|
| 8516 | 1 | 0.68635 | 0.8099 |
| 8062 | 1 | 0.68355 | 0.69275 |
| 8061 | 1 | 0.67205 | 0.67225 |
| 8227 | 1 | 0.6831 | 0.68435 |
| 8134 | 1 | 0.10785 | 0.12555 |
| 8235 | 1 | 0.7385 | 0.7643 |
| 4266 | 1 | 0.1502 | 0.1502 |
| 4267 | 1 | 0.1323 | 0.14475 |
| 4050 | 1 | 0.16065 | 0.1731 |
| 4269 | 1 | 0.1104 | 0.13515 |
| 4720 | 1 | 0.1517 | 0.3029 |
| 4945 | 1 | 0.0632 | 0.1554 |
| 9826 | 1 | 0.71885 | 0.8392 |
| 9827 | 1 | 0.7237 | 0.8006 |
| 9832 | 1 | 0.72155 | 0.81785 |
| 8519 | 1 | 0.77965 | 0.8225 |
| 8138 | 1 | 0.22805 | 0.39785 |
| 8325 | 1 | 0.5975 | 0.77875 |
| 8326 | 1 | 0.6549 | 0.65665 |
| 8330 | 1 | 0.64455 | 0.8026 |
| 7429 | 1 | 0.72645 | 0.80725 |
| 7430 | 1 | 0.1805 | 0.34085 |
| 8419 | 1 | 0.71655 | 0.8562 |
| 9648 | 1 | 0.74905 | 0.77395 |
| 9402 | 2 | 1.4679 | 1.5344 |
| 7074 | 1 | 0.1163 | 0.1163 |
| 228 | 5 | 3.31925 | 4.07875 |
| 9137 | 1 | 0.6466 | 0.6466 |
| 9825 | 1 | 0.7464 | 0.81245 |
| 5231 | 1 | 0.10435 | 0.2244 |
| 9838 | 1 | 0.6488 | 0.6488 |
| 9823 | 1 | 0.64345 | 0.79935 |
| 9824 | 1 | 0.66915 | 0.66915 |
| 9837 | 1 | 0.77885 | 0.82595 |
| 9836 | 1 | 0.8867 | 0.91295 |
| 4477 | 1 | 0.7165 | 0.7432 |
| 5478 | 1 | 0.6334 | 0.7034 |
| 9822 | 1 | 0.60415 | 0.7719 |
| 4268 | 1 | 0.2009 | 0.3742 |
| 3606 | 1 | 0.1972 | 0.3745 |
| 9835 | 1 | 0.80045 | 0.8208 |
| 9830 | 1 | 0.88695 | 0.92085 |
| 8238 | 1 | 0.78495 | 0.8973 |
| 714 | 2 | 0.2022 | 0.2022 |

Comparison of centrality values:

| BridgeID | UndamagedCentral | CENTRAL_damaged_doNothing | CENTRAL_damaged_opt |
|---|---|---|---|
| 8516 | 235 | 161.29225 | 190.3265 |
| 8062 | 223 | 152.43165 | 154.48325 |
| 8061 | 231 | 155.24355 | 155.28975 |
| 8227 | 261 | 178.2891 | 178.61535 |
| 8134 | 297 | 32.03145 | 37.28835 |
| 8235 | 331 | 244.4435 | 252.9833 |
| 4266 | 143 | 21.4786 | 21.4786 |
| 4267 | 179 | 23.6817 | 25.91025 |
| 4050 | 213 | 34.21845 | 36.8703 |
| 4269 | 263 | 29.0352 | 35.54445 |
| 4720 | 327 | 49.6059 | 99.0483 |
| 4945 | 389 | 24.5848 | 60.4506 |
| 9826 | 755 | 542.73175 | 633.596 |
| 9827 | 775 | 560.8675 | 620.465 |
| 9832 | 447 | 322.53285 | 365.57895 |
| 8519 | 253 | 197.25145 | 208.0925 |
| 8138 | 375 | 85.51875 | 149.19375 |
| 8325 | 429 | 256.3275 | 334.08375 |
| 8326 | 481 | 315.0069 | 315.84865 |
| 8330 | 529 | 340.96695 | 424.5754 |
| 7429 | 573 | 416.25585 | 462.55425 |
| 7430 | 613 | 110.6465 | 208.94105 |
| 8419 | 649 | 465.04095 | 555.6738 |
| 9648 | 87 | 65.16735 | 67.33365 |
| 9402 | 171 | 125.50545 | 131.1912 |
| 7074 | 251 | 29.1913 | 29.1913 |
| 228 | 327 | 217.07895 | 266.75025 |
| 9137 | 399 | 257.9934 | 257.9934 |
| 9825 | 825 | 615.78 | 670.27125 |
| 5231 | 817 | 85.25395 | 183.3348 |
| 9838 | 805 | 522.284 | 522.284 |
| 9823 | 789 | 507.68205 | 630.68715 |
| 9824 | 771 | 515.91465 | 515.91465 |
| 9837 | 709 | 552.20465 | 585.59855 |
| 9836 | 681 | 603.8427 | 621.71895 |
| 4477 | 155 | 111.0575 | 115.196 |
| 5478 | 97 | 61.4398 | 68.2298 |
| 9822 | 161 | 97.26815 | 124.2759 |
| 4268 | 87 | 17.4783 | 32.5554 |
| 3606 | 289 | 56.9908 | 108.2305 |
| 9835 | 171 | 136.87695 | 140.3568 |
| 9830 | 87 | 77.16465 | 80.11395 |
| 8238 | 87 | 68.29065 | 78.0651 |
| 714 | 87 | 8.7957 | 8.7957 |

Comparison of failure probability:

| | Retrofit Strategy | |
|---|---|---|
| Bridge ID | All “do nothing” | optimal. |
| 8516 | 0.31365 | 0.1901 |
| 8062 | 0.31645 | 0.30725 |
| 8061 | 0.32795 | 0.32775 |
| 8227 | 0.3169 | 0.31565 |
| 8134 | 0.89215 | 0.87445 |
| 8235 | 0.2615 | 0.2357 |
| 4266 | 0.8498 | 0.8498 |
| 4267 | 0.8677 | 0.85525 |
| 4050 | 0.83935 | 0.8269 |
| 4269 | 0.8896 | 0.86485 |
| 4720 | 0.8483 | 0.6971 |
| 4945 | 0.9368 | 0.8446 |
| 9826 | 0.28115 | 0.1608 |
| 9827 | 0.2763 | 0.1994 |
| 9832 | 0.27845 | 0.18215 |
| 8519 | 0.22035 | 0.1775 |
| 8138 | 0.77195 | 0.60215 |
| 8325 | 0.4025 | 0.22125 |
| 8326 | 0.3451 | 0.34335 |
| 8330 | 0.35545 | 0.1974 |
| 7429 | 0.27355 | 0.19275 |
| 7430 | 0.8195 | 0.65915 |
| 8419 | 0.28345 | 0.1438 |
| 9648 | 0.25095 | 0.22605 |
| 9402 | 0.26605 | 0.2328 |
| 7074 | 0.8837 | 0.8837 |
| 228 | 0.33615 | 0.18425 |
| 9137 | 0.3534 | 0.3534 |
| 9825 | 0.2536 | 0.18755 |
| 5231 | 0.89565 | 0.7756 |
| 9838 | 0.3512 | 0.3512 |
| 9823 | 0.35655 | 0.20065 |
| 9824 | 0.33085 | 0.33085 |
| 9837 | 0.22115 | 0.17405 |
| 9836 | 0.1133 | 0.08705 |
| 4477 | 0.2835 | 0.2568 |
| 5478 | 0.3666 | 0.2966 |
| 9822 | 0.39585 | 0.2281 |
| 4268 | 0.7991 | 0.6258 |
| 3606 | 0.8028 | 0.6255 |
| 9835 | 0.19955 | 0.1792 |
| 9830 | 0.11305 | 0.07915 |
| 8238 | 0.21505 | 0.1027 |
| 714 | 0.8989 | 0.8989 |

Chosen Optimum from Pareto Frontier
Case: Event M7.3
Optimization: Model 1, w = 0.9
GA maximum generation = 50
GA population = 10
Strategy:

| BridgeID | 8516 | 8062 | 8061 | 8227 | 8134 | 8235 | 4266 | 4267 | 4050 |
|---|---|---|---|---|---|---|---|---|---|
| Retrofit | 5 | 5 | 6 | 7 | 3 | 5 | 5 | 2 | 8 |
| BridgeID | 4269 | 4720 | 4945 | 9826 | 9827 | 9832 | 8519 | 8138 | 8325 |
| Retrofit | 3 | 3 | 5 | 2 | 8 | 3 | 5 | 6 | 3 |
| BridgeID | 8326 | 8330 | 7429 | 7430 | 8419 | 9648 | 9402 | 7074 | 228 |
| Retrofit | 3 | 2 | 4 | 3 | 2 | 5 | 4 | 4 | 2 |
| BridgeID | 9137 | 9825 | 5231 | 9838 | 9823 | 9824 | 9837 | 9836 | 4477 |
| Retrofit | 1 | 5 | 3 | 2 | 2 | 8 | 5 | 1 | 2 |
| BridgeID | 5478 | 9822 | 4268 | 3606 | 9835 | 9830 | 8238 | 714 | |
| Retrofit | 3 | 4 | 3 | 7 | 4 | 3 | 1 | 3 | |

Total retrofit cost at optimum= US $116.9 million

Comparison of average daily traffic:

| BridgeID | UndamagedADT | ADT_damaged_doNothing | ADT_damaged_opt |
|---|---|---|---|
| 8516 | 64400 | 43779.12 | 44171.96 |
| 8062 | 32200 | 22063.44 | 22111.74 |
| 8061 | 32200 | 21578.83 | 21979.72 |
| 8227 | 25800 | 17564.64 | 18305.1 |
| 8134 | 25800 | 2764.47 | 3261.12 |
| 8235 | 26500 | 19465.575 | 20067.125 |
| 4266 | 66700 | 10061.695 | 10131.73 |
| 4267 | 66700 | 8697.68 | 10338.5 |
| 4050 | 87200 | 13345.96 | 13520.36 |
| 4269 | 84000 | 9294.6 | 20949.6 |
| 4720 | 83300 | 12203.45 | 24290.28 |
| 4945 | 83300 | 5360.355 | 5102.125 |
| 9826 | 9100 | 6595.225 | 7246.33 |
| 9827 | 9300 | 6887.58 | 7473.48 |
| 9832 | 37750 | 27287.5875 | 31747.75 |
| 8519 | 39850 | 30768.185 | 30939.54 |
| 8138 | 26500 | 6036.7 | 7298.1 |
| 8325 | 26500 | 15881.45 | 20659.4 |
| 8326 | 22300 | 14706.85 | 16959.15 |
| 8330 | 22300 | 14333.325 | 17969.34 |
| 7429 | 22300 | 16236.63 | 16452.94 |
| 7430 | 22300 | 3959.365 | 7673.43 |
| 8419 | 22300 | 16000.25 | 19135.63 |
| 9648 | 40500 | 30447.9 | 31037.175 |
| 9402 | 26300 | 19338.39 | 20523.205 |
| 7074 | 10400 | 1191.84 | 1322.36 |
| 228 | 28200 | 18917.97 | 23050.68 |
| 9137 | 28200 | 18128.37 | 18128.37 |
| 9825 | 37750 | 27931.225 | 27831.1875 |
| 5231 | 83300 | 8417.465 | 19321.435 |
| 9838 | 7500 | 4843.125 | 6007.125 |
| 9823 | 75500 | 48044.425 | 60298.075 |
| 9824 | 75500 | 50513.275 | 52748.075 |
| 9837 | 21200 | 16658.96 | 16816.9 |
| 9836 | 6000 | 5346.9 | 5346.9 |
| 4477 | 25000 | 17818.75 | 21436.25 |
| 5478 | 6700 | 4230.715 | 5157.66 |
| 9822 | 75500 | 45922.875 | 50120.675 |
| 4268 | 88700 | 17283.195 | 32716.995 |
| 3606 | 87200 | 16999.64 | 19380.2 |
| 9835 | 37750 | 30175.4625 | 31645.825 |
| 9830 | 75500 | 67032.675 | 71351.275 |
| 8238 | 26500 | 20692.525 | 20692.525 |
| 714 | 16300 | 1652.005 | 3650.385 |

Comparison of historical significance values:

| BridgeID | UndamagedHS | HS_damaged_doNothing | HS_damaged_opt |
|---|---|---|---|
| 8516 | 1 | 0.6798 | 0.6859 |
| 8062 | 1 | 0.6852 | 0.6867 |
| 8061 | 1 | 0.67015 | 0.6826 |
| 8227 | 1 | 0.6808 | 0.7095 |
| 8134 | 1 | 0.10715 | 0.1264 |
| 8235 | 1 | 0.73455 | 0.75725 |
| 4266 | 1 | 0.15085 | 0.1519 |
| 4267 | 1 | 0.1304 | 0.155 |
| 4050 | 1 | 0.15305 | 0.15505 |
| 4269 | 1 | 0.11065 | 0.2494 |
| 4720 | 1 | 0.1465 | 0.2916 |
| 4945 | 1 | 0.06435 | 0.06125 |
| 9826 | 1 | 0.72475 | 0.7963 |
| 9827 | 1 | 0.7406 | 0.8036 |
| 9832 | 1 | 0.72285 | 0.841 |
| 8519 | 1 | 0.7721 | 0.7764 |
| 8138 | 1 | 0.2278 | 0.2754 |
| 8325 | 1 | 0.5993 | 0.7796 |
| 8326 | 1 | 0.6595 | 0.7605 |
| 8330 | 1 | 0.64275 | 0.8058 |
| 7429 | 1 | 0.7281 | 0.7378 |
| 7430 | 1 | 0.17755 | 0.3441 |
| 8419 | 1 | 0.7175 | 0.8581 |
| 9648 | 1 | 0.7518 | 0.76635 |
| 9402 | 2 | 1.4706 | 1.5607 |
| 7074 | 1 | 0.1146 | 0.12715 |
| 228 | 5 | 3.35425 | 4.087 |
| 9137 | 1 | 0.64285 | 0.64285 |
| 9825 | 1 | 0.7399 | 0.73725 |
| 5231 | 1 | 0.10105 | 0.23195 |
| 9838 | 1 | 0.64575 | 0.80095 |
| 9823 | 1 | 0.63635 | 0.79865 |
| 9824 | 1 | 0.66905 | 0.69865 |
| 9837 | 1 | 0.7858 | 0.79325 |
| 9836 | 1 | 0.89115 | 0.89115 |
| 4477 | 1 | 0.71275 | 0.85745 |
| 5478 | 1 | 0.63145 | 0.7698 |
| 9822 | 1 | 0.60825 | 0.66385 |
| 4268 | 1 | 0.19485 | 0.36885 |
| 3606 | 1 | 0.19495 | 0.22225 |
| 9835 | 1 | 0.79935 | 0.8383 |
| 9830 | 1 | 0.88785 | 0.94505 |
| 8238 | 1 | 0.78085 | 0.78085 |
| 714 | 2 | 0.2027 | 0.4479 |

Comparison of centrality values:

| BridgeID | UndamagedCentral | CENTRAL_damaged_doNothing | CENTRAL_damaged_opt |
|---|---|---|---|
| 8516 | 235 | 159.753 | 161.1865 |
| 8062 | 223 | 152.7996 | 153.1341 |
| 8061 | 231 | 154.80465 | 157.6806 |
| 8227 | 261 | 177.6888 | 185.1795 |
| 8134 | 297 | 31.82355 | 37.5408 |
| 8235 | 331 | 243.13605 | 250.64975 |
| 4266 | 143 | 21.57155 | 21.7217 |
| 4267 | 179 | 23.3416 | 27.745 |
| 4050 | 213 | 32.59965 | 33.02565 |
| 4269 | 263 | 29.10095 | 65.5922 |
| 4720 | 327 | 47.9055 | 95.3532 |
| 4945 | 389 | 25.03215 | 23.82625 |
| 9826 | 755 | 547.18625 | 601.2065 |
| 9827 | 775 | 573.965 | 622.79 |
| 9832 | 447 | 323.11395 | 375.927 |
| 8519 | 253 | 195.3413 | 196.4292 |
| 8138 | 375 | 85.425 | 103.275 |
| 8325 | 429 | 257.0997 | 334.4484 |
| 8326 | 481 | 317.2195 | 365.8005 |
| 8330 | 529 | 340.01475 | 426.2682 |
| 7429 | 573 | 417.2013 | 422.7594 |
| 7430 | 613 | 108.83815 | 210.9333 |
| 8419 | 649 | 465.6575 | 556.9069 |
| 9648 | 87 | 65.4066 | 66.67245 |
| 9402 | 171 | 125.7363 | 133.43985 |
| 7074 | 251 | 28.7646 | 31.91465 |
| 228 | 327 | 219.36795 | 267.2898 |
| 9137 | 399 | 256.49715 | 256.49715 |
| 9825 | 825 | 610.4175 | 608.23125 |
| 5231 | 817 | 82.55785 | 189.50315 |
| 9838 | 805 | 519.82875 | 644.76475 |
| 9823 | 789 | 502.08015 | 630.13485 |
| 9824 | 771 | 515.83755 | 538.65915 |
| 9837 | 709 | 557.1322 | 562.41425 |
| 9836 | 681 | 606.87315 | 606.87315 |
| 4477 | 155 | 110.47625 | 132.90475 |
| 5478 | 97 | 61.25065 | 74.6706 |
| 9822 | 161 | 97.92825 | 106.87985 |
| 4268 | 87 | 16.95195 | 32.08995 |
| 3606 | 289 | 56.34055 | 64.23025 |
| 9835 | 171 | 136.68885 | 143.3493 |
| 9830 | 87 | 77.24295 | 82.21935 |
| 8238 | 87 | 67.93395 | 67.93395 |
| 714 | 87 | 8.81745 | 19.48365 |

Comparison of failure probability:

| | Retrofit Strategies | |
|---|---|---|
| Bridge ID | All “do nothing” | optimal. |
| 8516 | 0.3202 | 0.3141 |
| 8062 | 0.3148 | 0.3133 |
| 8061 | 0.32985 | 0.3174 |
| 8227 | 0.3192 | 0.2905 |
| 8134 | 0.89285 | 0.8736 |
| 8235 | 0.26545 | 0.24275 |
| 4266 | 0.84915 | 0.8481 |
| 4267 | 0.8696 | 0.845 |
| 4050 | 0.84695 | 0.84495 |
| 4269 | 0.88935 | 0.7506 |
| 4720 | 0.8535 | 0.7084 |
| 4945 | 0.93565 | 0.93875 |
| 9826 | 0.27525 | 0.2037 |
| 9827 | 0.2594 | 0.1964 |
| 9832 | 0.27715 | 0.159 |
| 8519 | 0.2279 | 0.2236 |
| 8138 | 0.7722 | 0.7246 |
| 8325 | 0.4007 | 0.2204 |
| 8326 | 0.3405 | 0.2395 |
| 8330 | 0.35725 | 0.1942 |
| 7429 | 0.2719 | 0.2622 |
| 7430 | 0.82245 | 0.6559 |
| 8419 | 0.2825 | 0.1419 |
| 9648 | 0.2482 | 0.23365 |
| 9402 | 0.2647 | 0.21965 |
| 7074 | 0.8854 | 0.87285 |
| 228 | 0.32915 | 0.1826 |
| 9137 | 0.35715 | 0.35715 |
| 9825 | 0.2601 | 0.26275 |
| 5231 | 0.89895 | 0.76805 |
| 9838 | 0.35425 | 0.19905 |
| 9823 | 0.36365 | 0.20135 |
| 9824 | 0.33095 | 0.30135 |
| 9837 | 0.2142 | 0.20675 |
| 9836 | 0.10885 | 0.10885 |
| 4477 | 0.28725 | 0.14255 |
| 5478 | 0.36855 | 0.2302 |
| 9822 | 0.39175 | 0.33615 |
| 4268 | 0.80515 | 0.63115 |
| 3606 | 0.80505 | 0.77775 |
| 9835 | 0.20065 | 0.1617 |
| 9830 | 0.11215 | 0.05495 |
| 8238 | 0.21915 | 0.21915 |
| 714 | 0.89865 | 0.77605 |

GUI Implementation to Previous Case (Detail Retrofit Cost Included)

This re-run is of the objective function using the GUI with different solutions from Monte Carlo simulations. The setting was conducted in the GUI, with the tabular results directly copy-pasted from the generated table in Excel from the developed tool.
Case: Event M7.3
Optimization: Model 1, w = 0.9
Strategy:

| | | | | | | | | | |
|---|---|---|---|---|---|---|---|---|---|
| BridgeID | 8516 | 8062 | 8061 | 8227 | 8134 | 8235 | 4266 | 4267 | 4050 |
| Retrofit | 5 | 5 | 6 | 7 | 3 | 5 | 5 | 2 | 8 |
| BridgeID | 4269 | 4720 | 4945 | 9826 | 9827 | 9832 | 8519 | 8138 | 8325 |
| Retrofit | 3 | 3 | 5 | 2 | 8 | 3 | 5 | 6 | 3 |
| BridgeID | 8326 | 8330 | 7429 | 7430 | 8419 | 9648 | 9402 | 7074 | 228 |
| Retrofit | 3 | 2 | 4 | 3 | 2 | 5 | 4 | 4 | 2 |
| BridgeID | 9137 | 9825 | 5231 | 9838 | 9823 | 9824 | 9837 | 9836 | 4477 |
| Retrofit | 1 | 5 | 3 | 2 | 2 | 8 | 5 | 1 | 2 |
| BridgeID | 5478 | 9822 | 4268 | 3606 | 9835 | 9830 | 8238 | 714 | |
| Retrofit | 3 | 4 | 3 | 7 | 4 | 3 | 1 | 3 | |

Total retrofit cost at optimum= US $114.34 million

Comparison of average daily traffic:

| Order | NBI_StructNumber | OptStrategy(OS) | Pf_(s=1) | Pf_(s=OS) | UndamagedADT | DamagedADT(s=1) | DamagedADT(s=OS) |
|---|---|---|---|---|---|---|---|
| 1 | 8516 | 5 | 0.31065 | 0.3155 | 64400 | 44394.14 | 44081.8 |
| 2 | 8062 | 5 | 0.31195 | 0.317 | 32200 | 22155.21 | 21992.6 |
| 3 | 8061 | 6 | 0.3266 | 0.3191 | 32200 | 21683.48 | 21924.98 |
| 4 | 8227 | 7 | 0.32315 | 0.2939 | 25800 | 17462.73 | 18217.38 |
| 5 | 8134 | 3 | 0.89285 | 0.878 | 25800 | 2764.47 | 3147.6 |
| 6 | 8235 | 5 | 0.2638 | 0.25075 | 26500 | 19509.3 | 19855.125 |
| 7 | 4266 | 5 | 0.8501 | 0.84895 | 66700 | 9998.33 | 10075.035 |
| 8 | 4267 | 2 | 0.8682 | 0.847 | 66700 | 8791.06 | 10205.1 |
| 9 | 4050 | 8 | 0.84285 | 0.84155 | 87200 | 13703.48 | 13816.84 |
| 10 | 4269 | 3 | 0.8869 | 0.75415 | 84000 | 9500.4 | 20651.4 |
| 11 | 4720 | 3 | 0.85575 | 0.7004 | 83300 | 12016.025 | 24956.68 |
| 12 | 4945 | 5 | 0.9367 | 0.93675 | 83300 | 5272.89 | 5268.725 |
| 13 | 9826 | 2 | 0.27465 | 0.20685 | 9100 | 6600.685 | 7217.665 |
| 14 | 9827 | 8 | 0.26535 | 0.1973 | 9300 | 6832.245 | 7465.11 |
| 15 | 9832 | 3 | 0.27675 | 0.15965 | 37750 | 27302.6875 | 31723.2125 |
| 16 | 8519 | 5 | 0.22325 | 0.2257 | 39850 | 30953.4875 | 30855.855 |
| 17 | 8138 | 6 | 0.7722 | 0.7244 | 26500 | 6036.7 | 7303.4 |
| 18 | 8325 | 3 | 0.4106 | 0.21735 | 26500 | 15619.1 | 20740.225 |
| 19 | 8326 | 3 | 0.3466 | 0.23935 | 22300 | 14570.82 | 16962.495 |
| 20 | 8330 | 2 | 0.35375 | 0.19955 | 22300 | 14411.375 | 17850.035 |
| 21 | 7429 | 4 | 0.27075 | 0.26115 | 22300 | 16262.275 | 16476.355 |
| 22 | 7430 | 3 | 0.8295 | 0.6549 | 22300 | 3802.15 | 7695.73 |
| 23 | 8419 | 2 | 0.28215 | 0.14455 | 22300 | 16008.055 | 19076.535 |
| 24 | 9648 | 5 | 0.2483 | 0.2416 | 40500 | 30443.85 | 30715.2 |
| 25 | 9402 | 4 | 0.2675 | 0.21335 | 26300 | 19264.75 | 20688.895 |
| 26 | 7074 | 4 | 0.8808 | 0.87245 | 10400 | 1239.68 | 1326.52 |
| 27 | 228 | 2 | 0.33415 | 0.18165 | 28200 | 18776.97 | 23077.47 |
| 28 | 9137 | 1 | 0.35025 | 0.35025 | 28200 | 18322.95 | 18322.95 |
| 29 | 9825 | 5 | 0.25845 | 0.2576 | 37750 | 27993.5125 | 28025.6 |
| 30 | 5231 | 3 | 0.8952 | 0.76625 | 83300 | 8729.84 | 19471.375 |
| 31 | 9838 | 2 | 0.3553 | 0.19855 | 7500 | 4835.25 | 6010.875 |
| 32 | 9823 | 2 | 0.36645 | 0.20495 | 75500 | 47833.025 | 60026.275 |
| 33 | 9824 | 8 | 0.33215 | 0.30555 | 75500 | 50422.675 | 52430.975 |
| 34 | 9837 | 5 | 0.20905 | 0.20145 | 21200 | 16768.14 | 16929.26 |
| 35 | 9836 | 1 | 0.1157 | 0.1157 | 6000 | 5305.8 | 5305.8 |
| 36 | 4477 | 2 | 0.28165 | 0.14905 | 25000 | 17958.75 | 21273.75 |
| 37 | 5478 | 3 | 0.36425 | 0.22935 | 6700 | 4259.525 | 5163.355 |
| 38 | 9822 | 4 | 0.3942 | 0.33525 | 75500 | 45737.9 | 50188.625 |
| 39 | 4268 | 3 | 0.8027 | 0.62535 | 88700 | 17500.51 | 33231.455 |
| 40 | 3606 | 7 | 0.79735 | 0.78215 | 87200 | 17671.08 | 18996.52 |
| 41 | 9835 | 4 | 0.1969 | 0.1607 | 37750 | 30317.025 | 31683.575 |
| 42 | 9830 | 3 | 0.11055 | 0.055 | 75500 | 67153.475 | 71347.5 |
| 43 | 8238 | 1 | 0.21555 | 0.21555 | 26500 | 20787.925 | 20787.925 |
| 44 | 714 | 3 | 0.90085 | 0.77025 | 16300 | 1616.145 | 3744.925 |

| UndamagedHS | DamagedHS(s=1) | DamagedHS(s=OS) | UndamagedCentral | DamagedCentral(s=1) | DamagedCentral(s=OS) | RetrofitCost(s=OS) |
|---|---|---|---|---|---|---|
| 1 | 0.68935 | 0.6845 | 235 | 161.99725 | 160.8575 | 10358639.42 |
| 1 | 0.68805 | 0.683 | 223 | 153.43515 | 152.309 | 295521.5173 |
| 1 | 0.6734 | 0.6809 | 231 | 155.5554 | 157.2879 | 1359043.97 |
| 1 | 0.67685 | 0.7061 | 261 | 176.65785 | 184.2921 | 560497.3952 |
| 1 | 0.10715 | 0.122 | 297 | 31.82355 | 36.234 | 2575362.912 |
| 1 | 0.7362 | 0.74925 | 331 | 243.6822 | 248.00175 | 3226332.45 |
| 1 | 0.1499 | 0.15105 | 143 | 21.4357 | 21.60015 | 322533.1434 |
| 1 | 0.1318 | 0.153 | 179 | 23.5922 | 27.387 | 2045521.041 |
| 1 | 0.15715 | 0.15845 | 213 | 33.47295 | 33.74985 | 3279132.167 |
| 1 | 0.1131 | 0.24585 | 263 | 29.7453 | 64.65855 | 1394723.309 |
| 1 | 0.14425 | 0.2996 | 327 | 47.16975 | 97.9692 | 3291325.185 |
| 1 | 0.0633 | 0.06325 | 389 | 24.6237 | 24.60425 | 1590561.497 |
| 1 | 0.72535 | 0.79315 | 755 | 547.63925 | 598.82825 | 5518399.256 |
| 1 | 0.73465 | 0.8027 | 775 | 569.35375 | 622.0925 | 1343305.555 |
| 1 | 0.72325 | 0.84035 | 447 | 323.29275 | 375.63645 | 4175116.499 |
| 1 | 0.77675 | 0.7743 | 253 | 196.51775 | 195.8979 | 4143547.539 |
| 1 | 0.2278 | 0.2756 | 375 | 85.425 | 103.35 | 576410.4923 |
| 1 | 0.5894 | 0.78265 | 429 | 252.8526 | 335.75685 | 580747.5593 |
| 1 | 0.6534 | 0.76065 | 481 | 314.2854 | 365.87265 | 274794.5424 |
| 1 | 0.64625 | 0.80045 | 529 | 341.86625 | 423.43805 | 389977.8835 |
| 1 | 0.72925 | 0.73885 | 573 | 417.86025 | 423.36105 | 111814.6116 |
| 1 | 0.1705 | 0.3451 | 613 | 104.5165 | 211.5463 | 276376.5993 |
| 1 | 0.71785 | 0.85545 | 649 | 465.88465 | 555.18705 | 359321.7718 |
| 1 | 0.7517 | 0.7584 | 87 | 65.3979 | 65.9808 | 54997.06982 |
| 2 | 1.465 | 1.5733 | 171 | 125.2575 | 134.51715 | 376551.0863 |
| 1 | 0.1192 | 0.12755 | 251 | 29.9192 | 32.01505 | 182158.4187 |
| 5 | 3.32925 | 4.09175 | 327 | 217.73295 | 267.60045 | 3244952.952 |
| 1 | 0.64975 | 0.64975 | 399 | 259.25025 | 259.25025 | 0 |
| 1 | 0.74155 | 0.7424 | 825 | 611.77875 | 612.48 | 276105.1326 |
| 1 | 0.1048 | 0.23375 | 817 | 85.6216 | 190.97375 | 26391938.42 |
| 1 | 0.6447 | 0.80145 | 805 | 518.9835 | 645.16725 | 828213.0992 |
| 1 | 0.63355 | 0.79505 | 789 | 499.87095 | 627.29445 | 4281016.294 |
| 1 | 0.66785 | 0.69445 | 771 | 514.91235 | 535.42095 | 19572196.98 |
| 1 | 0.79095 | 0.79855 | 709 | 560.78355 | 566.17195 | 464698.6544 |
| 1 | 0.8843 | 0.8843 | 681 | 602.2083 | 602.2083 | 0 |
| 1 | 0.71835 | 0.85095 | 155 | 111.34425 | 131.89725 | 109165.684 |
| 1 | 0.63575 | 0.77065 | 97 | 61.66775 | 74.75305 | 3259096.815 |
| 1 | 0.6058 | 0.66475 | 161 | 97.5338 | 107.02475 | 1118335.887 |
| 1 | 0.1973 | 0.37465 | 87 | 17.1651 | 32.59455 | 2350185.809 |
| 1 | 0.20265 | 0.21785 | 289 | 58.56585 | 62.95865 | 871750.271 |
| 1 | 0.8031 | 0.8393 | 171 | 137.3301 | 143.5203 | 229514.0984 |
| 1 | 0.88945 | 0.945 | 87 | 77.38215 | 82.215 | 1742322.027 |
| 1 | 0.78445 | 0.78445 | 87 | 68.24715 | 68.24715 | 0 |
| 2 | 0.1983 | 0.4595 | 87 | 8.62605 | 19.98825 | 941625.9951 |